JOURNAL OF CAVE AND KARST STUDIES

December 2010
Volume 72, Number 3
ISSN 1090-6924
A Publication of the National Speleological Society

IN THIS ISSUE:

CONE KARST IN THE BAHAMAS? MICROCLIMATE MONITORING IN SHOW CAVES, A NEW GENUS, AND MORE...

Published By
The National Speleological Society

Editor-in-Chief
Malcolm S. Field
National Center of Environmental
Assessment (8623P)
Office of Research and Development
U.S. Environmental Protection Agency
1200 Pennsylvania Avenue NW
Washington, DC 20460-0001
703-347-8601 Voice 703-347-8692 Fax
field.malcolm@epa.gov

Production Editor
Scott A. Engel
CH2M HILL
700 Main Street, Suite 400
Baton Rouge, LA 70802
225-381-8454
scott.engel@ch2m.com

Journal Copy Editor
Bill Mixon

JOURNAL ADVISORY BOARD

Penelope Boston
Dave Culver
Derek Ford
Louise Hose
Wil Orndorf
Benjamin Schwartz
Elizabeth White
William White
Carol Wicks

BOARD OF EDITORS

Anthropology
George Crothers
University of Kentucky
211 Lafferty Hall
Lexington, KY 40506-0024
859-257-8208 • george.crothers@uky.edu

Conservation-Life Sciences
Julian J. Lewis & Salisa L. Lewis
Lewis & Associates, LLC.
Cave, Karst & Groundwater Biological Consulting
17903 State Road 60 • Borden, IN 47106-8608
812-283-6120 • lewisbioconsult@aol.com

Earth Sciences
Gregory S. Springer
Department of Geological Sciences
316 Clippinger Laboratories
Ohio University • Athens, OH 45701
740-593-9436 • springeg@ohio.edu

Exploration
Paul Burger
Cave Resources Office
3225 National Parks Highway • Carlsbad, NM 88220
505-785-3106 • paul_burger@nps.gov

Microbiology
Kathleen H. Lavoie
Department of Biology
State University of New York
Plattsburgh, NY 12901
518-564-3150 • lavoiekh@plattsburgh.edu

Paleontology
Greg McDonald
Park Museum Management Program
National Park Service
1201 Oakridge Dr. Suite 150
Fort Collins, CO 80525
970-267-2167 • greg_mcdonald@nps.gov

Social Sciences
Joseph C. Douglas
History Department
Volunteer State Community College
1480 Nashville Pike • Gallatin, TN 37066
615-230-3241 • joe.douglas@volstate.edu

Book Reviews
Arthur N. Palmer & Margaret V. Palmer
Department of Earth Sciences
State University of New York
Oneonta, NY 13820-4015
607-432-6024 • palmeran@oneonta.edu

The *Journal of Cave and Karst Studies* (ISSN 1090-6924, CPM Number #40065056) is a multi-disciplinary, refereed journal published three times a year by the National Speleological Society, 2813 Cave Avenue, Huntsville, Alabama 35810-4431 USA; Phone (256) 852-1300; Fax (256) 851-9241, email: nss@caves.org; World Wide Web: http://www.caves.org/pub/journal/.
Check the *Journal* website for subscripion rates. Back issues and cumulative indices are available from the NSS office.

POSTMASTER: send address changes to the *Journal of Cave and Karst Studies*, 2813 Cave Avenue, Huntsville, Alabama 35810-4431 USA.

The *Journal of Cave and Karst Studies* is covered by the following ISI Thomson Services Science Citation Index Expanded, ISI Alerting Services, and Current Contents/Physical, Chemical, and Earth Sciences.

Copyright © 2010 by the National Speleological Society, Inc.

Front cover: Plate 1 from Walker and Mylroie in this issue.

FSC
www.fsc.org
MIX
Paper from responsible sources
FSC® C006300

T.M. Hurd, A. Brookhart-Rebert, T.P. Feeney, M.H. Otz, and I. Otz – Fast, regional conduit flow to an exceptional-value spring-fed creek: implications for source-water protection in mantled karst of south central Pennsylvania. *Journal of Cave and Karst Studies,* v. 72, no. 3, p. 129–136. DOI: 10.4311/jcks2009es0112

FAST, REGIONAL CONDUIT FLOW TO AN EXCEPTIONAL-VALUE SPRING-FED CREEK: IMPLICATIONS FOR SOURCE-WATER PROTECTION IN MANTLED KARST OF SOUTH-CENTRAL PENNSYLVANIA

Todd M. Hurd[1], Ashley Brookhart-Rebert[2], Thomas P. Feeney[3], Martin H. Otz[4], and Ines Otz[5]

Abstract: Karst springs of Cumberland County, Pennsylvania, are important water resources, but their sources and flow paths are unknown. We traced flow in a mantled-karst groundwater system in the Great Valley section of the Valley and Ridge Physiographic Province using fluorescent dyes, with focus on Big Spring Creek. Upper Big Spring Creek is assigned High Quality/Exceptional Value status by Pennsylvania based on its high water quality and value as a multi-use resource with exceptional recreational or ecological significance. Subsurface flow followed the geologic strike after Sulpho Rhodamine B (Acid Red 52) dye was released on exposed carbonates. Subsurface flow had a maximum effective linear velocity of 2.5 km d^{-1}, which is 8 times greater than sodium fluorescein (Acid Yellow 73) dye released separately into a losing stream over colluvium (0.3 km d^{-1}). Sulpho Rhodamine B was detected strongly 8.9 km away at Big Spring Creek's largest source spring (~250 ppt water; 50 ppb eluate), but weakly in an east source (2.5 ppb eluate). Sodium fluorescein was detected after four weeks at 0.07 to 0.15 ppb in eluate at springs at Huntsdale Hatchery, 9.5 km from release atop the colluvial mantle. Slow flow derived from losing streams on the colluvial mantle likely maintains water quality of Big Spring Creek and similar systems. However, this recharge is distant, and the flow passes below karst recharge features in the valley center, creating many opportunities for contamination. Future studies of contaminant and sediment loadings to subterranean basins and of source-water protection strategies that recognize these patterns are necessary to protect these streams.

Introduction

Limestone springs and spring-fed creeks in south-central Pennsylvania are well known as valuable cold-water fisheries supporting wild trout (e.g., Letort Spring Run, Big Spring Creek), and some are utilized as water supplies for trout hatcheries (Hurd et al., 2008) and municipalities. Nevertheless, source areas for these springs remain largely undetermined. Specific reaches of several spring-fed creeks are designated Exceptional Value Waters, Pennsylvania's most distinguished category of water use (Pennsylvania Code Chapter 93), even though groundwater contributes substantial quantities of non-point nitrogen and pesticide pollution to springs and wells in the region (Lindsey et al., 2003; Lindsey et al., 2009). Lindsey et al. (2009) note that in the Ridge and Valley Aquifer, more than 10% of well samples contained over six pesticides. Moreover, nitrate levels in groundwater of the Mid-Atlantic region are highest in areas mapped as carbonate rocks (Greene et al., 2004; Low and Chichester, 2006). Spring-fed creeks consistently show elevated nitrate, with highest concentrations of 6 to 8 mg L^{-1} in summer (Walderon and Hurd, 2009), and localized, rapid volatile organic compounds (VOCs) contamination of springs and wells has occurred via preferential flow in the region's karst (Aley et al., 2004).

The Cumberland Valley of south-central Pennsylvania is a complex regolith-mantled carbonate hydrogeological system located in the central part of the Great Valley section of the Valley and Ridge Physiographic Province. The valley is bordered to the north by North or Blue Mountain and to the south by South Mountain (Blue Ridge Physiographic Province), a resistant upland source of quartzite and schist (Chichester, 1996). Conodoguinet Creek and Yellow Breeches Creek drain Cumberland County between North and South Mountains. Flow is east-northeast into the Susquehanna River (Fig. 1). Most of the valley carbonates, and almost all of the shale near North Mountain, are in the Conodoguinet Creek basin. South Mountain and much of the eastern quarter of Cumberland Valley are drained by the Yellow Breeches Creek (Becher and Root, 1981). Several tributaries farther

[1] Corresponding Author - Shippensburg University Department of Biology, 1871 Old Main Drive, Shippensburg, Pennsylvania 17257, tmhurd@ship.edu
[2] Pennsylvania Department of Conservation and Natural Resources, Bureau of Recreation and Conservation, P.O. Box 8475, Harrisburg, PA 17105-8475, arebert@state.pa.us
[3] Shippensburg University Department of Geography and Earth Science, 1871 Old Main Drive, Shippensburg, Pennsylvania 17257, tpfeen@ship.edu
[4] Nano Trace Technologies, Gartenstrasse 6, CH-3252 Worben, Switzerland, mhotz@nanotracetech.com
[5] Nano Trace Technologies, 5858 East Molloy Road, Suite 171, Syracuse, New York 13211, iotz@nanotracetech.com

to the southwest originate on South Mountain and flow into the Conodoguinet Creek (Earle, 2009) via Burd Run and Middle Spring along the western boundary of Cumberland County. The Burd Run/Middle Spring system forms the only continuous surface stream between South Mountain and Conodoguinet Creek, and accessible caves are clustered within its surface watershed (Smeltzer, 1958). The southern half of the valley is underlain primarily by a sequence of carbonate rocks of variable thickness, collectively referred to as the Cumberland Valley sequence (Becher and Root, 1981). A thick wedge of colluvium on the north flank of South Mountain covers the older rocks in this sequence (Becher and Root, 1981) and reaches up to 137 m thick (Chichester, 1996). This mantle thins toward the valley center to reveal some carbonate outcrops. Hollyday et al. (1997) describe this mantled karst as part of the larger regional Elkton Aquifer or West Toe Aquifer of the western Blue Ridge Aquifer. Seepage-run data indicate that Yellow Breeches Creek is losing its water through the mantle to the underlying carbonates, and most stream reaches in the lower and middle part of the basin are gaining water from the groundwater system (Chichester, 1996). Other low-order tributaries sink near the carbonate contacts, suggesting complexity of recharge to the karst aquifer and in flow patterns to the spring-fed creeks that discharge in the valley center (Fig. 1). Typical karst features occur in the valley, including closed depressions, caves, sinking streams, springs, and dry channels. Direct groundwater-recharge features include sinkholes, fractured bedrock, sinking streams, and sinkhole ponds. Triassic-age diabase dikes that extend north/south through the valley act as groundwater dams and diversions in a few locations, and many of the springs discharge at faults or where diabase dikes cross the valley (Chichester, 1996).

The primary objective of this study was to determine source areas for Big Spring Creek, a valued wild-brook trout fishery (Cooper and Scherer, 1967) and water supply with increased development within its surface watershed. Big Spring Creek is designated an Exceptional Value Stream and exhibits complex karst hydrology. Big Spring Creek has two major source springs, with generally low variation in discharge, temperature, and turbidity (USGS, 2009), but occasionally with increased turbidity in the larger source spring in response to storms. A third contributing spring to Big Spring Creek serves as the municipal water supply to Newville, Pennsylvania. Becher and Root (1981) and Chichester (1996) suggested that surface water is lost to the groundwater system from South Mountain/Yellow Breeches Creek and flows through the karst of the Cumberland Valley toward north-flowing springs, including Big Spring. We sought to delineate a portion of Big Spring Creek's source areas with fluorescent dye tracing, including tracer release points in a colluvial losing reach in the upper Yellow Breeches watershed directly to the south and in a failed storm-water detention basin (sink collapse) in exposed carbonates farther west.

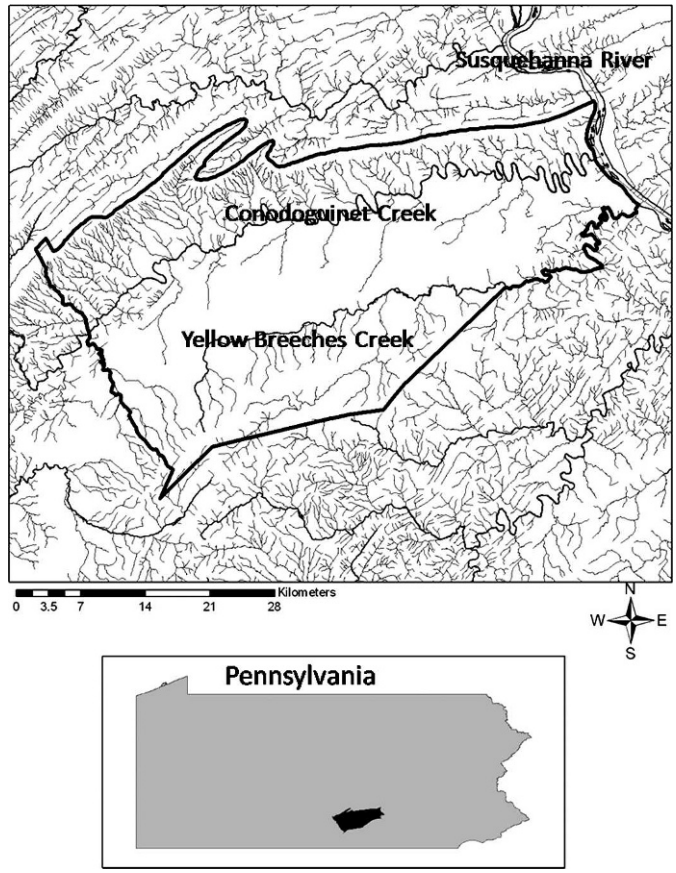

Figure 1. Study region showing boundary of Cumberland County in south-central Pennsylvania and major tributaries of the Susquehanna River within the carbonate valley (Conodoguinet and Yellow Breeches Creeks).

These contrasting release points also facilitated an initial comparison of groundwater-flow characteristics between mantled karst and exposed carbonates of the Great Valley section of the Valley Ridge Province in Cumberland County, Pennsylvania.

METHODS

Eight springs were sampled for dye breakthrough, including the two main sources of Big Spring Creek and six other springs within several kilometers of Big Spring Creek (Fig. 2). Seven of the springs are located in the Conodoguinet Creek drainage basin: Big Spring (both east and west source springs), Cool Spring, Green Spring, Bullshead Branch, Mt. Rock Spring, and Alexander Spring. The two spring sources of Big Spring are located about 4.5 km south of Newville and collectively discharged an average of 765 L s^{-1} during this study (USGS, unpublished data). The Cool Spring resurgence occurs near the channel of Big Spring Creek in the Borough of Newville, and is the source of Newville municipal water supply. Discharge and source areas for this spring have not

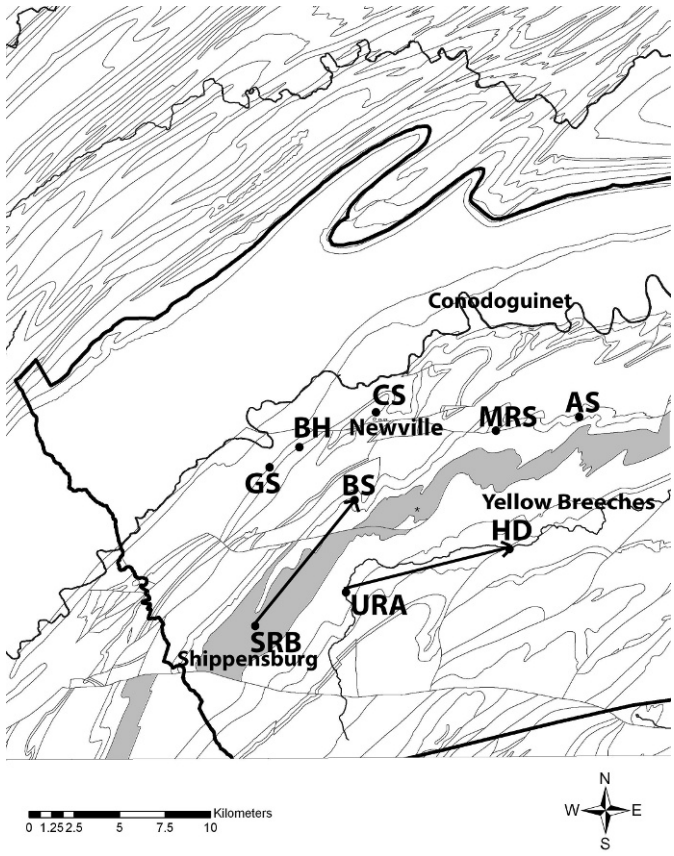

Figure 2. Release points, study springs, and groundwater flow paths (arrows) determined by fluorescent dye tracing in western Cumberland County, Pennsylvania. Tracer release points SRB – Sulpho Rhodamine-B dye, URA – sodium fluorescein dye. Study springs GS – Green Spring, BH – Bullshead Spring, BS – Big Spring, CS – Cool Spring (Newville, Pennsylvania, municipal supply), MRS – Mount Rock Spring, AS – Alexander Spring, HD – Huntsdale Hatchery Springs. The asterisk denotes location of a recently permitted quarry 2.1 km east and south of Big Spring Creek sources. Extensive tectonic deformation has folded the rock so that it generally has a steep dip to the northwest, with a northeast-southwest strike. The Zullinger Formation is shaded. Note south of Big Spring an example of major faulting in the region.

been determined. Green Spring, which currently supplies water to a private fish hatchery, originates about 6.4 km southwest of Newville. Discharge was estimated once in 2005 to be approximately 670 L s^{-1}. Bullshead Branch is a spring tributary to Green Spring Creek, located about 6.4 km from Newville. Discharge for Bullshead Branch was not measured, but appears comparable to or less than that of Green Spring. Bullshead Branch and Green Spring possess relatively long, intermittent surface channels above their resurgence points. Mt. Rock Spring discharged approximately 500 L s^{-1} during spring and summer measurements in 2005 and is about 7.6 km east of Newville. Alexander Spring emerges from several spring seeps with lower total discharge than the other springs studied and is about 12 km east of Newville. The streams flowing from Mt. Rock Spring and Alexander Spring lose water in their lower reaches, with frequent lack of surface flow to Conodoguinet Creek during the summer and fall (Earle, 2009). A group of springs located in the mantled karst of the Yellow Breeches Creek drainage basin was sampled at their confluence at Huntsdale State Fish Culture Station of the Pennsylvania Fish and Boat Commission (Fig. 2).

We used fluorescent dye tracing to determine groundwater-flow patterns, with sodium fluorescein (C.I. Acid Yellow 73) and Sulpho Rhodamine B (C.I. Acid Red 52) chosen for tracers based on their low detection limits and safety to humans and organisms (Field et al., 1995; Käss, 1998). Charcoal receptors were purchased from the Crawford Hydrology Laboratory and consisted of vinyl-coated fiberglass-screen mesh filled with 10 g of activated coconut charcoal. Pairs of background receptors were exchanged from springs weekly during the summer of 2005, until suitable tracer-release conditions occurred, defined as one week of complete sinking of the surface flow in the upper Yellow Breeches. Duplicate receptors continued to be exchanged weekly for seven weeks following dye injection. Water from the two main source springs of Big Spring Creek was collected in 60 ml brown glass bottles, beginning immediately before the first dye release and then daily thereafter. The background fluourescence corresponded to only 15 ppt for Sulpho Rhodamine B in the pre-release water samples from the source springs and 7 to 25 ppt for sodium fluorescein in detectors collected the week before release, resulting in low detection limits in the post-release samples. Receptors and water samples were kept dark and cool in an ice chest during transport and refrigerated afterward.

On the afternoon of August 25, 2005, receptors were exchanged and water samples were collected for background fluorescence. At 8:00 p.m. that day, 0.9 kg of sodium fluorescein dye dissolved in 9.5 L of water was released in the sinking reach of the Yellow Breeches at Route 174 in Walnut Bottom, Pennsylvania, directly south of Big Spring (Fig. 2). This reach was losing water along its entire surface flow to within 50 m downstream of the release point. By dawn on August 26, only a trace of the dye was visible along the stream edge in back-current areas, and there was no dye visible by 11:00 a.m. At 9:00 p.m. on August 27, 2005, 0.9 kg of Sulpho Rhodamine B dissolved in 9.5 L of water was released into a sinkhole collapse in the Zullinger Formation during a rain event. This site is located within an engineered detention basin near the surface watershed boundaries of Middle Spring and Bullshead Branch, west of Big Spring (Figs. 1, 2). It drains impervious runoff via open culverts under Interstate Highway 81.

Charcoal receptors were eluted and the solution was analyzed with a Shimadzu scanning spectrofluoropho-

tometer at the Crawford Hydrology Lab (Crawford and Associates, 2004). We also used a Shimadzu scanning spectrofluorophotometer to analyze water samples.

The average daily Sulpho Rhodamine B concentration was estimated from the breakthrough curve at Big Spring west and combined with hourly discharge data (USGS, unpublished) to estimate the approximate mass of recovered tracer, assuming that the west spring contributed 90% of the discharge and 90% purity of the Sulpho Rhodamine B released. Mean discharge for the breakthrough period (USGS unpublished) and mean transit time were also used to obtain preliminary estimates of conduit system volume and radius (Goldsheider et al., 2008). To estimate system volume for the west spring, average discharge of 688 L s^{-1} (90% of average 765 L s^{-1} for both source springs; USGS unpublished) was multiplied by mean transit time (6 days), the time when one half of the detected tracer passed the sampling site. We then estimated conduit radius based on flow distance and system volume, assuming one phreatic pipe.

The approximate drainage area for Big Spring Creek (both source springs) was estimated using values of precipitation (98.6 cm) and evaporation (63.3 cm) at Shippensburg, Pennsylvania (Chichester, 1996; Rense, 1997) and four years of mean discharge (849.5 L s^{-1}) from USGS (2009). We assumed mean discharge during this time approximated mean discharge during the period of precipitation record.

RESULTS

Both injected dyes followed regional, linear patterns paralleling the valley topography and trend in strike, with resurgence at specific springs (Fig. 2). Sulpho Rhodamine B was detected in water samples 3.5 days after release, 8.9 km to the northeast in the west source spring of Big Spring (Figs 2, 3), indicating a maximum effective linear velocity of 2.5 km d^{-1} in the exposed carbonates. Peak concentrations of 250 to 316 ppt occurred between August 31 and September 3, 2005, then tailed, indicating a mean transport time of 6 days and mean linear velocity of 1.5 km d^{-1}. A longer period of detection existed for the charcoal receptors at this site, continuing through September and into the first week of October (Fig. 3). The Crawford Laboratory designated the dye connection to the west spring as extremely positive, their most confident designation for charcoal receptors, with peak eluate concentration of 45 to 50 ppb. In the east source of Big Spring, Sulpho Rhodamine B dye was not clearly detectable from the charcoal receptors until the week of September 1–8 (approximately 2 ppb in eluate), then tailed to even lower levels by October 2005 (Fig. 3). The Sulpho Rhodamine B detection limit for water samples at the east source of Big Spring was 10 ppt, but we did not detect the dye in water samples there.

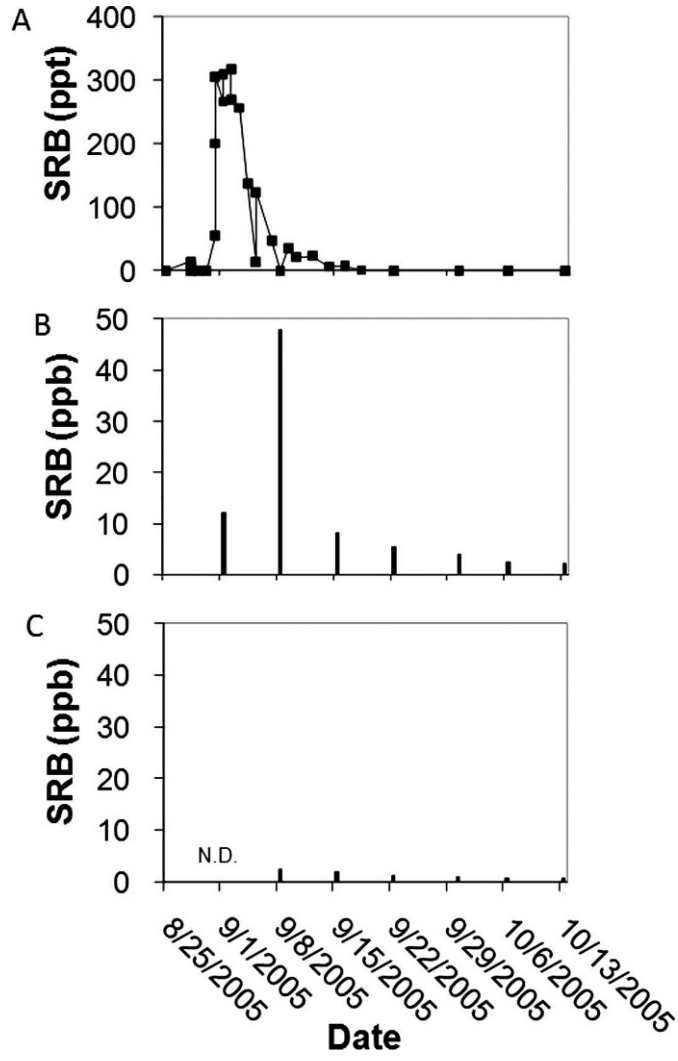

Figure 3. Differential breakthrough of Sulpho Rhodamine B (SRB) at Big Spring source springs following injection on August 27, 2005. A. Strong and rapid breakthrough curve at the larger west source spring based on water samples. B. Strong dye detection at the larger west source spring on receptors. C. Dye detection at the smaller east source spring on receptors. SRB was not detected clearly in water samples for the east spring.

Calculations of dye-mass recovery for Sulpho Rhodamine B suggest that approximately 9% of the released tracer was recovered in the west source of Big Spring, using the data shown in Figure 4. A preliminary estimate for volume of the west source conduit is approximately 357,000 m^3, with a conduit radius of 3.6 m.

The sodium fluorescein released 5.2 km south of Big Spring was detected 9.5 km east of the release point, at the springs at Huntsdale Hatchery, approximately one month after release as 77 to 140 ppt in the eluate from charcoal (Fig. 2). This dye was not detected in Big Spring or other springs draining to the north, but apparently remained in the Yellow Breeches surface watershed. Flow to the

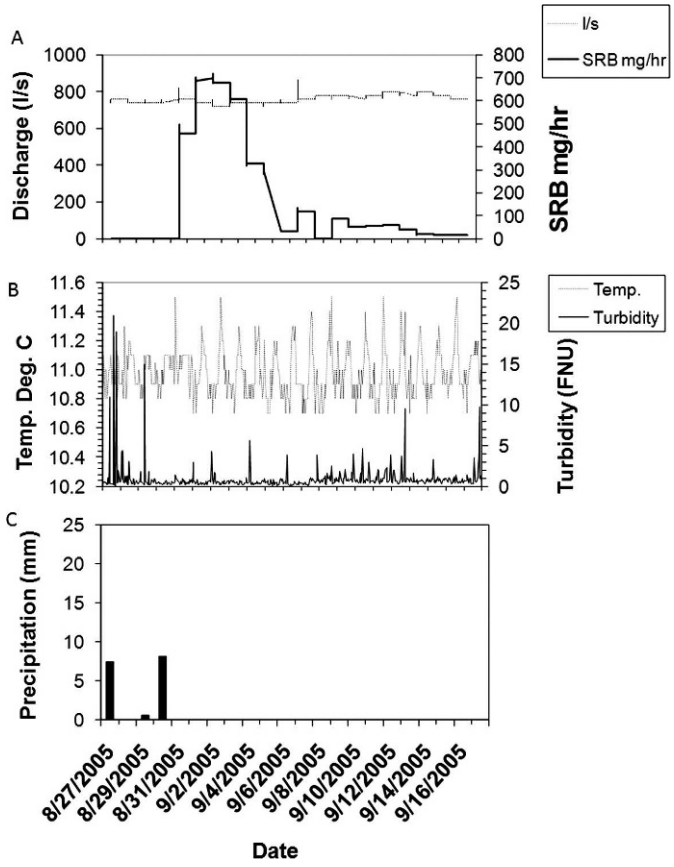

Figure 4. A. Estimated mass breakthrough of Sulpho Rhodamine B in Big Spring with discharge, assuming 90% contribution of west source spring to total flow, and 90% tracer purity. B. Temperature and turbidity of Big Spring. C. Precipitation recorded at Shippensburg University. Discharge, temperature, and turbidity data were provided courtesy of the U.S. Geological Survey (Bruce Lindsey).

Huntsdale springs was comparatively slow through the mantled karst, approximately 0.3 km d^{-1} versus 1.5 to 2.5 km d^{-1} in the exposed carbonates. Using precipitation (Chichester, 1996) and evaporation (Rense, 1997) estimates for Shippensburg, Pennsylvania, and discharge for Big Spring Creek (USGS, 2009), we estimated approximate drainage area of 76 km^2 for both of the main source springs of Big Spring Creek. Further dye tracing will lead to a better understanding of the extent of the Big Spring drainage basin.

Discussion

Regional groundwater flow patterns closely followed trends in geologic strike from west and south (Fig. 2). For Big Spring Creek, flow from outside the surface watershed can be rapid and follow preferential flow paths from karst recharge features to primary springs. This pattern is common in Appalachian karst (Ginsberg and Palmer, 2002) and confirms the importance of rapid surface contribution to conduits where the colluvial mantle thins. The west and east sources of Big Spring Creek had very different breakthrough responses (Fig. 3), which suggests that the two source springs have distinct flow paths or that the east spring discharges more diffuse flow. The west source of Big Spring can become turbid during very strong precipitation events, a characteristic of fast flow systems (Quinlan, 1989; Otz and Azzolina, 2007; Herman et al., 2008). Nevertheless, this spring usually demonstrates relatively low variability in discharge, temperature, and turbidity (USGS, 2009). These patterns suggest cave-stream flow from the Sulpho Rhodamine B release point, fed by moderated flow from the colluvial mantle. White and White (2001) note that many groundwater basins in Appalachian karst consist of a branch-work cave flow system, where subterranean tributaries interacting with allogenic surface water feed dominant conduit flow. These authors also note how flow through Appalachian karst can be moderated by flow into smaller fractures from main conduits during events, with subsequent slower drainage back to the conduit system. Lindsey et al. (2006) noted dual flow characteristics of Dykeman Spring, in the Middle Spring Creek watershed, and Big Spring, based on geochemical measurements, hydrological monitoring, and results of this study. It is reasonable to envision relatively slow flow in colluvium or colluvial fill, followed by rapid delivery to springs via conduit flow. White (2007) notes that carbonate springs may be fed by conduits, yet exhibit little or no hydrograph response to storms due to primary storage in the epikarst. Smeltzer (1958) mapped a number of caves in the Shippensburg area, most of which consist of interconnected main passages that trend northeast-southwest along the strike, although most do not currently carry streams. White (1958) notes that Shippensburg-area caves are probably remnants of a formerly more complex cavern system, dating possibly to the late Tertiary, and that this long history has likely contributed to complex patterns of fillings and re-excavations. Such history would also contribute to the complex hydrology of the mantled karst.

Karst systems are extremely vulnerable to anthropogenic impacts and may rapidly transport water and contaminants on a regional scale (Vesper et al., 2001). Surface runoff to the collapsed sinkhole where Sulpho Rhodamine B was released originates in zones of residential and industrial development, flows through an engineered drainage system open to contaminant spills near an interstate-highway exit (the IH 81 and Highway 174 interchange), and sinks immediately upon entering a failed storm-water detention basin (Fig. 5a). Maximum effective linear velocity of groundwater flow from this recharge feature to the west source of Big Spring Creek was 2.5 km d^{-1}, higher than velocities (0.02 to 1.7 km d^{-1}) derived from first-arrival times for groundwater in the region between an army depot and springs farther west and north (Aley et al., 2004).

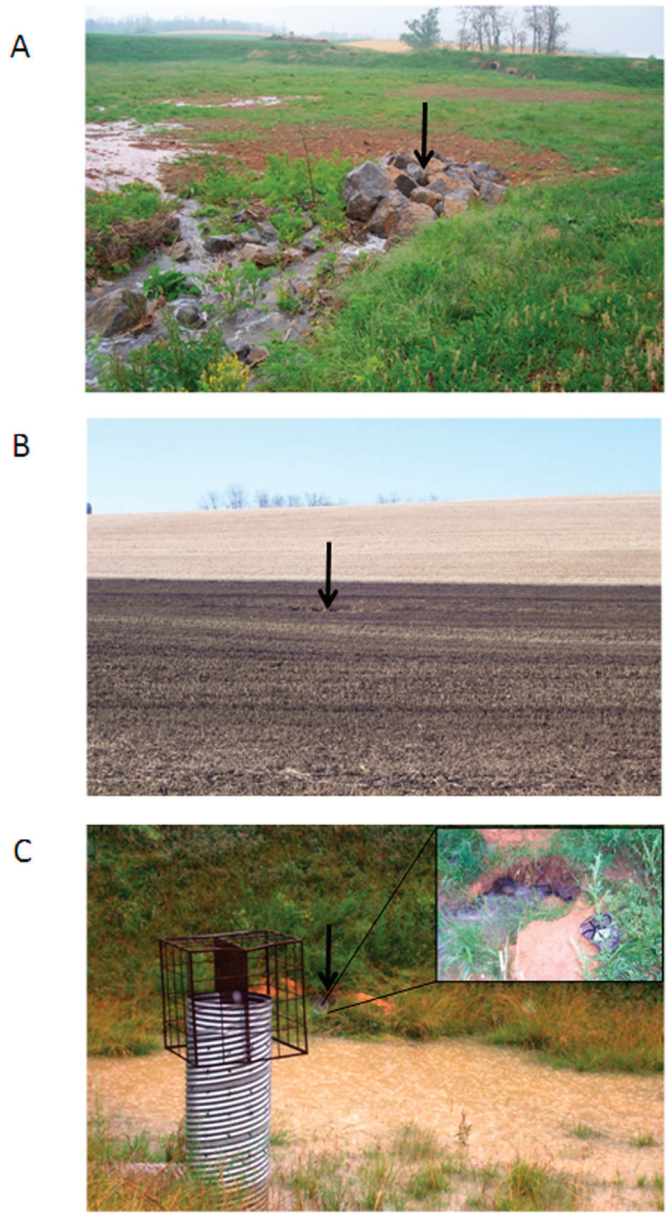

Figure 5. Critical recharge areas associated with karst features in Cumberland County, Pennsylvania. A. Runoff from impervious surface and interstate-highway drainage into a failed detention basin. This was the release point of Sulpho Rhodamine B traced to the west source spring of Big Spring Creek. B. Liquid manure spread over an active sink where the colluvial mantle thins. C. Sink collapse in an infiltration gallery of a recently permitted quarry and asphalt production facility, 2.1 km southeast of Big Spring source springs.

Karst recharge features in close proximity to intensive agricultural or urban land use present a direct threat to Big Spring Creek and sensitive receptors. Such features should be better buffered or controlled when associated with intensive land use (Petersen and Vondracek, 2006) to allow for more gradual infiltration and natural attenuation of potential contaminants from agricultural and industrial areas. Similar drainage into the subsurface occurs in the region within fields receiving agricultural runoff, in a military installation leaching volatile organics (Aley et al., 2004), and in a quarry and asphalt plant within 2 km of Big Spring Creek (Fig. 5).

Our results do not support previous suggestions that groundwater flows predominantly across the valley from South Mountain toward Big Spring and Conodoguinet Creek (Becher and Root, 1981; Chichester, 1996; Continental Placer, 2003), although there is need for further dye-tracing tests under varying hydrological conditions to better determine these patterns. Well data showing northward flow with hydraulic conductivity of only 0.2 to 1.1 m day^{-1} (Continental Placer, 2003) on the southeast boundary of the Big Spring surface watershed may be reflecting slower fracture flow within the Zullinger Formation, in which we demonstrated rapid conduit flow (Fig. 2). There is need for dye tracing of conduit systems to be incorporated into permitting and monitoring processes (Quinlan, 1989) in Pennsylvania karst, particularly when development occurs in close proximity to Exceptional Value spring-fed creeks and municipal springs.

Sodium fluorescein released in the upper Yellow Breeches watershed appeared to remain in this watershed (Fig. 2). Neither tracer was detected in Cool Spring, Green Spring, Bullshead Branch, Mt. Rock Spring, or Alexander Spring, suggesting that these are separate flow systems. Nevertheless it is important to acknowledge that false negative results can be obtained for a number of reasons in fluorescent dye-tracing tests (Quinlan, 1989), and so they should be interpreted cautiously. Groundwater flow from the Yellow Breeches release site was substantially slower than from the other release site, with sodium fluorescein taking about one month to travel the distance it took the Sulpho Rhodamine B to travel in 3 to 5 days. This is likely due to the slowing of surface water as it infiltrates the colluvial material along South Mountain prior to phreatic flow toward springs associated with Yellow Breeches Creek. Detection of sodium fluorescein at the Huntsdale springs was not as strong as Sulpho Rhodamine B in the valley center and did not meet the criterion of two consecutive detections at 10-times background for a certain positive following the Crawford Laboratory protocol (Crawford and Associates, 2004). Nevertheless, sodium fluorescein was detected at least 3 to 5 times background for two consecutive weeks one month following release. At Huntsdale, there are multiple springs combined into a larger hatchery source. Collectively, the geologic setting and complexity of the Huntsdale springs and hatchery system may call for further source water delineation with different tracers and injection locations.

We estimate that the drainage area for Big Spring is approximately 76 km^2, whereas the surface watershed area is only 8.8 km^2. Given that the springs are within

approximately 5 to 10 km of one another and dye traveled 9 km along strike, subterranean basins associated with these systems may be narrow and parallel to one another. This conceptual model fits well with the ''rule of thumb'' approach for estimating source areas in Appalachian karst, where vadose flow follows dip from local topographic highs, then turns 90° to follow phreatic conduits along the strike (Ginsberg and Palmer, 2002). The pattern is also consistent with contamination of Cumberland County groundwater in 1969 by a gasoline spill close to Harrisburg (Becher and Root, 1981), other Appalachian karst systems (e.g. Dasher and Boyer, 1997; White and White, 2001; Herman et al., 2008), and trends of major cave passages in the region (Smeltzer, 1958). We made preliminary estimates for system volume (357,000 m^3) and radius (3 to 4 m) assuming one phreatic pipe. While this approach is useful for preliminary conceptualization, it is likely that the associated conduit system includes both open passage and flooded sumps, as other mapped Pennsylvania caves demonstrate (Smeltzer, 1958; White, 2007). Low recovery of Sulpho Rhodamine B also suggests hydrological complexity. This low recovery is likely due to adsorption and dilution in the aquifer due to the small quantity used (1 kg) and the distance traveled (9 km). Some SRB was missed after concentrations fell below detection limits. (Fig. 3).

Conclusions

We have documented fast, regional conduit flow along strike (approximately 3 km d^{-1} based on first arrival time) and vulnerability to intensive land use for a high-quality/exceptional-value spring-fed creek in Pennsylvania, Big Spring Creek. Slower flow from losing streams over the colluvial mantle likely maintains the relatively high quality of Big Spring Creek and similar springs in the region. Nevertheless, these recharge areas are distant, with groundwater traveling through conduits open to surface runoff in exposed carbonates of the valley center.

In the study area, nutrients and other contaminants in the discharge of karst springs can come from recharge features along the path of the underground flow, and not principally from losing surface streams. Therefore, mitigation focus and best management practices should be redirected from riparian buffers to spring head, well head, and source area protection, along with improved storm water engineering, joint municipal planning, and permitting in these areas. Regional planning and source-water protection strategies (e.g., Doerfliger et al., 1997; Kastning and Kastning, 1997; Kacaroglu, 1999) need to be implemented based on definitive hydrological studies and identification of critical recharge features along delineated karst groundwater flows. Such focus would not only protect local spring water and its existing uses, but would more effectively reduce non-point nutrient, sediment, and contaminant loadings to the Susquehanna/Chesapeake Bay watersheds via karst valleys.

Acknowledgements

We thank Drs. Nicholas Crawford (Center for Cave and Karst Studies), Donald Siegel (Syracuse University), and Heinz Otz (Otzhydro, Switzerland) for assistance in the study design, along with Doug Chichester of U.S. Geological Survey. Bruce Lindsey of U.S. Geological Survey provided data shown in Figure 4. We also thank the Crawford Hydrology Laboratory for charcoal-receptor analysis and Big Spring Watershed Association, Inc. and land owners whose support was invaluable. An Alexander Stewart Foundation Grant to Big Spring Watershed Association and a Pennsylvania State System of Higher Education Professional Development Grant to T.M. Hurd provided funding for the study.

References

Aley, T., Tucker, M., and Stone, P.R. III, 2004, Letterkenny Army Depot Southeastern Area National Priorities List site, Operable Unit Six off-post groundwater, Appendix A-4 Groundwater Tracing Study, Off-Post Trace 3. Prepared by Ozark Underground Laboratory. Protem, Missouri, *in* SEOU6 Southeastern Area Off-Post Groundwater Remedial Investigation Report LEADSEOU6RI1104 compiled by Shaw Environmental, Inc., Cherry Hill, New Jersey, 141 p.

Becher, A., and Root, S., 1981, Groundwater and Geology of the Cumberland Valley, Cumberland County, Pennsylvania: Pennsylvania Geological Survey, 4th ser., Water Resource Report 50, 95 p.

Chichester, D.C., 1996, Hydrogeology of, and simulation of ground-water flow in, a mantled carbonate-rock system, Cumberland Valley, Pennsylvania: U.S. Geological Survey Water-Resources Investigations Report 94-4090, 39 p.

Continental Placer, 2003, Quarry Dewatering Impact Evaluation, Produced for Pennsy Supply Inc., Penn Township Operation, Penn Township, Pennsylvania, December 2003, Continental Placer, Inc., 7 p.

Cooper, E.L., and Scherer, R.C., 1967, Annual production of brook trout (*Salvelinus fontinalis*) in fertile and infertile streams of Pennsylvania, *in* Proceedings of the Pennsylvania Academy of Science, v. 41, p. 65–70.

Crawford and Associates, 2004, Laboratory Profile, Center for Cave and Karst Studies, Applied Research and Technology Program of Distinction, Department of Geography and Geology, Bowling Green, Kentucky, Crawford and Associates, 73 p.

Dasher, G., and Boyer, D., 1997, Dye tracings in the Spring Creek area, Greenbrier County, West Virginia, *in* Younos, T., Burbey, T.J., Kastning, E.H., and Poff, J.A., eds., Proceedings, Karst Water Environment Symposium, October 30–31, 1997, Roanoke, VA: Virginia Water Resource Center, v. P3-1997, p. 18–30.

Doerfliger, N., Jeannin, P.-Y., and Zwahlen, F., 1997, EPIK: A new method for outlining of protection areas in karstic environments, *in* Günay, G., and Johnson, A.I., eds., Karst Waters and Environmental Impacts, Rotterdam, Balkema, p. 117–123.

Earle, J., 2009, Watershed Restoration Action Strategy, State Water Plan Sub basin 07B, Conodoguinet Creek Watershed, Franklin and Cumberland Counties: Pennsylvania Department of Environmental Protection, Bureau of Watershed Management. http://www.dep.state.pa.us/dep/DEPUTATE/Watermgt/WC/Subjects/WSNoteBks/WRAS-07B.htm [accessed September 10, 2009].

Field, M.S., Wilhelm, F.G., Quinlan, J.F., and Aley, T.J., 1995, An assessment of the potential adverse properties of fluorescent tracer dyes used for groundwater tracing: Environmental Monitoring and Assessment, v. 38, p. 75–96.

Ginsberg, M., and Palmer, A., 2002, Delineation of Source-Water Protection Areas in Karst Aquifers of the Ridge and Valley and

Appalachian Plateaus Physiographic Provinces: Rules of Thumb for Estimating the Capture Zones of Springs and Wells: U.S. Environmental Protection Agency, EPA 816-R-02-015, 41 p.

Goldsheider, N., Meiman, J., Pronk, M., and Smart, C., 2008, Tracer tests in karst hydrogeology and speleology, International Journal of Speleology, v. 37, no. 1, p. 27–40.

Greene, E.A., LaMotte, A.E., and Cullinan, K.A., 2004, Ground-water Vulnerability to Nitrate Contamination at Multiple Thresholds in the Mid-Atlantic Region Using Spatial Probability Models: U.S. Geological Survey Scientific Investigations Report 2004-5118, 24 p.

Herman, E.K., Toran, L., and White, W.B., 2008, Threshold events in spring discharge: Evidence from sediment and continuous water level measurement: Journal of Hydrology, v. 351, p. 98–106.

Hollyday, E.F., Hileman, G.E., and Duke, J.E., 1997, The Elkton aquifer or Western Toe aquifer of the Blue Ridge Mountains— A regional perspective, *in* Younos, T., Burbey, T.J., Kastning, E.H., and Poff, J.A., eds., Proceedings, Karst Water Environment Symposium, October 30–31, 1997, Roanoke, Va.:Virginia Water Resource, v. P3-1997, p. 71–77.

Hurd, T.M., Jesic, S., Jerin, J.L., Fuller, N.W., and Miller, D. Jr., 2008, Stable isotope tracing of trout hatchery carbon to sediments and foodwebs of limestone spring creeks: Science of the Total Environment, v. 405, p. 161–172. doi:10.1016/j/scitotenv.2008.06.036.

Kacaroglu, F., 1999, Review of groundwater protection and pollution in karst areas, Water Air and Soil Pollution:, v. 113, p. 337–356.

Käss, W., 1998, Tracing technique in geohydrology, Rotterdam, Balkema, 581 p.

Kastning, E.H., and Kastning, K.M., 1997, Buffer zones in karst terrains, *in* Younos, T., Burbey, T.J., Kastning, E.H., and Poff, J.A., eds., Proceedings, Karst Water Environment Symposium, October 30–31, 1997, Roanoke, Va.: Virginia Water Resource Center, v. P3-1997, p. 80–87.

Lindsey, B.D., Phillips, S.W., Donnelly, C.A., Speiran, G.K., Plummer, L.N., Böhlke, J.K., Focazio, M.J., Burton, W.C., and Busenberg, E., 2003, Residence Times and Nitrate Transport in Groundwater Discharging to Streams in the Chesapeake Bay Watershed: U.S. Geological Survey Water-Resources Investigations Report 03-4035, 201 p.

Lindsey, B.D., Berndt, M.P., Katz, B.G., Ardis, A.F., and Skach, K.A., 2009, Factors affecting water quality in selected carbonate aquifers in the United States, 1993–2005: U.S. Geological Survey Scientific Investigations Report 2008-5240, 177 p.

Lindsey, B.D., Brookhart, A., Hurd, T.M., Feeney, T.P., Otz, M., and Otz, I., 2006, Multi-velocity transport of water through mantled karst aquifers: The potential effect on aquifers used for water supply: The Geological Society of America Northeastern Section - 41st Annual Meeting, March 20–22, 2006, Camp Hill/Harrisburg, Pennsylvania, Abstracts, v. 38, no. 2, 74 p.

Low, D.J., and Chichester, D.C., 2006, Ground-Water-Quality Data in Pennsylvania—A Compilation of Computerized [Electronic] Databases, 1979–2004: U.S. Geological Survey Data Series 150, 22 p.

Otz, M.H., and Azzolina, N.A., 2007, Preferential ground-water flow: Evidence from decades of fluorescent dye tracing: Geological Society of America, October 28–31, 2007, Denver, CO, Abstracts with programs, v. 39, no. 6, 350 p.

Pennsylvania Code Chapter 93: Water Quality Standards. http://www.pacode.com/secure/data/025/chapter93/chap93toc.html, [accessed September 10, 2009].

Petersen, A., and Vondracek, B., 2006, Water quality in relation to vegetative buffers around sinkholes in karst terrain: Journal of Soil and Water Conservation, v. 61, no. 6, p. 380–390.

Quinlan, J.F., 1989, Ground-water monitoring in karst terraines: Recommended protocols and implicit assumptions (unpublished), U.S. Environmental Protection Agency Report EPA/600/X-89/050, 79 p.

Rense, W.C., 1997, A 65-year water budget history of Shippensburg, Pennsylvania: Pennsylvania Geographical Society Annual Meeting, York, Pennsylvania, November 1997.

Smeltzer, B., 1958, Additional data on Shippensburg caves, *in* White, W.B., ed., MAR Bulletin 4, University Park, Pennsylvania, Mid-Appalachian Region of the NSS, p. 3–17.

United States Geological Survey (USGS), 2009, National Water Information System. Department of the Interior, U.S. Geological Survey, http://waterdata.usgs.gov/nwis/uv?01569460 [accessed September 10, 2009].

Vesper, D.J., Loop, C.M., and White, W.B., 2001, Contaminant transport in karst aquifer: Theoretical and Applied Karstology, v. 13–14, p. 101–111. [Reprinted 2003: Speleogenesis and Evolution of Karst Aquifers, v. 1, no. 2, 11 p., http://www.speleogenesis.info/pdf/SG2/SG2_artId19.pdf.]

Walderon, M., and Hurd, T.H., 2009, Nutrient dynamics in carbonate vs. non-carbonate streams: Seasonality, sources, and relative loading: 94th Annual Meeting of the Ecological Society of America, Abstract with Programs, COS 19-4 Biogeochemistry: Above Ground –Below Ground Interactions, in press.

White, W.B., 1958, Note on the geology of the Shippensburg area, *in* White, W.B., ed., MAR Bulletin 4, University Park, Pennsylvania, Mid-Appalachian Region of the NSS, p. 1–2.

White, W.B., 2007, A brief history of karst hydrogeology: Contributions of the NSS: Journal of Cave and Karst Studies, v. 69, no. 1, p. 13–26.

White, W.B., and White, E.L., 2001, Conduit fragmentation, cave patterns, and the localization of karst groundwater basins: The Appalachians as a test case: Theoretical and Applied Karstology, v. 13–14, p. 9–23. [Reprinted 2003: Speleogenesis and Evolution of Karst Aquifers v. 1 no. 2, www.speleogenesis.info/pdf/SG2/SG2_artId22.pdf, 15 p.]

L.N. Walker, J.E. Mylroie, A.D. Walker, and J.R. Mylroie – Symmetrical cone-shaped hills, Abaco Island, Bahamas: karst or pseudokarst? *Journal of Cave and Karst Studies,* v. 72, no. 3, p. 137–149. DOI: 10.4311/jcks2009es0100

SYMMETRICAL CONE-SHAPED HILLS, ABACO ISLAND, BAHAMAS: KARST OR PSEUDOKARST?

LINDSAY N. WALKER[1], JOHN E. MYLROIE[2]*, ADAM D. WALKER[1], AND JOAN R. MYLROIE[2]

Abstract: Abaco Island, Bahamas, contains a large number of conical hills that strongly resemble cone karst, a dissolutional landform associated with karst processes in tropical carbonate localities around the world. Field investigation demonstrated that the conical hills are roughly symmetrical in shape and consist of mid to late Pleistocene eolian calcarenites (carbonate sand dunes) partly mantled by talus. The original hummocky depositional topography of the eolian ridges has been dissected by a variety of processes including dissolution pit formation that enhances slope failure, vegetative disruption of the rock surface, and fire-induced exfoliation of the bedrock. The original asymmetrical shape of continuous dune ridges has thus been modified into a series of hills with a symmetrical cone shape, in which the steeper leeward depositional slopes of the dunes have been masked by talus to create a lesser slope that approximates the dip of the exposed bedrock slope of the more gentle windward depositional faces of the dunes. The conical hills are primarily constructional in nature, modified by mass-wasting slope processes only partly influenced by dissolution; therefore these conical hills are not true cone karst, but pseudokarst, despite their cone shape and their development in soluble carbonate rock. Abaco is the only island in the Bahamian Archipelago with both high eolian relief and a significant positive water budget; that water budget supports the degree of dissolution and forest growth necessary to create the root wedging and fire-induced exfoliation that most modify the steep leeward slopes of the dunes. As the eolian calcarenites were deposited only during the brief glacioeustatic sea-level highstands of the last few hundred thousand years, the development of cone-shaped hills in these eogenetic rocks has been geologically very rapid.

INTRODUCTION

The presence of residual limestone hills is well documented in tropical localities around the world (Ford and Williams, 2007 and references therein; Jennings, 1985 and references therein; Lehmann, 1936; Sweeting, 1973 and references therein; Day, 2004 and references therein). Some of the best known localities are China, Malaysia, Vietnam, Jamaica, New Guinea, Java, Puerto Rico, Cuba, and the Philippines. These landscapes may be referred to as tower karst. Ford and Williams (2007, p. 371), state: ''The word 'tower' therefore subsumes a myriad of forms, and a variety of terms in different languages has been used to describe them, including *turm*, *mogote*, *cone*, *piton*, *hum and pepino*.'' Cone karst (or kegelkarst) refers specifically to cone-shaped hills produced by karst processes (Day, 2004). Cone karst is considered by most karst scientists as a subdivision of tower karst, and these two karst landforms often exist in close proximity to one another (Ford and Williams, 2007).

The presence of such landforms has been attributed to incision of a thick limestone plateau by stream action as the landscape adjusts to a new, lower base level, leaving residual hills of cone or tower shape (Ford and Williams, 1989; 2007; Tang and Day, 2000). Changing base levels are often preserved within the landscape as terraces and abandoned caves exposed in the residual hills, which indicates that tower-karst development is typically a prolonged process (Gillieson, 1996; White, 1988). Residual hills can also form due to high-density development of karst depressions, called dolines or cockpits (Haryono and Day, 2004; Sweeting, 1973; Trudgill, 1985; Versey, 1972; White 1988; 1990; Williams, 1972). Cockpit is the preferred term in some regions of tropical karst, while doline is more commonly used in temperate climates. Adjustment to base-level lowering results in depression development downward at a rate comparable to depression widening, leaving residual hills at the intersections of the depressions (White, 1988). Tropical karst areas where depressions dominate are often referred to as cockpit karst (Sweeting, 1973) or polygonal karst (Williams, 1972).

Residual limestone hills may also form from corrosion of the surrounding landscape, in which denudation takes place almost entirely by subaerial dissolution (Ford and Williams, 1989). Lowering of the surface continues until base level is reached. This landscape lowering implies a large amount of subaerial dissolution with minimal contribution by mechanical processes over a long period of time.

* Corresponding Author, mylroie@geosci.msstate.edu

[1] 60200 Glacier Drive, Canmore, AB T1W 1K6, Canada, s03.lmccullough@wittenberg.edu

[2] Department of Geosciences, Mississippi State University, Mississippi State, MS 39762 USA

Figure 1. Symmetrical cone-shaped hill E on Abaco, along the N-S profile of the ridge. This cone is approximately 22 m in height. The photographer is facing east, with north to the left of the photograph and south to the right.

Though cone and tower karst are well documented on the limestone terrains of many islands (Haryono and Day, 2004; Lehmann, 1936; Sweeting, 1973; Versey, 1972; Williams, 1972), they have never been described in the Bahamas. These island tower karst settings fall into the category of karst on islands, as opposed to island karst (Vacher and Mylroie, 2002). Karst on islands does not differ from that found in continental settings, while island karst is influenced by sea-level position and marine or fresh water geochemistry. In other words, the island setting is not critical to the development of tower karst.

The purpose of this study is to document and describe the morphology of landforms on Abaco Island, Bahamas, that bear a striking resemblance to tropical cone karst in order to understand their formation (Figs. 1 and 2). The shape of the residual hills on Abaco is most similar to cone karst found in Puerto Rico and the Philippines, which is why the landforms on Abaco will be referred to as cone-shaped hills; they are certainly not towers. Cone-shaped hills on limestones that display a variety of other karst features (karren, caves, pits, etc.), as do the hills on Abaco, lead the casual observer to assume the hills are cone karst. The presence of cone-shaped landforms on Abaco is particularly interesting because Abaco lacks many of the features and processes that have been attributed to cone karst formation in other localities, such as surface streams and interlocking karst depressions. In addition, the eogenetic limestones that comprise the surficial geology of Abaco are too young in age (mid to late Pleistocene) for uplift and corrosion to be solely responsible for landscape denudation, implying that other processes are at work. Are the cone-shaped hills of Abaco Island true cone karst, or pseudokarst?

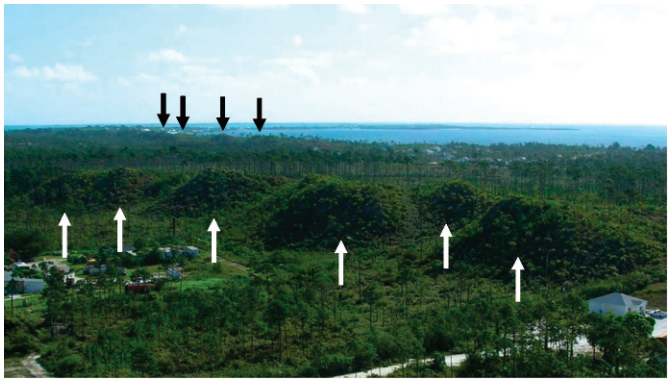

Figure 2. Areal view of Abaco cone-shaped hills; note how the overview reveals aspects of asymmetry of the hills not obvious from the ground view of Figure 1. White arrows identify foreground hills, black arrows hills in the distance.

STUDY AREA

The Commonwealth of the Bahamas forms a NW-SE–trending archipelago of thick carbonate banks located southeast of Florida and northeast of Cuba (Fig. 3). Abaco Island, located on Little Bahama Bank at the northern end of the archipelago, is the eastern-most island on the bank, which itself is the northernmost bank in the archipelago (Figs. 3 and 4A). Abaco is bordered on the east by the deep waters of the Atlantic Ocean, on the south by the deep waters of the NW Providence Channel and the NE Providence Channel, and on the west by the shallow waters of the Little Bahama Bank (Fig. 3). The landmass of Abaco consists of two main islands, Great Abaco Island and Little Abaco Island, and numerous outlying cays (Fig. 4A).

Cone-shaped landforms occur in many separate localities on Abaco, but are particularly concentrated on the eastern side of Great Abaco Island south of Marsh Harbour. The work for this study was conducted at a site approximately 10 km south of Marsh Harbour (Fig. 4). The geology of the area consists dominantly of Pleistocene eolianite ridges and interdune areas that are locally covered by a patchy terra rossa paleosol (Walker et al., 2008a). The paleosol has been largely removed from the land surface by denudation and only remains in cracks and solution pits. The entire land surface of the study area, including both the eolianite ridges and the surrounding lows, has been highly weathered and modified by karst processes resulting in a high density of dissolution pits, extensive karren development, and the presence of a hard calcrete layer on exposed limestone bedrock (Walker et al., 2008a; 2008b). The vegetation in the study area is dominated by Caribbean pines (*Pinus caribae*) and abundant low scrub vegetation (Fig. 5); this vegetation pattern was later understood to be of great importance. The low areas surrounding the ridges are covered by a veneer of loose rock (Fig. 6). In discussions with other workers on Abaco,

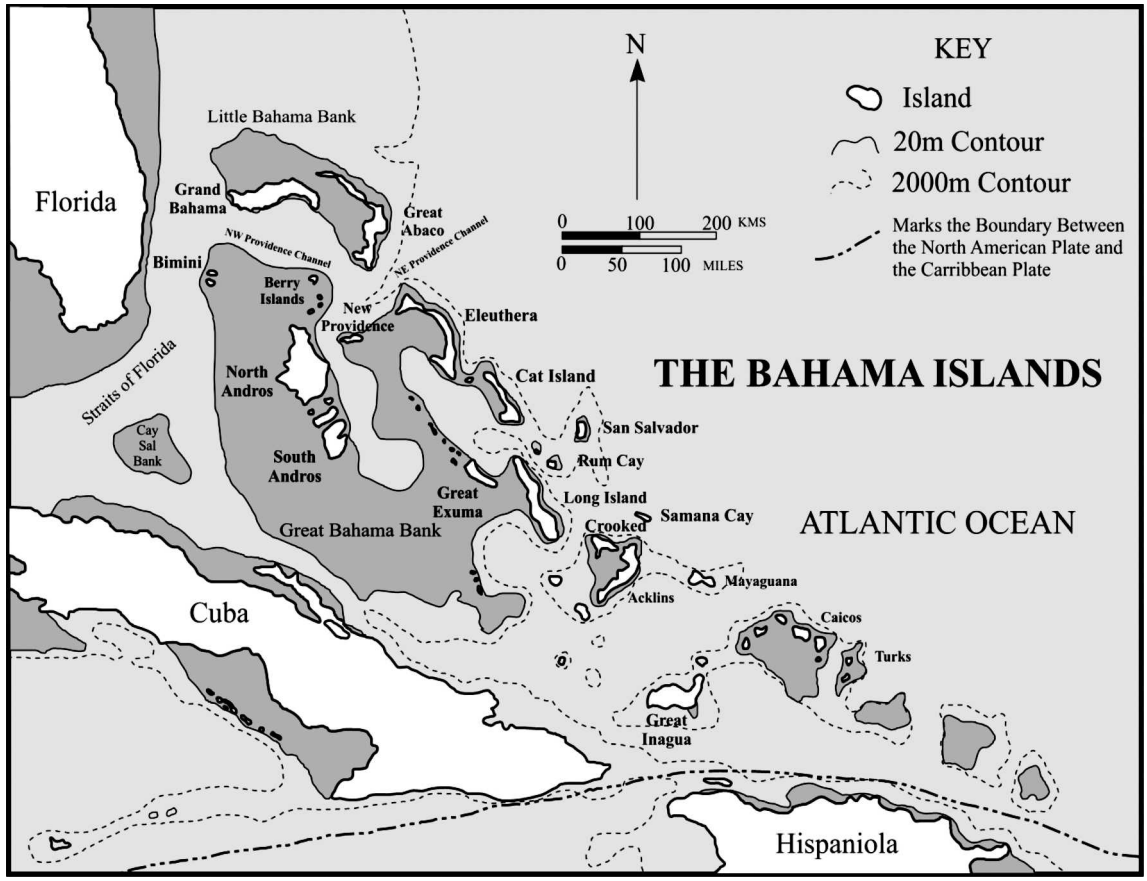

Figure 3. Map of the Commonwealth of the Bahamas (modified from Carew and Mylroie, 1995).

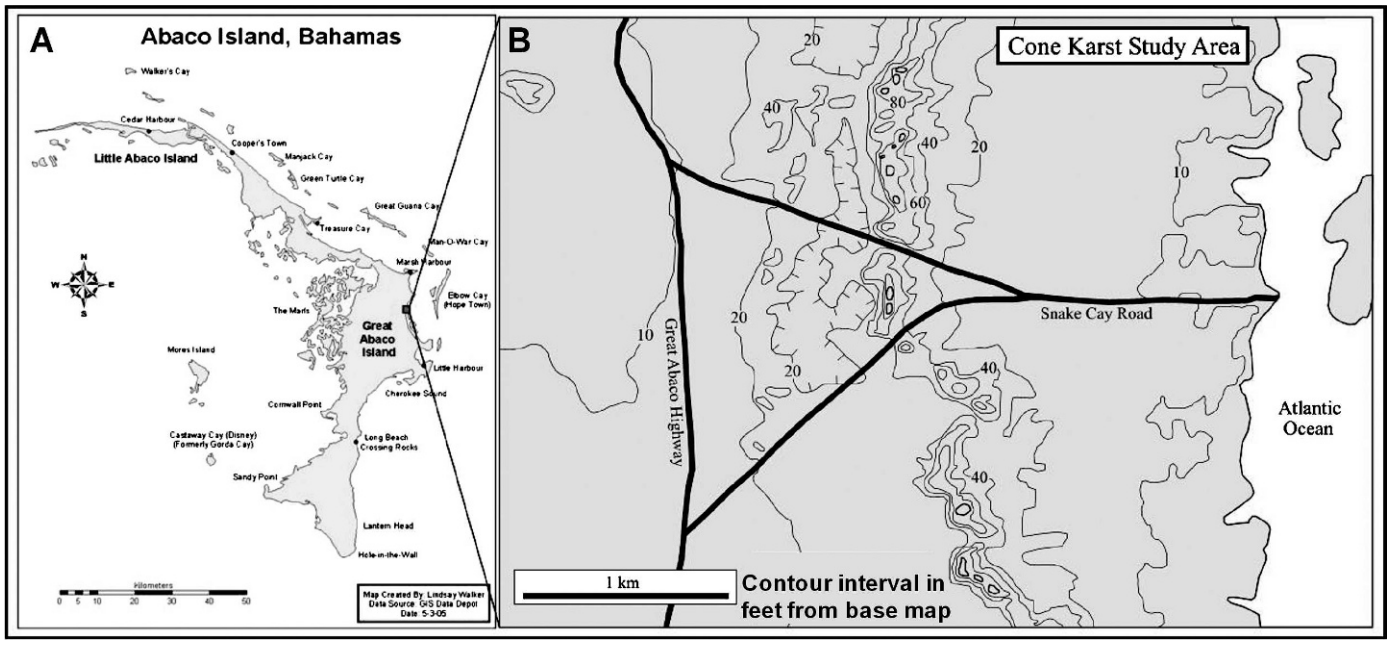

Figure 4. (A) Map of Abaco Islands, Bahamas, showing the location of the cone study area. (B) Topographic map of the cone study area showing the presence of individual isolated hills within a larger eolianite dune ridge (modified from Department of Lands and Surveys, 1975).

Figure 5. General view of the vegetation of Abaco, dominated by the Caribbean pine (*Pinus caribae*). A small cone-shaped hill is barely visible in the background.

this surface has been referred to descriptively as felsenmeer (sea of stones, without any implications of arctic or alpine origin). On the low areas surrounding the ridges, this weathered rock cannot be mechanically transported and becomes part of a stony soil profile on an epikarst surface.

Eolian calcarenites, or carbonates dunes (commonly referred to as eolianites), form all high ground in the Bahamas above 8 m elevation, and can reach elevations over 60 m (Carew and Mylroie, 1997; 2001). They contain an internal architecture produced by eolian processes that controls their overall morphology. Classic studies of Bahamian eolianites by White and Curran (1985), Curran and White (2001), and Caputo (1995) provide detailed descriptions of Holocene and Pleistocene dune suites, respectively. Comparison with ancient carbonate dune suites is provided by Carew and Mylroie (2001). Simplifying from those studies, the dunes form transverse to the prevailing wind direction as hummocky, lobate ridges, with gentle slopes on the windward side and steeper slopes of the leeward side. The gentle windward sides consist of climbing-translatent stratifications (Loucks and Ward, 2001), also called wind-ripple laminations (Curran and White, 2001), that are deposited upslope in the downwind direction. This downwind, but uphill, layering can account for the majority of the stratification in carbonate dunes (Loucks and Ward, 2001). The leeward sides of the dunes are steeper, associated with grainfall and sand-flow units that commonly produce foreset beds that dip steeply in the downwind direction.

Methods

In order to understand the formation of the cone landforms on Abaco, it was necessary to quantify their shape and size. Dimensions of the cone-shaped landforms

Figure 6. The felsenmeer surface in the cone study area. (A) Rock surface covered by loose blocks, machete in center-foreground 1-m long for scale. (B) Larger blocks typically found between the conical hills.

were determined by making basic height and slope measurements of 31 cone-shaped hills (labeled A–EE in the tables), paying special attention to identifying the extent of their symmetry. Heights were measured using a Suunto inclinometer and tape measure. Slope angles were measured in all four cardinal directions, also using a Suunto inclinometer. Slope measurements were not taken in locations where a cone-shaped hill had been artificially cliffed, such as road cuts. The orientation and dip of preserved stratification were noted to relate the primary dune structure to the resulting hill shape. Cone-shaped hills were classified as belonging either to the large main eolianite ridge or to smaller spur ridges oblique to the main ridge in the study area (Fig. 4B). Field observations as to the location and density of dissolution pits and other possible erosional mechanisms were also documented.

Results

The cone-shaped landforms are approximately symmetrical in shape, and are formed from the dissection and modification of Pleistocene eolianite ridges (Figs. 2 and

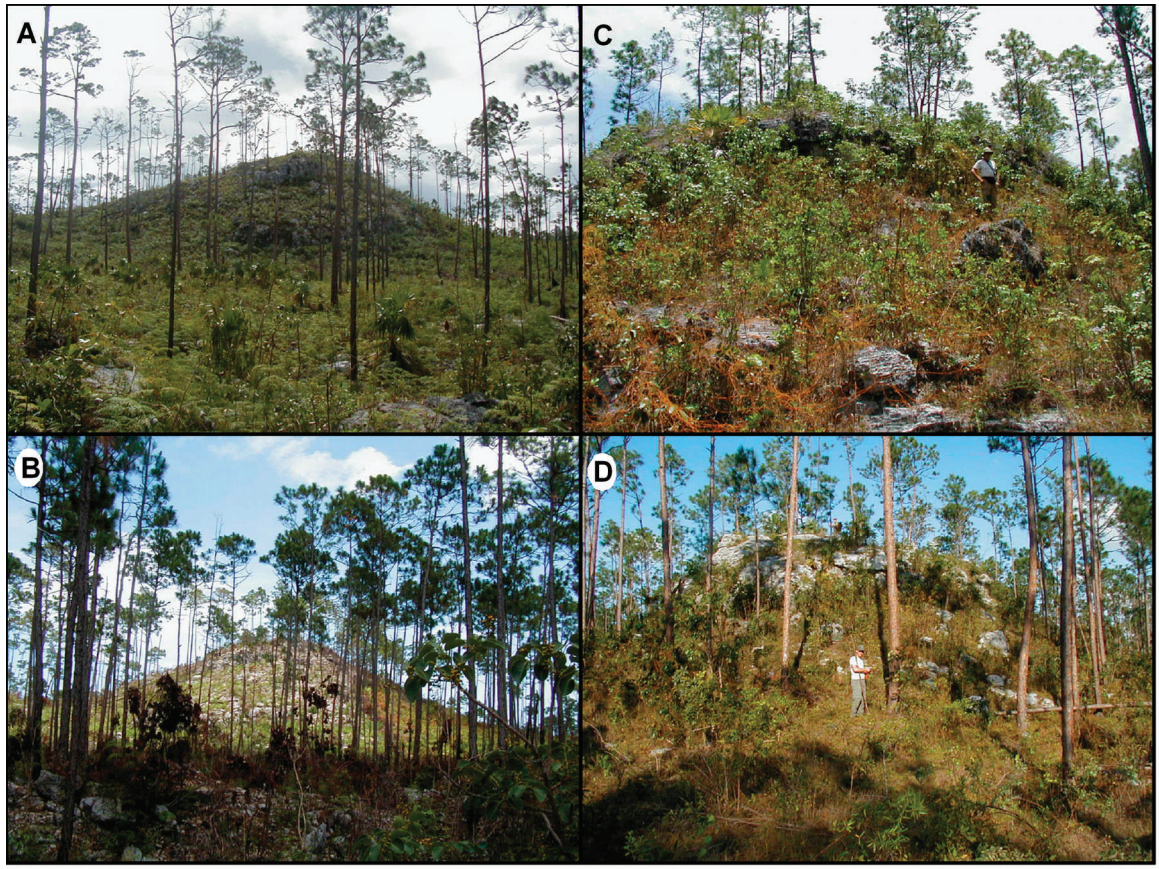

Figure 7. The shapes of typical cone-karst landforms in the study area. (A) Cone-shaped landform J showing some residual asymmetry along the E-W profile of the main ridge as a result of the originally asymmetrical eolianite depositional pattern. This cone is approximately 19 m in height. The photographer is facing south, with the east, or gentler windward side, on the left of the photograph and the west, or steeper leeward side, on the right. (B) Cone-shaped landform I showing the symmetrical shape along the E-W profile of the main ridge. This cone is approximately 21 m in height. The photographer is facing south, with east on the left of the photograph and west on the right. (C) Small cone-shaped hill, showing an apron of talus in the foreground. (D) Small cone-shaped hill with talus to the right of the figure.

4B). The east slope of the hill follows the dip of the windward, translatent or wind-ripple bed stratification of the dune, while the other slopes are formed by truncation of tranlatent or wind-ripple beds and production of talus slopes to form a nearly symmetrical cone (Figs. 1, 2 and 7). Cone-karst landforms in other localities, such as China, have also been known to cut across geologic structure, suggesting that the conical form is more dependent on weathering processes than structural controls (Ford and Williams, 2007). In some cases, the Abaco cone-shaped hills may preserve some of the asymmetry of the original dune ridge (Figs. 2 and 7A).

The cone-shaped hills range in height from 2 to 22 m above the surrounding land surface, with a mean height for all cones of 11.2 m (Tables 1 and 2). The east slopes of the cone-shaped hills were usually the gentlest, with a mean slope of 13.6° (Tables 1 and 2). The west slopes were generally the steepest, with a mean slope of 25.0° (Tables 1 and 2 and Fig. 7A). The north and south slopes had similar means of 20.9 and 21.0 respectively (Tables 1 and 2 and Fig. 7B).

The cone-shaped hills can be divided into two populations. The first population consists of 19 cone-shaped hills dissected from a large, main ridge that trends generally N-S, and the second population consists of 12 cone-shaped hills dissected from smaller spur ridges oblique to the main ridge, trending NE to SW. Cone-shaped hills formed from the main ridge are generally larger, with a mean height of 14.0 m (Table 1), while those from the spur population are smaller, with a mean height of 6.7 m (Table 2). The main-ridge cone-shaped hills have slopes that are always steepest on the west and gentlest on the east (Table 1 and Figs. 2 and 7A). The spur-ridge cones have slopes that are, on average, gentlest on the east, but do not show a side that is consistently steeper based on the slope measurements taken (Table 2 and Fig. 7D).

Main-ridge cone-shaped hills show foreset beds dipping to the west (leeward) and gentler translatent or wind-ripple

Table 1. Main ridge cones.

Cone	Height (m)	N Slope (°)	S Slope (°)	E Slope (°)	W Slope (°)
D	6.1	30.0	24.0	15.0	34.0
E	22.0	29.0	26.0	17.0	30.0
F	18.4	N/A	N/A	14.0	29.0
G	15.7	N/A	22.0	14.5	30.0
H	13.8	16.0	26.0	13.0	32.0
I	21.4	24.0	18.0	20.0	33.0
J	19.1	27.0	23.0	16.0	32.0
K	19.0	12.0	27.0	10.0	32.0
L	6.0	14.0	15.0	17.0	32.0
M	14.1	30.0	12.0	13.0	33.0
N	17.4	29.0	31.0	N/A	28.0
O	15.5	N/A	26.0	15.0	30.0
P	9.5	22.0	19.0	10.0	21.0
Q	12.9	26.0	24.0	11.0	29.0
R	12.5	N/A	24.0	11.0	28.5
W	12.7	N/A	25.0	22.0	27.0
X	18.7	12.0	21.0	10.0	26.0
DD	7.1	18.0	12.0	10.0	20.0
EE	4.1	19.0	15.0	11.0	20.0
Mean Values	14.0	22.0	21.7	13.9	28.8

N/A = areas where slope data unavailable because of artifical cliffing of the dune.

stratification dipping to the east (windward). The east-facing slope of the main-ridge cones generally follows the dip of the original translatent or wind-ripple stratification, while the west-facing slopes are not as steep as the original slip-face of the dune due to truncation of the beds and the formation of talus slopes (Fig. 8). Spur-ridge cone-shaped hills show foreset beds dipping generally to the southwest. The current southwest slope of the cone is not as steep as the original slip-face of the dune, again due to truncation of the beds and the formation of talus slopes. The northeast slopes of the spur-ridge cones follow the dip of the original translatent or wind-ripple stratification of the dune ridge.

Field observations show that dissolution pits are commonly found in lines along the flanks of the cone-shaped landforms (Fig. 9). These lines of dissolution pits are often coexistent with small-scale breaks in slope that allow for the collection of run-off during high-intensity rainfall events and thus increased dissolution. In addition, forest fires, which occur frequently in the pine forests of Abaco, cause cracking and exfoliation of the bedrock (Fig. 10A–B). Another common erosional mechanism in

Table 2. Spur ridge cones.

Cone	Height (m)	N Slope (°)	S Slope (°)	E Slope (°)	W Slope (°)
A	8.2	31.0	32.0	11.0	29.0
B	5.8	17.0	22.0	N/A	27.0
C	7.2	19.0	30.0	8.0	21.0
S	7.5	13.0	10.0	29.0	25.0
T	10.0	15.0	23.0	10.0	29.0
U	9.9	39.0	8.0	19.0	26.0
V	10.6	32.0	11.0	9.0	18.0
Y	3.6	16.0	15.0	14.0	10.0
Z	3.4	13.0	9.0	10.0	11.0
AA	7.6	21.0	35.0	10.0	8.0
BB	5.0	9.0	24.0	15.0	10.0
CC	2.1	11.0	20.0	9.0	16.0
Mean Values	6.7	19.7	19.9	13.1	19.2

N/A = areas where slope data unavailable because of artificial cliffing of the dune.

Figure 8. Initial depositional configuration of the cone-shaped hills, and subsequent alteration. (A) Outcrop on a hill crest, showing dip to the right, slightly steeper than the 1-m-long machete for scale. Note to the left that the dipping translatent or wind-ripple beds are truncated. (B) Cone-shaped hill, dip of the eolian beds shown by the black and white arrows. To the right, the hill slope is mostly bare rock following the windward shallow dip (dashed line) of the translatent or wind ripple stratification; to the left, talus has collected to lessen the steeper lee side dip. Person in white oval for scale.

the study area occurs from the disruption of the bedrock surface by the roots of vegetation, particularly pine trees (Fig. 10C–D).

Discussion

Cone-karst landscapes in the world are formed by processes such as incision of a thick limestone plateau by stream action, lowering of the surface by doline or cockpit development, and corrosion of the surrounding landscape, leaving residual hills. Abaco, however, has no surface streams or broad karst depressions (Mylroie, et al. 1995; Walker et al., 2008a; 2008b), and the rock from which the cones are formed is so young that it is unlikely that corrosion alone could have caused cone-shaped hills to form. In the absence of surface streams, subaerial chemical and physical erosive processes are dominant.

The eolianite ridges from which the cone-shaped hills form are constructional landforms, created by wind transport of carbonate grains in a subaerial environment. As a result, they are subject to subaerial erosion immediately upon deposition. Because the Bahamas are tectonically stable, with only minor subsidence of 1 to 2 m per 100,000 years (Carew and Mylroie, 1995) and fluvial erosion is not a factor, much of the relief above present sea level and all relief above 8 m, is the result of these constructional eolian processes (Carew and Mylroie, 1997; 2001). This is, overall, a very different depositional and erosional history than the marine limestones of cone-karst landscapes around the world. The deposition of Bahamian eolianite ridges also takes place in geologic time periods (the approximately 10,000 year-long sea-level highstand events of the Quaternary) that are relatively short compared to the deposition time of limestones in other environments (Carew and Mylroie, 1997). Thus, the erosional processes, both chemical and physical, acting on Bahamian limestone landscapes take place on different time scales and in different ways than would otherwise be expected.

One element of these erosion processes is the rapid development of a karst landscape with a high density of dissolution pits. In Bahamian karst areas, dissolution pits act as vadose fast-flow routes through the carbonate bedrock (Mylroie and Carew, 1995; Harris et al, 1995). Dissolution pits in the study area often form in lines along the flanks of the cone-shaped landforms, causing weak zones on the periphery of the landforms as the pits enlarge and coalesce (Fig. 9A). Eventually, the weak zones develop into fissures, allowing degradation of the slopes by rock fall (Fig. 9B).

The land surface is further mobilized by forest-fire–induced exfoliation of the eolianites (Fig. 10A–B) and disruption of the bedrock surface by vegetation (Fig. 10C–D). As eolian ridges initiate with high relief, rock loosened by fire, vegetative, and karst processes mass-wastes down slope as talus. Talus slopes, or debris aprons, are common on cone-karst landforms, due to erosion of the steep slopes (Jakucs, 1977; Marker, 1970). As can be seen in Figures 6B, 7C, and 8B, the talus blocks produced are subangular to rounded and do not interlock well, creating a lower angle of repose than expected, compared to talus from dense, hard telogenetic limestones in continental settings. The advanced degree of weathering of the limestone on Abaco due to these processes has also resulted in the rock-rubble veneer on the low areas surrounding the cones (Fig. 6). Thus, the cones and the surrounding land surface form from a combination of dissolutional and mechanical processes, and the formation

Figure 9. The effects of dissolutional karst processes in the study area (machete 1-m long for scale in A–C). (A) Vertical downward-looking view of dissolution pits forming along the flank of a cone-shaped landform. As these pits enlarge and merge, they will form a weak zone that will eventually fail, causing degradation of the slope. (B) Imminent rock-fall as a result of dissolution-pit formation (machete indicated by the arrow). (C) Terra-rossa paleosol preserved within a dissolution crack (material above and parallel to the machete). Dissolutional denudation has stripped this material from the adjacent flat bedrock surfaces. (D) Small dissolutional cave in a small residual hill.

of the talus slopes causes the originally steep leeward face of the eolianite ridge to become less steep (Fig. 11).

Eolian calcarenites are originally deposited as hummocky ridges, with a predisposition to a cone shape that is subsequently modified by erosion (Fig. 12). A formerly continuous, but asymmetrical, eolian ridge takes on a relatively symmetrical profile (Fig. 13). In the case of the main-ridge cones, this modification takes place along the E-W profile, with the east-facing slope maintaining its original gentle slope, and the west-facing slip or leeward face becoming less steep (Figs. 1 and 8B). In the case of the spur-ridge cones, this modification takes place along the NE-SW profile, with the NE-facing slope maintaining its original gentle slope and the SW-facing leeward face becoming less steep. The remaining asymmetry is often difficult to see under the thick vegetative cover of the study area.

The main ridge cone-shaped hills are predisposed to dissection along the N-S ridge profile due to the original hummocky depositional pattern (Fig. 12) of eolian dune ridges in the Bahamas (White and Curran, 1985). Some residual hummocky topography is still evident in the study area, where cone-shaped hills have not been completely isolated from the ridge, despite the intense weathering processes (Fig. 2). Main ridge cone-shaped hills appear more symmetrical in the N-S direction than the E-W direction because the original dip of the beds is not a factor in those directions (Fig. 7A versus 7B). Instead, the cone-shaped hills are dissected from the main ridge by the above described fire, vegetative, and karst processes to form

Figure 10. Non-dissolutional erosion mechanisms in the cone study area. (A) Fire-induced exfoliation of the bedrock surface, machete 1-m long for scale. (B) Recent fire exfoliation, rock flakes charred and sooty, flashlight 15 cm long for scale. (C) Disruption of the bedrock surface in the study area by the roots of pine trees, machete 1-m long for scale. (D) Pine tree bulging out of a dissolution pit, creating strain on the surrounding rock.

relatively symmetrical profiles (Figs. 1, 11 and 13). Again, the cone-shaped hills appear even more symmetrical under the thick vegetative cover of the study area.

The spur ridge cone-shaped hills do not show such an obvious relationship to bed dip and slope as the main ridge cones. This is because the beds of the spur ridge do not dip exactly in the cardinal directions from which the slope measurements were taken. Nevertheless, the relationship

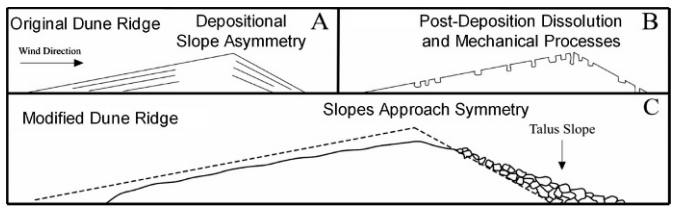

Figure 11. Modification of an originally asymmetrical eolianite ridge into relatively symmetrical cone-shaped landforms by the formation of talus slopes due to karst, vegetative, and fire processes. This modification takes place along the E-W profile of the main ridge.

can still be seen, in that the eastern slopes are usually the gentlest and generally follow the angle of the beds that dip to the east-northeast. The east-northeast beds represent the climbing slope of the dune, the translatent or wind-ripple strata, while the west-southwest foresets represent the steeper slip slope of the leeward side of the dune.

Such cone-shaped hills are not known from other Bahamian islands. Abaco, however, is the only Bahamian island with high eolian relief in a climate that has a significant positive water budget (Fig. 14). Grand Bahama Island to the west of Abaco is also quite wet but lacks significant eolian relief (no elevations above 8 m), and so, has no cone-shaped hills. High eolianite ridges are known to the south and east of Abaco, but on islands with significantly dryer climates. These dry islands do not display cone-shaped hills. This observation implicates meteoric water flux as an important factor in formation of the cone shape. Pine forests, which are the major vegetation type in the cone study area (Fig. 5), only grow on islands with sufficient rainfall (O'Brien, 2006). As pine forests provide ample leaf litter for forest fires, Bahamian islands with pine forests have frequent fires, while,

Figure 12. The original depositional topography of Bahamian hummocky dunes can be preserved as dune segmentation by erosion occurs. (A) Holocene North Point Member dunes (~5000 years old) on San Salvador Island, showing original hummocky topography. (B) Pleistocene dunes on Great Abaco; original hummocky topography, though degraded by erosion, still visible.

somewhat counter-intuitively, drier islands with no pine forests do not have extensive or common fire events (O'Brien, 2006). Thus, the wet climate of Abaco supports the growth of pine forests, which in turn cause forest fires and disruption of the bedrock surface by their roots, and this further contributes to dissection of the eolian ridges into cones and the formation of the rock-rubble surface. The high denudation rate of Abaco relative to other islands in the Bahamas is also evident from the almost complete removal of the terra rossa paleosol from the Pleistocene land surface of the study area (Fig. 9C).

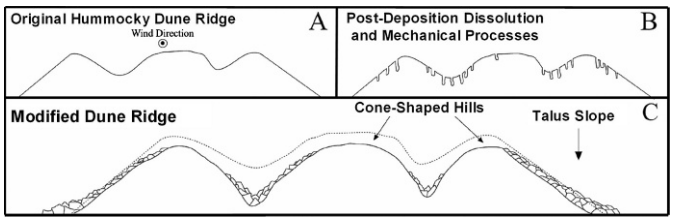

Figure 13. Dissection of an originally hummocky eolianite ridge (A) into cone-shaped landforms (C) by the formation of talus slopes due to karst, vegetative, and fire processes (B). This dissection takes place along the N-S profile of the main ridge.

The original, asymmetrical structure of the dunes as shown by the depositional strata is in agreement with current prevailing wind directions in the Bahamas. Today, winds in the summer are dominantly from the east and southeast and winds in the winter are dominantly from the northeast (Tucker and Wright, 1990). Assuming the situation was similar in the Pleistocene when the dunes were deposited, the two populations could represent seasonal variations in wind direction (Caputo, 1995; Carew and Mylroie, 1997). The main ridge would represent deposition under a predominent wind direction or the wind direction during times of higher sediment production or transport. The smaller spur ridges would represent deposition under a secondary wind direction or the wind direction at a time of lower sediment production or transport. The two populations could also represent two separate eolianite packages associated with different sea-level highstands. Obtaining proof of either scenario would require large-scale sampling of both ridge populations. At this stage, only preliminary petrographic analysis has been conducted (Walker, 2006). The presence of eolianite ridges

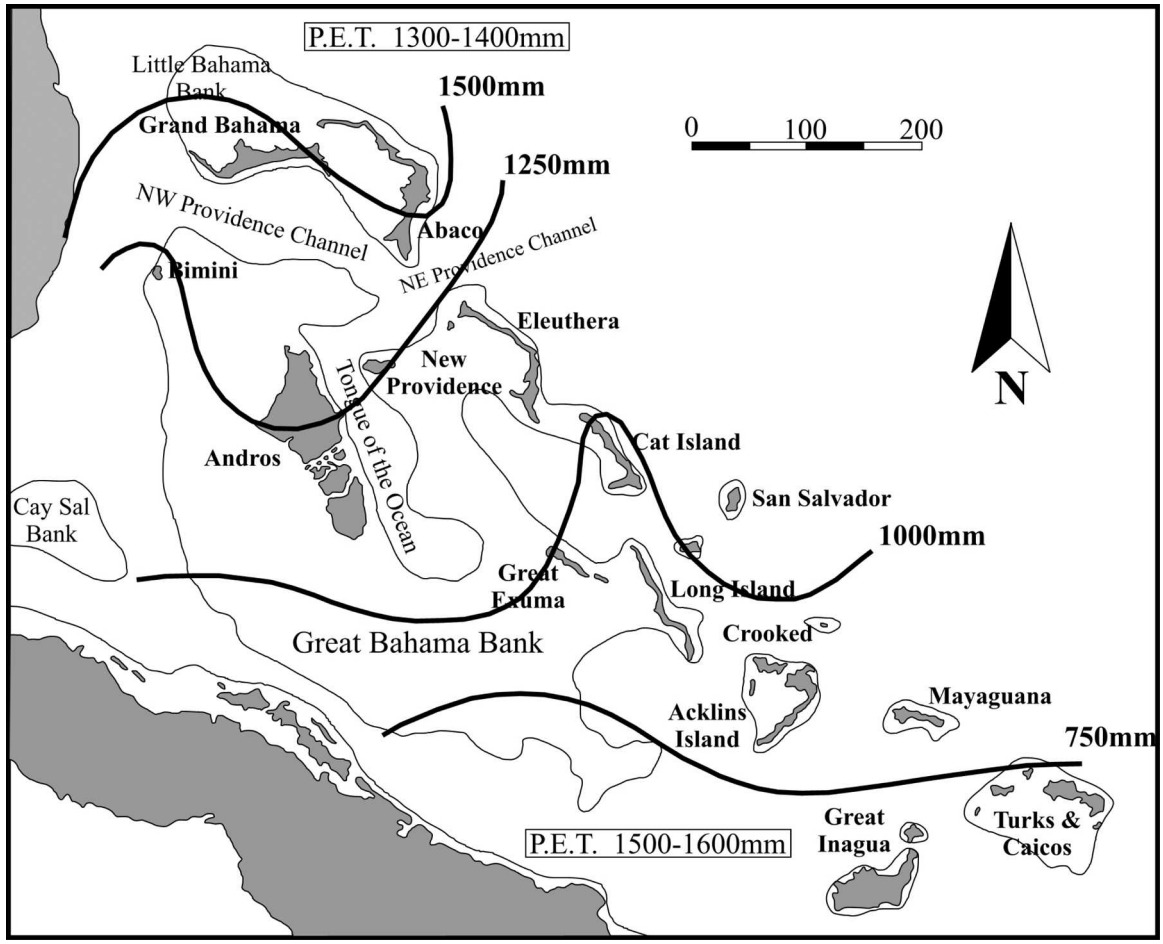

Figure 14. Climate map of the Bahamas showing yearly rainfall (solid contour lines) and P.E.T (Potential Evapotranspiration, in boxes). As shown, Abaco has the largest positive water budget of all the Bahamian islands (modified from Whitaker and Smart, 1997).

in two different orientations is common on other Bahamian islands, such as San Salvador Island (Carew and Mylroie, 1997).

The post-depositional evolution of the porosity of carbonate rocks can be divided into three stages, eogenetic, the time of early burial, mesogenetic, the time of deeper burial, and telogenetic, the stage of erosion of carbonates that have been deeply buried and are now near the surface (Choquette and Pray, 1970). Telogenetic karst is the landscape developed on, and the secondary permeability developed in, ancient rocks that are now exposed after experiencing deep burial (Vacher and Mylroie, 2002). Most traditional forms of karst in continental interiors are formed in telogenetic limestones. Telogenetic rocks are characterized by a low matrix permeability and high fracture and conduit permeability.

Eogenetic karst is a term that refers to the ''land surface developing on, and the pore system developing in, young rocks undergoing eogenetic, meteoric diagenesis'' (Vacher and Mylroie, 2002, p. 183). The eogenetic rocks of Abaco have a high primary porosity, and consequent high matrix permeability that has not been greatly rearranged. Dissolution pits in eogenetic rocks are not obligated to form along joints and fractures, and so develop in a fashion sensitive to available recharge (Harris, et al., 1995). This situation allows the pits to form on the sides of the eolian ridges without regard to structure and participate in the dissolutional dissection of the ridges. The landforms develop quickly, because mechanical mass-wasting processes interact with dissolutional dissection and modification of the eolianite ridges. Bahamian karst is both syndepositional (caves and karst form while deposition is on-going) and syngenetic (caves and karst form while the carbonates are being consolidated), as reported by Mylroie and Mylroie (2009). Therefore, karst processes were acting on the eolianite ridges starting during the actual formation of the dunes to initiate some of the necessary conditions for weathering and talus accumulation.

It has long been recognized that the characteristic geometries of the residual hills in cone and tower karst landscapes are not solely the result of lithologic and structural controls (Ford and Williams, 2007). Similar

landforms, for example, have been described in the dense, telogenetic Devonian and Carboniferous limestones of China and in the eogenetic Tertiary limestones of Caribbean islands such as Cuba and Puerto Rico, which have a much higher primary porosity (Ford and Williams, 2007). Does the degree of dissolutional dissection provided by epikarst development and pit cave formation on the eolian ridges of Abaco qualify those cone-shaped hills as cone karst? The initial review of the evidence would suggest not. The cone-shaped hills of Abaco are constructional features modified by a degree of dissolutional dissection coupled with mechanical weathering. The cone shape is derived more from the depositional topography than from the subsequent chemical and mechanical erosion. However, the restriction of these cone-shaped hills to the wettest Bahamian island that also has high-relief dunes argues that the dissolutional component could be critical to the final expression of a cone shape. It could also be argued that the rainfall-sensitive pine-forest vegetation, with its significant root-wedging and forest-fire inducement, causes the mechanical weathering and talus accumulation that is an important component of the final cone shape.

SUMMARY

The cone-shaped landforms on Abaco represent a unique form of an eogenetic limestone landscape that has not been previously described. The cone-shaped hills form from a combination of dissolutional and mechanical processes as rock loosened by fire, vegetation, and karst processes mass-wastes down slope as talus, acting on a depositional eolian shape predisposed to cone configuration. Thus, formerly asymmetrical eolianite ridges are dissected and modified into relatively symmetrical cone-shaped hills. Much of the residual asymmetry is hidden under the thick vegetation of the study area. Cone-shaped landforms have yet to be reported on other Bahamian islands, and none have been seen on the fourteen other Bahamian Islands spanning the entire archipelago visited by the authors. Abaco, however, is most likely the only island in the Bahamas with both the high eolian relief and the large positive water budget necessary for the formation of the landforms.

The cone-shaped landforms on Abaco are obviously in an environment entirely different from that of traditional cone-karst landscapes. The cone-shaped hills on Abaco are not residual remnants resulting from a lowering of the surrounding surface of the land to base level. Their placement above the surrounding landscape is the result of constructional eolian processes. The formation of eolian ridges on carbonate platforms such as the Bahamas is known to take place only during high interglacial sea levels, when flooding of the platform allows for the creation and mobilization of carbonate sediments (Carew and Mylroie, 1997; 2001). Therefore these cone-shaped hills are initially the result of base level rising instead of falling. Erosional modification and dissection initiates immediately upon deposition and continues throughout subsequent sea-level oscillations to form landforms of surprising symmetry given the asymmetrical interior dune structure. Thus, they record a strikingly unique modification of a very young limestone ridge into cone-shaped landforms that are similar to those arising from apparently different karst processes elsewhere. Despite the cone shape of the hills on Abaco and their development in soluble carbonate rock, they are primarily a pseudokarst feature.

ACKNOWLEDGEMENTS

The authors thank the Karst Waters Institute, Total SA, and Mississippi State University for providing the funding that made this study possible; the Bahamian government for providing the research permit; Friends of the Environment, Marsh Harbour, Abaco, for providing logistical support; all of the residents of Abaco Island that made this study possible, particularly Nancy and Michael Albury, Anita Knowles, Allison Ball, Diane Claridge, and David Knowles. Brenda Kirkland and Grady Dixon of Mississippi State University, Tony Waltham, and an anonymous reviewer, are thanked for all of their insights and comments during the development of this manuscript. Photo in Figure 2 provided by Nancy Albury.

REFERENCES

Caputo, M.V., 1995, Sedimentary architecture of Pleistocene eolian calcarenites, San Salvador Island, Bahamas, *in* Curran, H.A., and White, B., eds., Geological Society of America Special Paper 300, Terrestrial and Shallow Marine Geology of the Bahamas and Bermuda, p. 63–76.

Carew, J.L., and Mylroie, J.E., 1995, Quaternary Tectonic Stability of the Bahamian Archipelago: Evidence from Fossil Coral Reefs and Flank Margin Caves: Quaternary Science Reviews, v. 14, p. 145–153.

Carew, J.L., and Mylroie, J.E., 1997, Geology of the Bahamas, *in* Vacher, H.L., and Quinn, T.M., eds., Geology and Hydrogeology of Carbonate Islands. Developments in Sedimentology 54, Amsterdam, Elsevier, p. 91–139.

Carew, J.L., and Mylroie, J.E., 2001, Quaternary Carbonate Eolianites of the Bahamas: Useful analogues for the interpretation of ancient rocks?, *in* Abegg, F.E., Harris, P.M., and Loope, D.B., eds., Modern and Ancient Carbonate Eolianites: Sedimentology, Sequence Stratigraphy, and Diagenesis. SEPM Special Publication No. 71, p. 33–45.

Choquette, P.W., and Pray, L.C., 1970, Geologic Nomenclature and Classification of Porosity in Sedimentary Carbonates: American Association of Petroleum Geologists Bulletin, v. 54, p. 207–250.

Curran, H.A., and White, B., 2001, Ichnology of Holocene carbonate eolianites of the Bahamas, *in* Abegg, F.E., Harris, P.M., and Loope, D.B., eds., Modern and Ancient Carbonate Eolianites: Sedimentology, Sequence Stratigraphy, and Diagenesis. SEPM Special Publication No. 71, p. 33–45.

Day, M.J., 2004, Cone Karst, *in* Gunn, J., ed., Encyclopedia of Cave and Karst Science, London, Fitzroy Dearborn Publishers, p. 241–243.

Department of Lands and Surveys, 1975, Topographic map of Abaco, Bahamas. Sheet 20. Nassau, New Providence, Bahamas.

Ford, D.C., and Williams, P.W., 1989, Karst Geomorphology and Hydrology, London, Chapman and Hall, 601 p.

Ford, D.C., and Williams, P.W., 2007, Karst Hydrogeology and Geomorphology, West Sussex, John Wiley & Sons Ltd., 562 p.

Gillieson, D.G., 1996, Caves: Processes, Development and Management, Oxford, Blackwell Publishers Ltd., 324 p.

Harris, J.G., Mylroie, J.E., and Carew, J.L., 1995, Banana holes: Unique karst features of the Bahamas: Carbonates and Evaporites, v. 10, p. 215–224.

Haryono, E., and Day, M., 2004, Landform differentiation within the Gunung Kidul Kegelkarst, Java, Indonesia: Journal of Cave and Karst Studies, v. 66, p. 62–69.

Jakucs, L., 1977, Morphogenetics of Karst Regions, New York, John Wiley and Sons, 284 p.

Jennings, J.N., 1985, Karst Geomorphology. 2nd ed., Oxford, Basil Blackwell, 293 p.

Lehmann, H., 1936, Morphological Studies in Java, Stuggart, Engelhorn, 114 p.

Loucks, R.G., and Ward, W.C., 2001, Eolian stratification and beach-to-dune transition in a Holocene carbonate eolianites complex, Isla Cancũn, Quintana Roo, Mexico, *in* Abegg, F.E., Harris, P.M., and Loope, D.B., eds., Modern and Ancient Carbonate Eolianites: Sedimentology, Sequence Stratigraphy, and Diagenesis. SEPM Special Publication No. 71, p. 57–76.

Marker, M.E., 1970, Some problems of a karst area of the eastern Transvaal, South Africa: Transactions of the Institute of British Geographers, v. 50, p. 73–85.

Mylroie, J.E., and Carew, J.L., 1995, Chapter 3, Karst Development on Carbonate Islands, *in* Budd, D.A., Harris, P.M., and Saller, A.H., eds., Unconformities and Porosity in Carbonate Strata, American Association of Petroleum Geologists Memoir 63, p. 55–76.

Mylroie, J.E., Carew, J.L., and Vacher, H.L., 1995, Karst development in the Bahamas and Bermuda, *in* Curran, H.A., and White, B., eds., Geological Society of America Special Paper 300, Terrestrial and Shallow Marine Geology of the Bahamas and Bermuda, p. 251–267.

Mylroie, J.E., and Mylroie, J.R., 2009, Flank margin cave development as syndepositional caves: Examples from The Bahamas, *in* White, W.B., ed., Proceedings of the 15th International Congress of Speleology Huntsville, Alabama, National Speleological Society, v. 2, p. 533–539.

O'Brien, J.J., 2006, Direct and Indirect Effects of Fire on the Ecology of Bahamian Pineyards. [Abstract]. In: 2nd Abaco science alliance conference. Marsh Harbour, Abaco, Bahamas: [not paged].

Sweeting, M.M., 1973, Karst Landforms, New York, Columbia University Press, 362 p.

Tang, T., and Day, M.J., 2000, Field survey and analysis of hillslopes on tower karst in Guilin, southern China: Earth Surface Processes and Landforms, v. 25, p. 1221–1235.

Trudgill, S., 1985, Limestone Geomorphology. Geomorphology Texts Volume 8, New York, Longman, 196 p.

Tucker, M.E., and Wright, P.W., 1990, Carbonate Sedimentology, Oxford, Blackwell Scientific Publications, 482 p.

Vacher, H.L., and Mylroie, J.E., 2002, Eogenetic karst from the perspective of an equivalent porous medium: Carbonates and Evaporites, v. 17, p. 182–196.

Versey, H.R., 1972, Karst of Jamaica, *in* Herak, M., and Stringfield, V.T., eds., Karst: Important Karst Regions of the Northern Hemisphere, Amsterdam, Elsevier, p. 445–466.

Walker, L.N., 2006, The caves, karst, and geology of Abaco Island, Bahamas. MSc thesis, Mississippi State University, 241 p. http://sun.library.msstate.edu/ETD-db/theses/available/etd-03292006-153441/

Walker, L.N., Mylroie, J.E., Walker, A.D., and Mylroie, J.R., 2008a, A preliminary geologic reconnaissance of Abaco Island, Bahamas, *in* Freile, D., and Park, L., eds., Proceedings of the 13th Symposium on the Geology of the Bahamas and Other Carbonate Regions, San Salvador, Bahamas, Gerace Research Centre, p. 89–97.

Walker, L.N., Mylroie, J.E., Walker, A.D., and Mylroie, J.R., 2008b, The caves of Abaco Island, Bahamas: Keys to Geologic Timelines: Journal of Cave and Karst Studies, v. 70, p. 108–119.

Whitaker, F.F., and Smart, P.L., 1997, Chapter 4, Hydrogeology of the Bahamian Archipelago, *in* Vacher, H.L., and Quinn, T., eds., Geology and Hydrogeology of Carbonate Islands, Amsterdam, Elsevier, Developments in Sedimentology 54, p. 183–216.

White, B., and Curran, H.A., 1985, The Holocene carbonate eolianites of North Point and the modern marine environments between North Point and Cut Cay, *in* Curran, H.A., ed., Pleistocene and Holocene Carbonate Environments on San Salvador Island, Bahamas—Guidebook for Geological Society of America, Orlando annual meeting field trip, p. 73–93.

White, W.B., 1988, Geomorphology and Hydrology of Karst Terrains, New York, Oxford University Press, 464 p.

White, W.B., 1990, Surface and Near-Surface Karst Landforms, *in* Higgins, C.G., and Coates, D.R., eds., Groundwater Geomorphology: The Role of Subsurface Water in Earth-Surface Processes and Landforms. Geological Society of America Special Paper 252, Boulder, Colorado, Geological Society of America, p. 157–175.

Williams, P.W., 1972, Morphometric analysis of polygonal karst in New Guinea: Geological Society of America Bulletin, v. 83, p. 761–796.

G. Li, Y. Shang, and J. Gao – Scale analysis of the significance of dispersion in mixing-transport in conduits. *Journal of Cave and Karst Studies,* v. 72, no. 3, p. 150–155. DOI: 10.4311/jcks2009es0106

SCALE ANALYSIS OF THE SIGNIFICANCE OF DISPERSION IN MIXING-TRANSPORT IN CONDUITS

GUANGQUAN LI, YULEI SHANG, AND JUN GAO
Department of Geophysics, Yunnan University, 2 North Green Lake Road, Kunming, Yunnan 650091, P. R. China, guangquanli74@gmail.com

Abstract: Mixing-transport of solute entering at sinkholes or from within the limestone matrix in cavernous conduits is an important process for contaminant migration in karst aquifers. This process may be described with a one-dimensional advection-dispersion equation incorporating the fluxes of solute and water across the conduit wall. For the dilution-dispersion equation, which does not include solute flux across the wall but has the flux of water through the wall, the sufficient and necessary condition for neglecting conduit dispersion is showed by scale analysis to be $L_P \gg a$, where a is the conduit radius, and L_P is the spatial scale of the solute plume. A straightforward necessary and practically, though not strictly, sufficient condition is $a/WT_B \ll 1$, where W is the mean velocity of conduit flow, and T_B is the time scale of the breakthrough curve. For the releasing-dispersion equation, which includes the fluxes of water and solute across the wall, $L_P \gg a$ is still a sufficient condition, but no longer a necessary one. The inequality $a \ll WT_B$ is neither a necessary condition nor a sufficient condition.

INTRODUCTION

The most distinctive feature of karst aquifers is a set of interconnected caves or conduits that form complex underground drainage systems for water and contaminants (Shuster and White, 1971; Kiraly, 1998). These large conduits, often connected to sinkholes and perennial springs at their upstream and downstream ends, respectively, are formed by the dissolving action of acid and aggressive rainwater on carbonate bedrock (usually limestone, dolomite, or marble) over thousands to millions of years. Because the scales of water flow and solute concentration of interest for karst aquifers is typically comparable to, or smaller than, the conduit lengths, sinkholes, springs, and conduits behave like singular points and lines, the prevalence of which makes it a formidable task to accurately model flow and transport in the aquifers.

There are some important works regarding modeling contaminant transport in karst conduits with leaky walls. Tang et al. (1981) developed a model for solute transport in a single fracture, in which the mass transfer between the fracture and the rock matrix is assumed to be diffusive. The weakness of the model is the absence of active solute and water exchange between the fracture and the matrix, which is not realistic for karst aquifers. Contaminant transport in aquifers containing numerous small fractures is often described by a dual-porosity model and a continuum approach, in which contaminant exchange between fractures and porous matrix is modeled by a transfer coefficient representing a diffusive process (Millington and Quirk, 1961; Bear et al., 1993). There are two problems when applying the dual-porosity model to karst aquifers. One is that the exchange of solute between conduits and the matrix is assumed to be diffusive, and the other is that the aforementioned singularity caused by the prevalence of several large conduits was not considered. A numerical model called CAVE (Carbonate Aquifer Void Evolution) developed by Clemens et al. (1996) aims to model the water and calcium exchange between a conduit and the matrix. The liability of CAVE is that the calcium transfer between the matrix and the conduit is diffusion-like (Dreybrodt and Eisenlohr, 2000). In reality, the solute transfer from the matrix to the conduit can be advective or dispersive.

Equations including advection and dispersion were developed to account for retention in immobile-fluid regions (2RNE) and describe transport in a single conduit (Field and Pinsky, 2000; Goldscheider, 2008). The idea is use of the Green's function for the boundary value problem to model solute transport in a conduit. Weaknesses of this analytical model are that advective dilution caused by seepage flow from the matrix is neglected and the conduit dispersion is held constant to facilitate solution. Instead, retention in immobile-fluid regions is used to simulate the tailing phenomena observed in breakthrough curves at springs. Birk et al. (2005) addressed the mixing of matrix water and conduit water and the consequences with respect to interpretation of the spring breakthrough curve. In that scenario, there was no solute flux from the matrix into the conduit. A weakness of their model is the advective dilution induced by the seepage flow from the matrix was not considered.

Water in karst conduits is typically a combination of the water entering at sinkholes and water released from the limestone matrix. In a similar vein, contaminants in karst conduits consist of those entering through sinkholes and those released from the matrix. The mixing-transport of contaminants in a conduit, for the case of negligible conduit dispersion, is analytically solved using the method of characteristics (Li, 2009a; Li, 2009b). The motivation of this article is to investigate when conduit dispersion can be

neglected for mixing-transport of contaminants in a karst conduit. The results can provide us with insight on when the analytical solution to a simplified equation neglecting dispersion is applicable, as well as when numerical solution of the full equation is needed.

Mixing-Transport of Contaminants in a Conduit

The transport of solute by flow in a solid-wall pipe can be described with a one-dimensional advection-dispersion equation (Taylor, 1954). Our problem is different in that both water and solute seep into the conduit from the permeable wall. Though complicated, the mixing-transport of contaminants (solute) in a karst conduit may be described using a relatively simple one-dimensional equation. With a consideration of conduit dispersion, solute-mass conservation gives (Li et al., 2008; Li, 2009a)

$$\frac{\partial C}{\partial t}+\frac{\partial}{\partial z}\left(WC-D_c\frac{\partial C}{\partial z}\right)=\frac{2}{a}J, \tag{1}$$

where t [T] is time, z [L] is the conduit-wise distance from the sinkhole, a [L] is the conduit radius, C [M L^{-3}] is the concentration of solute in the conduit (averaged over the cross-sectional area), W [L T^{-1}] is the mean speed of conduit flow, D_c [L^2 T^{-1}] is conduit dispersion, and J [M L^{-2} T^{-1}] is the specific solute flux across the conduit wall.

Water mass conservation gives

$$W(z)=W_0+\frac{z}{\tau}, \tag{2}$$

where W_0 is the mean speed of flow at the sinkhole, and τ is defined as:

$$\tau=\frac{a}{2q}, \tag{3}$$

where q is the specific water flux across the wall.

The conduit dispersion can be parameterized by (Li, 2004; Li et al., 2008)

$$D_c=aW. \tag{4}$$

This equation for the dispersion coefficient is for turbulent conduit flow, not for laminar flow. The dispersion coefficient for laminar flow is dependent of the square of velocity, often called Taylor dispersion (Bear, 1972).

Scale Analysis of Dilution-Dispersion Equation without Wall Solute Flux

There is an inhomogenous term on the right side of Equation (1). Also, both the flow velocity W and the conduit dispersion D_c are dependent variables. For these reasons, it is difficult to directly evaluate the equation. Two steps are taken to evaluate the equation. The first step is to simplify the equation into an equation that ignores the solute flux but includes the water flux across the wall, which is called the dilution-dispersion equation because clean seepage water dilutes contaminants that have entered at sinkholes. Scale analysis is used decide about the significance of conduit dispersion. Then the conclusion from the first step is used to evaluate whether or not it can apply to the mixing-transport equation incorporating the fluxes of water and solute across the wall, called the (solute) releasing-dispersion equation.

A Sufficient and Necessary Condition for Neglecting Dispersion in Dilution-Dispersion Equation

Ignoring the flux of solute across the conduit wall, Equation (1) simplifies to

$$\frac{\partial C}{\partial t}+\frac{\partial}{\partial z}(WC)=\frac{\partial}{\partial z}\left(D_c\frac{\partial C}{\partial z}\right). \tag{5}$$

Without losing generality and considering the rising limbs of the breakthrough curves, scale analysis of the above equation yields

$$\frac{C}{T_B}-W\frac{C}{L_P}=D_c\frac{C}{L_P^2}, \tag{6}$$

where T_B and L_P are the time and spatial scales of the solute plume, respectively. Because Equation (6) consists of three terms, it follows that the dispersion term can be neglected when and only when

$$L_P^2\gg D_cT_B. \tag{7}$$

A more straightforward necessary condition

In the above section, a sufficient and necessary condition for neglecting conduit dispersion in the dilution-dispersion equation is defined. This subsection aims to derive another, more straightforward sufficient and necessary condition.

If dispersion can be neglected in Equation (6), inequality (7) must be valid as a necessary condition. Substituting Equation (7) into (6) yields:

$$L_P\sim WT_B, \tag{8}$$

which states that the transport is advection-dominated. Substituting Equations (4) and (8) into Equation (7) yields

$$a\ll WT_B, \tag{9}$$

which is a necessary condition for neglecting conduit dispersion in Equation (5).

Below is a proof that the inequality in Equation (9) alone is not a sufficient condition for neglecting conduit dispersion. Suppose that with condition Equation (9), the dispersion term in Equation (5) cannot be neglected with respect to the advection term, or more explicitly,

$$W\frac{C}{L_P}\sim <D_c\frac{C}{L_P^2}, \tag{10}$$

where $\sim<$ means being roughly equal to or smaller than. Then

$$L_P \sim < a. \tag{11}$$

Combining this inequality with Equation (9) yields

$$WT_B \gg a > \sim L_P, \tag{12}$$

From the first and last terms of this inequality, the unsteady term, or the first term in Equation (5), can be neglected with respect to the advection term. Thus the transport is nearly steady, and thus we get $L_P \sim a$. Inequality (12) becomes

$$WT_B \gg L_P \sim a. \tag{13}$$

If there is a solution allowed under restraint by Equation (13), the condition imposed by Equation (9) will not be a sufficient for neglecting conduit dispersion.

Now we investigate whether or not there is a solution allowed under restraint by Equation (13). As above, the problem is nearly steady, and thus from Equation (5), we have

$$\frac{\partial}{\partial z}\left(WC - D_c\frac{\partial C}{\partial z}\right) = 0. \tag{14}$$

Note that the terms in the parentheses are exactly the solute flux in the conduit. Equation (14) means that the solute flux is a constant through the conduit. This equation is a second-order ordinary differential equation, the solution of which requires two boundary conditions, one at the conduit entrance and the other at the exit. We would let the conduit length roughly equal to the radius, and at the same time, prescribe two constant-concentration conditions for the two ends. Thus, a physically meaningful solution is found that satisfies the restraint imposed by Equation (13). Therefore, condition imposed by Equation (9) is not strictly sufficient for neglecting conduit dispersion.

However, in practical field circumstances, such as dye-tracing experiments, the problem becomes better specified. For instance, the breakthrough curves of dye or contaminants at the conduit entrance and the exit, or the boundary conditions at the two ends, are invariably transient or unsteady. Thus the above boundary conditions are not met in field cases, and Equation (14) is typically not satisfied. Therefore, the above supposition that the dispersion term in Equation (5) cannot be neglected with respect to the advection term under the condition imposed by Equation (9), is invalid for field cases. In other words, the condition imposed by Equation (9) is sufficient for neglecting conduit dispersion in practical field cases.

The condition imposed by Equation (9) is not strictly sufficient for neglecting conduit dispersion, because the inequality in Equation (13) may be satisfied. Naturally, a violation of the inequality in Equation (13) may result in a sufficient condition such as

$$L_P \gg a. \tag{15}$$

Actually, if the above inequality is satisfied, through Equation (6), the dispersion term must be negligible with respect to the advection term (a sufficient condition). On the other hand, if conduit dispersion can be neglected in Equation (6), the above inequality must be valid (a necessary condition). Therefore, inequality (15) is a necessary and sufficient condition.

ANALYSIS FOR RELEASING-DISPERSION EQUATION

Whether or not inequality Equation (7), namely, $L_P^2 \gg D_c T_B$, is a condition sufficient or necessary or both for neglecting dispersion in the releasing-dispersion equation, where some solute enters through the conduit wall (Equation (1)), will be investigated in this section. This category is more difficult to analyze in that the right side of the equation is non-zero.

When $L_P^2 \gg D_c T_B$ is satisfied, the dispersion term in Equation (1) must be negligible. However, it is no longer a necessary condition. Suppose the first term of Equation (1) is roughly equal to or smaller than the third term, and the third term, the dispersion, can be neglected. Then both terms can be ignored, in which case the main balance is between the second term and the right-hand side. That is

$$W\frac{C}{L_P} \sim \frac{2}{a}J. \tag{16}$$

With the use of $J = C_m q$, wherein C_m is the concentration of solute released from the matrix, the above equation transforms to $L_P \sim aWC/2qC_m$. It follows that the initial supposition is possible, in which case the spatial scale of the solute plume is described by this equation. Therefore, $L_P^2 \gg D_c T_B$ is no longer a necessary condition for neglecting conduit dispersion.

We now ask whether or not the inequality in Equation (9), $a \ll WT_B$, is a sufficient condition. Following the discussion in the last section, a physical solution can be found, except that the right side of Equation (14) now has a non-homogeneous term resulting from the wall solute flux. Therefore, as before, the inequality in Equation (9) is not a strictly sufficient condition.

In the previous section, we showed that the inequality in Equation (9) is a necessary condition for neglecting conduit dispersion. This is because the main balance in the dilution-dispersion equation is between the first and second terms when dispersion is negligible. However, for the releasing-dispersion equation, that is not valid any longer, because the non-homogenous term now complicates the equation. Thus, we can not always get the inequality in Equation (9) as in the last section. Therefore, the inequality in Equation (9) is not a strictly necessary condition for neglecting conduit dispersion in the releasing-dispersion equation. In a quick summary, the inequality in Equation (9) is neither a sufficient nor a necessary condition.

Table 1. The parameters of the designed numerical example.

Parameter	Value	Units
Conduit radius, a	2.0	m
Conduit length, L	100.0	m
Matrix solute concentration, C_m	30.0	mg L^{-1}
Water flux at sinkhole, Q_0	0.18	m^3 s^{-1}
Water flux from conduit wall, Q_r	1.62	m^3 s^{-1}
Total water flux at spring, Q_s	1.8	m^3 s^{-1}
Specific water flux across wall, q	0.00129	m s^{-1}
Reynolds number[a], Re(cell)	0.028	

[a] The Reynolds number controls the accuracy of spatial discretization in the numerical solution.

At the beginning of this section, $L_P^2 \gg D_c T_B$ is shown to be a sufficient but not a necessary condition for neglecting conduit dispersion in the releasing-dispersion equation. Similarly, condition $L_P \gg a$ is not a necessary condition. Supposing $L_P \sim < a$ and following the same procedure, the second term in Equation (1) can be roughly equal to or smaller than the third term, while the third term can be neglected. Thus, both the second and third terms can be ignored in the equation. In this case, the main balance is between the first and last terms, and the time-scale of the breakthrough curve is determined by a similar equation, $T_B \sim aC/2qC_m$. Therefore, $L_P \gg a$ is no longer a necessary condition for neglecting conduit dispersion. Of course, this equality is a sufficient condition, because the dispersion term can be neglected with respect to the advection term, and therefore, can be neglected from Equation (1).

A Numerical Example

In the above two sections, through scale analysis, we investigate whether or not three inequalities, $L_P^2 \gg D_c T_B$, $WT_B \gg a$, and $L_P \gg a$, are sufficient and/or necessary conditions. In this section, a numerical method is used to verify that $L_P \gg a$ is a sufficient condition for neglecting conduit dispersion in the releasing-dispersion equation.

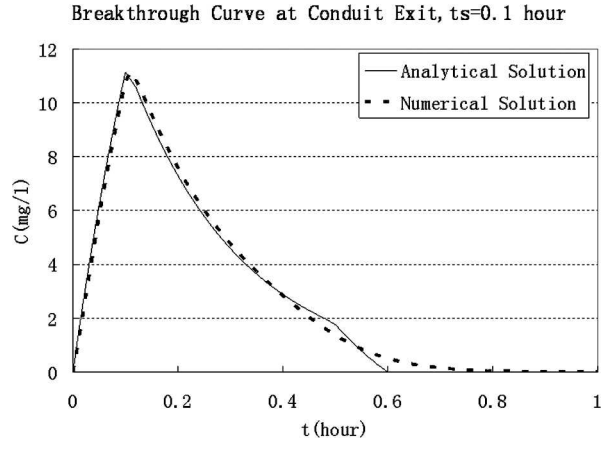

Figure 1. Comparison between the breakthrough curves from the numerical solution of the releasing-dispersion equation and the analytical solution, in which the duration of release t_s= 0.1 hour.

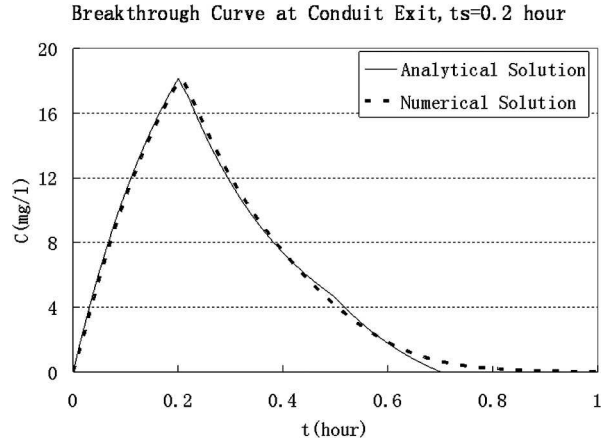

Figure 2. Same as Figure 1, except that t_s= 0.2 hour.

In the numerical example, solute and water are released from the matrix into a conduit, but no solute enters via a sinkhole. The analytical solution of this problem is presented as online supplementary documents to Li (2009a), while the numerical solution is sought by the implicit and stable Crank-Nicolson scheme (Li, 2004). Table 1 lists the parameters of the defined example, in which the cell Reynolds number is very small, which guarantees the accuracy of the numerical solution. Matches between the numerical solution and the analytical solution are plotted in Figures 1 through 5. The durations of release t_s in Figures 1 through 5 are 0.1, 0.2, 0.5, 2.0, and 6.0 hours, respectively. Because inequality $L_P \gg a$ is satisfied, the matches between the numerical solutions and the analytical solutions appear to be good. This numerical result verifies that the inequality $L_P \gg a$ is a sufficient condition, as showed by the preceding scale analysis.

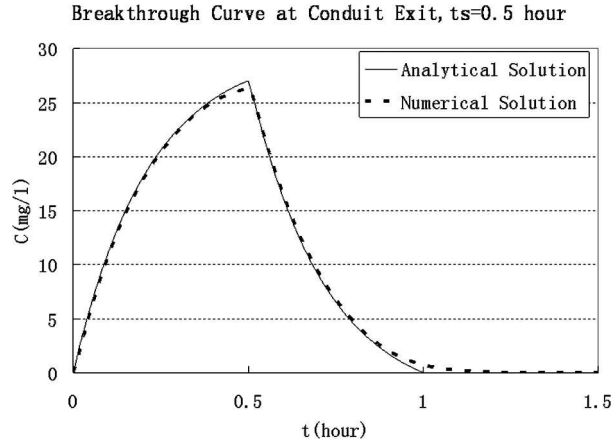

Figure 3. Same as Figure 1, except that t_s= 0.5 hour.

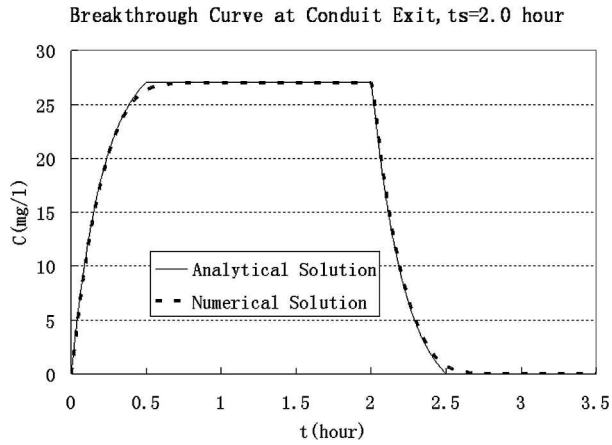

Figure 4. Same as Figure 1, except that t_s= 2.0 hours.

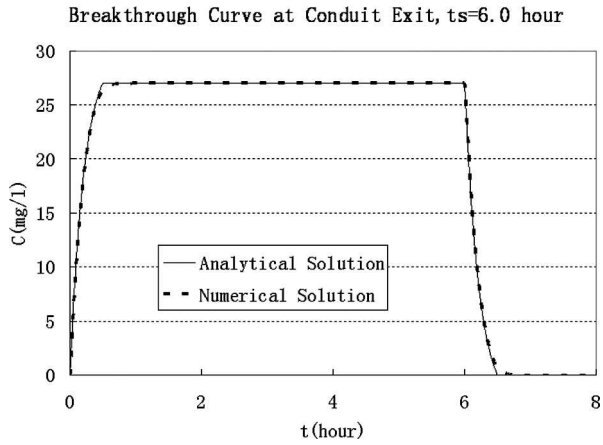

Figure 5. Same as Figure 1, except that t_s= 6.0 hours.

DISCUSSION

The results of our scale analysis of the significance of dispersion in mixing-transport in karst conduits are summarized in Table 2. For the dilution-dispersion equation that includes flux of water but not solute from the wall, a straightforward necessary and practically sufficient condition for neglecting conduit dispersion is $WT_B \gg a$. A potential application of this condition is the case where no contaminants are flowing from the matrix and the released matrix water dilutes contaminants entering via sinkholes, i.e., dye-tracing experiments.

Suppose that a dye-tracing experiment has a mean flow velocity (W_0) of 0.1 m s^{-1} and a conduit has a radius a of 1 m. In order to neglect conduit dispersion, a ratio of $a/WT_B = 0.01$ would require dye release to have a duration satisfying $T_B > 100a/W = 1000$ seconds. In other words, a dye trace with a release duration of tens of minutes would result in negligible conduit dispersion, and the dilution-transport model developed in Li (2009b) should be applicable. If applying that model yields an unreasonable overestimation of the conduit length and spring water flux, we would conclude that the drainage system most likely consists of a network of conduits, rather than a single conduit, or there is a strong interaction between conduit and matrix. Notably, vortices at conduit enlargements could contribute to greater dispersion than usual. To exclude that possibility, a dye-release duration up to several hours would be desirable to neglect conduit dispersion. Such a requirement is seldom satisfied when implementing dye-tracing experiments. Nevertheless, a long duration induced by rain events may mimic the suggested dye-input rate.

When there is solute flux being released from the matrix, things become more difficult to analyze because the inhomogenous term, i.e., the solute flux across the wall, complicates the releasing-dispersion equation so that scale analysis is more difficult to conduct. However, we nonetheless get the results listed in Table 2. A notable feature of the numerical solutions in Figures 1 through 5 is the long tail in the numerical solution, which is believed to result from variable conduit dispersion. Nevertheless, the tail caused by variable conduit dispersion is much smaller than that observed in field experiments; see Birk et al. (2005). This illustrates that retention in immobile-water region is a more important mechanism to produce tailing.

CONCLUSIONS

The mixing-transport of contaminants in a karst conduit can be described using a one-dimensional advection-dispersion equation incorporating fluxes of water and solute across the conduit wall. We call the equation without solute flux but with water flux across the wall the dilution-dispersion equation, while calling the equation with fluxes of water and solute across the wall the releasing-dispersion equation.

Scale analysis was performed to investigate the significance of dispersion in the dilution-dispersion equation. As dye-tracing experiments may be described with the equation, the result of our scale analysis has important applications to dye tracing experiments and similar physical processes, such as surface contaminants being carried into a sinkhole and transported in a conduit. A rule of thumb is that when and only when $a/WT_B \ll 1$, conduit dispersion can be ignored. This inequality, in conjunction with the dilution-transport model (Li, 2009b), provides us with a tool to investigate whether the drainage system under dye-tracing experiments mainly consists of a single conduit or a conduit network. More specifically, if applying the model results in an unreasonable estimate of conduit parameters such as the length, the conduit system is likely to consist of a network, or there is a strong interaction between conduit and matrix.

When contaminants sequestered in the rock matrix are released into the conduit, the process may be described with the releasing-dispersion equation. In this case, our scale analysis reveals that $L_P \gg a$ is a sufficient but not

Table 2. Results from our scale analysis of the significance of dispersion in mixing-transport in a karst conduit. Note that $WT_B \gg a$ is a practically sufficient condition for neglecting conduit dispersion in the dilution-dispersion equation.

Condition	Conduit Dispersion Neglected in Dilution-Dispersion Equation	Conduit Dispersion Neglected in Releasing-Dispersion Equation
$L_P^2 \gg D_c T_B$	Sufficient and Necessary	Sufficient and Unnecessary
$WT_B \gg a$	Necessary but not Sufficient	Neither Necessary nor Sufficient
$L_P \gg a$	Sufficient and Necessary	Sufficient and Unnecessary

necessary condition for neglecting conduit dispersion, which is verified by a preliminary numerical study. In reality, solute transport in karst conduits is a result of different interactive processes. If conduit dispersion can be shown to be negligible, we may be able to detect other mechanisms, such as retention in immobile water and multiple pathways, dominating the mixing-transport, thus being able to resolve different mechanisms. This is the primary aim of our study.

Acknowledgements

Financial support of this research was provided by the University Fund of Yunnan University under contract KL090020. The authors are deeply grateful to the Editor Malcolm S. Field, the Associate Editor Gregory S. Springer (who edited the paper for English usage), and two anonymous reviewers for their insightful comments and constructive suggestions.

References

Bear, J., 1972, Dynamics of Fluids in Porous Media, New York, Dover, 764 p.

Bear, J., Tsang, C-F., and de Marsily, G., 1993, Flow and Contaminant Transport in Fractured Rock, San Diego, Academic Press, 560 p.

Birk, S., Geyer, T., Liedl, R., and Sauter, M., 2005, Processed-based interpretation of tracer tests in carbonate aquifers: Ground Water, v. 43, no. 3, p. 381–388.

Clemens, T., Huckinghaus, D., Sauter, M., Liedl, R., and Teutsch, G., 1996, A combined continuum and discrete network reactive transport model for the simulation of karst development, *in* Calibration and Reliability in Groundwater Modeling: Proceedings of the ModelCARE 96 Conference: International Association of Hydrological Sciences Publ. 237, p. 309–318.

Dreybrodt, W., and Eisenlohr, L., 2000, Limestone dissolution rates in karst environments, *in* Klimchouk, A., Ford, D., Palmer, A., and Dreybrodt, W., eds., Speleogenesis, Evolution of Karst Aquifers, Huntsville, Ala., National Speleological Society, p. 136–148.

Field, M.S., and Pinsky, P.F., 2000, A two-region nonequilibrium model for solute transport in solution conduits in karstic aquifers: Journal of Contaminant Hydrology, v. 44, no. 3–4, p. 329–351.

Goldscheider, N., 2008, A new quantitative interpretation of the long-tail and plateau-like breakthrough curves from tracer tests in the artesian karst aquifer of Stuttgart, Germany: Hydrogeology Journal, v. 16, p. 1311–1317.

Kiraly, L., 1998, Modeling karst aquifers by the combined discrete channel and continuum approach: Bulletin du. Centre d'Hydrogeologie, v. 16, p. 77–98.

Li, G., 2004, Laboratory Simulation of Solute Transport and Retention in a Karst Aquifer [Ph. D. thesis], Tallahassee, Florida State University, 194 p.

Li, G., Loper, D.E., and Kung, R., 2008, Contaminant sequestration in karstic aquifers: Experiments and quantification: Water Resources Research, v. 44, W02429 p. doi:10.1029/2006WR005797.

Li, G., 2009a, Analytical solution of advective mixing in a conduit: Ground Water, v. 47, no. 5, p. 714–722. doi:10.1111/j.1745-6584.2009.00575.x.

Li, G., 2009b, Analytical solution of advective dilution of conduit flow. in preparation.

Millington, R.J., and Quirk, J.M., 1961, Permeability of porous solids: Faraday Transactions, v. 57, p. 1200–1207.

Shuster, E., and White, W., 1971, Seasonal fluctuations in the chemistry of limestone springs: A possible means for characterizing carbonate aquifers: Journal of Hydrology, v. 14, p. 93–128.

Tang, D.H., Frind, E.O., and Sudicky, E.A., 1981, Contaminant transport in fractured porous media: Analytical solution for a single fracture: Water Resources Research, v. 17, p. 555–564.

Taylor, G.I., 1954, The dispersion of matter in turbulent flow through a pipe: Proceedings of the Royal Society (London) A, v. 223, p. 446–468. doi:10.1098/rspa.1954.0130.

A. Vojtechovska, J. Bruthans, and F. Krejca – Comparison of conduit volumes obtained from direct measurements and artificial tracer tests. *Journal of Cave and Karst Studies,* v. 72, no. 3, p. 156–160. DOI: 10.4311/jcks2009es0095

COMPARISON OF CONDUIT VOLUMES OBTAINED FROM DIRECT MEASUREMENTS AND ARTIFICIAL TRACER TESTS

ANNA VOJTECHOVSKA[1], JIRI BRUTHANS[1], AND FRANTISEK KREJCA[2]

Abstract: An isolated phreatic loop in a natural cave was used to test the reliability of artificial-tracer tests for estimating the volume of a flooded karst conduit. The volume of a phreatic tube was measured by filling a drained phreatic loop with a constant inflow over a known time period. The volume of the phreatic loop is 190 ± 20 m^3, and it was compared to independent calculations of conduit volumes based on values based on tracer breakthrough curves. The best results were for mean transit time, where tracer-test calculations yielded volumes very similar to the volume obtained by direct filling of the loop. On the other hand, using the first-arrival time or peak time in the volume calculation resulted in considerable underestimation of the phreatic tube's volume, and these methods should be avoided except when breakthrough curves are affected by molecular diffusion. This demonstrates that volume estimation by tracer tests may be quite precise for common natural conduits, but results are strongly affected by the breakthrough-curve parameter chosen by the experimenter.

INTRODUCTION

Karst conduits are the primary drains of karst aquifers and act as fast groundwater-flow paths (Atkinson, 1977). Thus, understanding the hydrodynamic character of such conduits is important for understanding groundwater flow and hydraulic response propagation and for protection of groundwater sources in karst areas.

Quantitative tracer tests are typically used to estimate the basic characteristics of flooded karst conduits (Atkinson et al., 1973; Käss, 1998; Field, 2002; Goldscheider et al., 2008). Test results are used to approximate karst conduit volumes and mean cross-section areas (only the water-filled part of conduits is considered here). Such test results, especially if obtained for various flow rates, help to distinguish phreatic conduits (i.e., sumps) from vadose streams and are useful for estimating the static volume of conduits (Goldscheider et al., 2008). The maximum discharge and mean cross-sectional area of a conduit are used to estimate mean flow velocity at peak discharge. The velocities, combined with conduit geometries, are useful for studies of sediment-transport processes (Bruthans and Zeman, 2003). Moreover, the mean cross-sectional area is an important indicator for determining if sumps are large enough for divers to explore. Many different trace times are used to calculate conduit volumes (see below). But, unlike the case of artificial tubing, it is hard to test the reliability of volume estimates for natural karst conduits.

The purpose of this study was to compare the volume of a cave loop calculated from a tracer test with the volume measured by actually filling an empty sump. The study area is in Chýnov Cave, located 100 km south of Prague, Czech Republic, where it was possible to completely empty an isolated phreatic loop (sump) by pumping away the water.

CONDUIT DESCRIPTION

Chýnov Cave is situated in a thin layer of calcite-pure metamorphosed limestone. The cave contains an array of deep-phreatic conduits (*sensu* Ford and Ewers, 1978) and is traversed by a small stream with discharge varying between 6 and 13 L s^{-1}. We studied the Kaskady phreatic loop, which is a single underwater passage with a length of about 105 m and a maximum water depth of 11 m (Fig. 1). Cross-sections are variable (Fig. 1). Walls are undulating but not covered by scallops. The absence of scallops is attributed to predominantly slow flow rates. On the conduit's bottom there is about 30 m^3 of detritus and insoluble materials with particles diameters up to several tens of centimeters. Upstream and downstream of the phreatic loop the flow rates of the underground stream are similar, and no underwater inflows were observed on complete draining of the loop during a pumping test. Therefore, we consider the phreatic loop isolated from any significant water-filled fractures or matrix porosity, which would have yielded water into the emptied loop.

METHODS

The flow-rate through the loop was measured by timing the filling of a 50 L vessel. A tracer (NaCl) was injected directly into a stream cascade located at point IP (Fig. 1) to ensure good mixing of the tracer. A NaCl breakthrough curve was determined using electrical-conductivity measurement of the underground stream at SP (Fig. 1).

[1] Department of Hydrogeology, Engineering Geology, and Applied Geophysics, Faculty of Sciences, Charles University in Prague, Albertov 6, 128 43 Prague, Czech Republic, bruthans@natur.cuni.cz
[2] Management of Chýnov Cave, Dolní Hořice 54, 391 55 Chýnov, Czech Republic

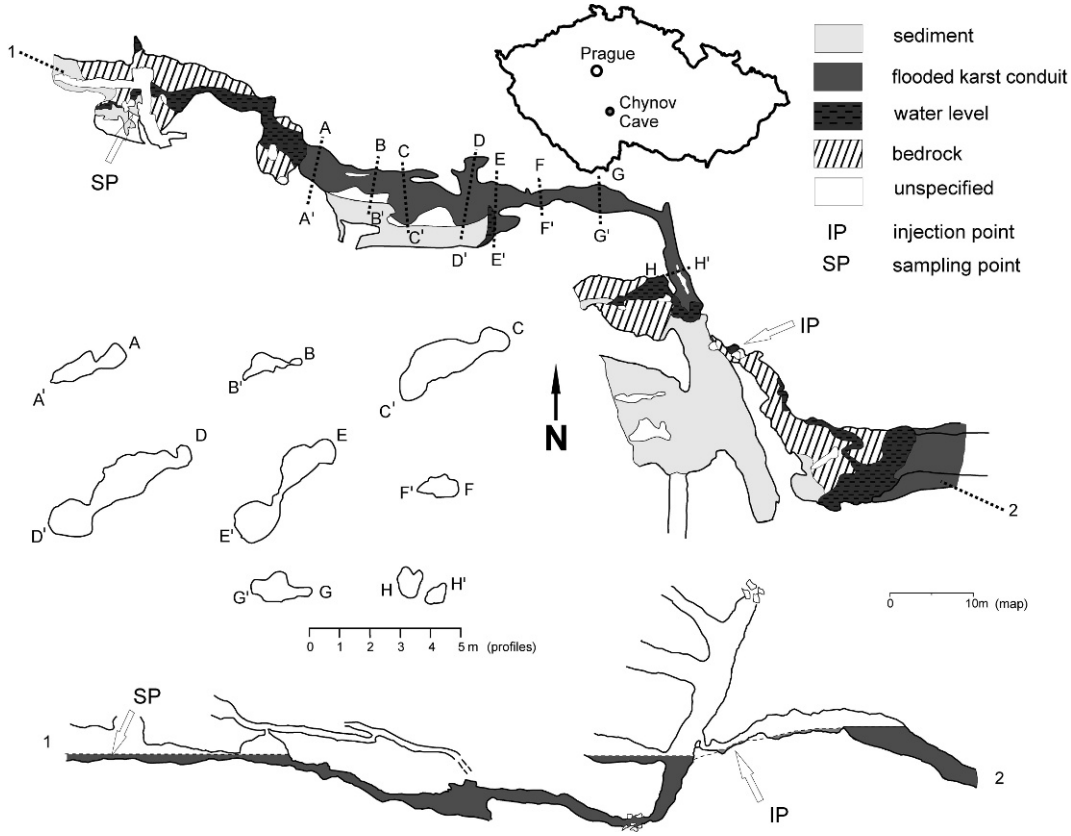

Figure 1. Map and projected vertical section of sump in Chýnov Cave (49°25′47.317″N, 14°49′57.576″E). Locations of injection of tracer (IP) and sampling point (SP) are indicated.

Measurements were made at one-minute intervals by a Cond 340i (WTW Co.) device equipped with a data logger. After the sodium chloride content decreased considerably from peak values (360 minutes after injection), the logging interval was changed to five minutes. The tracer test was monitored for 23 hours. Because conductivity is dependent on temperature, the water temperature was monitored as well. The temperature was stable during the tracer test (8.7 °C). In addition to logging conductivity, we collected water samples for analysis of Cl^- by argentometric titration. The relationship between the conductivity and measured the Cl^- content was linear ($R^2 = 0.999$) with a positive correlation between conductivity and the NaCl content in the water. The computer program Qtracer2 (Field and Nash, 1997; Field, 2002) was used to analyze the breakthrough curve, and the conduit volume was calculated as $V = Q \times t$, where Q is the stream flow rate or discharge (L s^{-1}) and t is time (s). It was possible to use a variety of times taken from the breakthrough curve, and we tested many of these (Fig. 2, Table 1).

After the tracer test, the water in the isolated phreatic loop was pumped out completely, and the phreatic loop was surveyed and documented (Fig. 1). The loop was allowed to refill, and the volume of the phreatic loop was calculated as $V_F = Q_F \times t_F$, where t_F is the time needed to fill the drained phreatic loop by inflowing water and Q_F is the measured inflow.

Results and Discussion

The volume of phreatic loop measured by refilling was 190 m^3 with an estimated error of ± 20 m^3) due to a 10% uncertainty in discharge. The measured breakthrough curve of the tracer test is depicted in Figure 3. The tracer arrived 116 minutes after injection and reached its maximum concentration 176 minutes after the injection. A relatively long tail was observed (Fig. 3). Tracer times are summarized in Table 1. We recovered 92% of the tracer mass, which shows that part of the tracer was apparently lost. If this was not just due to an error in discharge estimation, it might have been caused by a very long tail below our detection limit due to diffusion into the static water trapped in the detritus on the bottom of the sump.

Comparing the karst conduit's refilling volume (V_F) with calculations of conduit volumes based on timing of the tracer-breakthrough curve, the best breakthrough curve estimates are based on mean transit time, both centroid and half-recovery (Table 1). On the other hand, using first arrival time or peak time in volume calculation

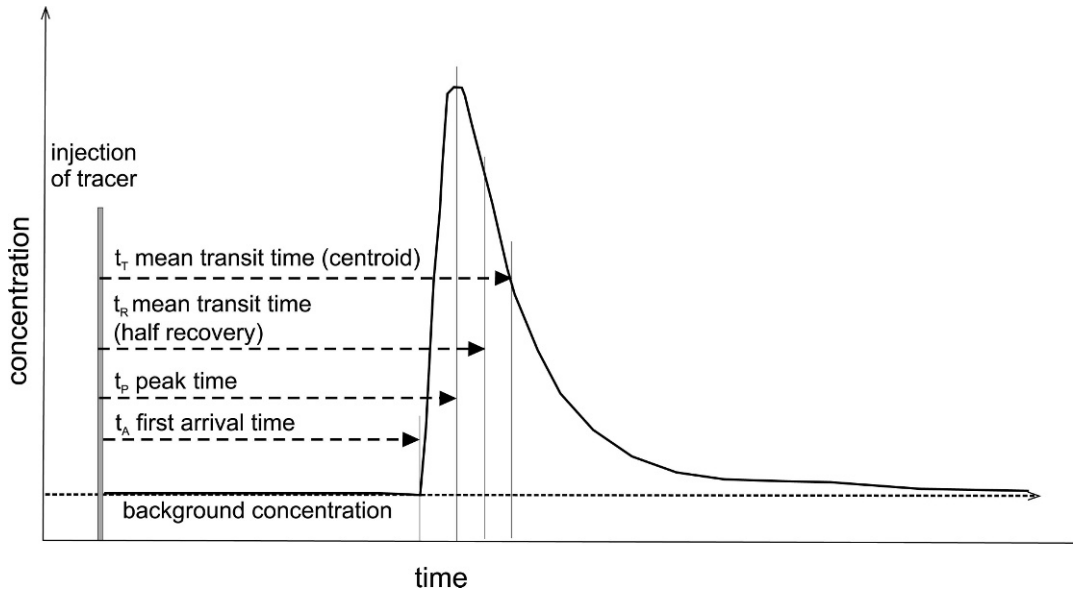

Figure 2. Definition of various times used in this paper for a hypothetical breakthrough curve. First arrival time is defined by raising the concentration of tracer well above the background. Peak time is defined by maximum concentration of the tracer. Mean transit time (half recovery) is defined by passage of 50% of tracer mass (background is subtracted). Mean transit time (centroid) is defined by centroid of the tracer (background is subtracted).

resulted in considerable underestimation of the conduit volume.

When the discharge from cave opening is constant, $V = Q \times t$ can be used to calculate its volume (Atkinson et al., 1973; Field and Nash, 1997). Estimates of cave volumes from tracer-test data have relied on various definitions of t. Atkinson et al. (1973), who assumed that water moves through the system like piston in a cylinder, used the peak time. Smart (1988), Field and Nash (1997), and Goldscheider et al. (2008) used the mean tracer transit time. The centroid generally lags behind the peak concentration of the tracer mass of the tracer-breakthrough curve (Fig. 2). On the other hand, Birk et al. (2004) used the first arrival or peak times as better measures of the conduit geometry than the mean tracer transit time because their calculation of conduit volumes was based on the assumption of plug flow conditions.

Thrailkill et al. (1991) suggests that average velocity is probably best calculated from the centroid of the breakthrough curve (mean transit time). However, because of the skew of the breakthrough curve, the position of the

Table 1. Times and corresponding calculated volumes of flooded parts of phreatic loop in Chýnov Cave. For explanation see the text and Figure 2.

Time	Minutes after Injection	Corresponding Volume (m^3)	Comparison with True Volume (%)
Real volume (pumping)	NA	190	100
t_A = first arrival time	116	85	45
t_P = peak time	176	129	68
t_{R1} = mean transit time (recovery 46% of injected tracer; 50% of recovered tracer)	231	169	89
t_{R2} = mean transit time (recovery 50% of injected tracer)	242	177	93
t_T = mean transit time (centroid- no extrapolation)	290	212	112
t_T = mean transit time (centroid - extrapolation)	291–310	213–227	112–119

NA = not applicable.

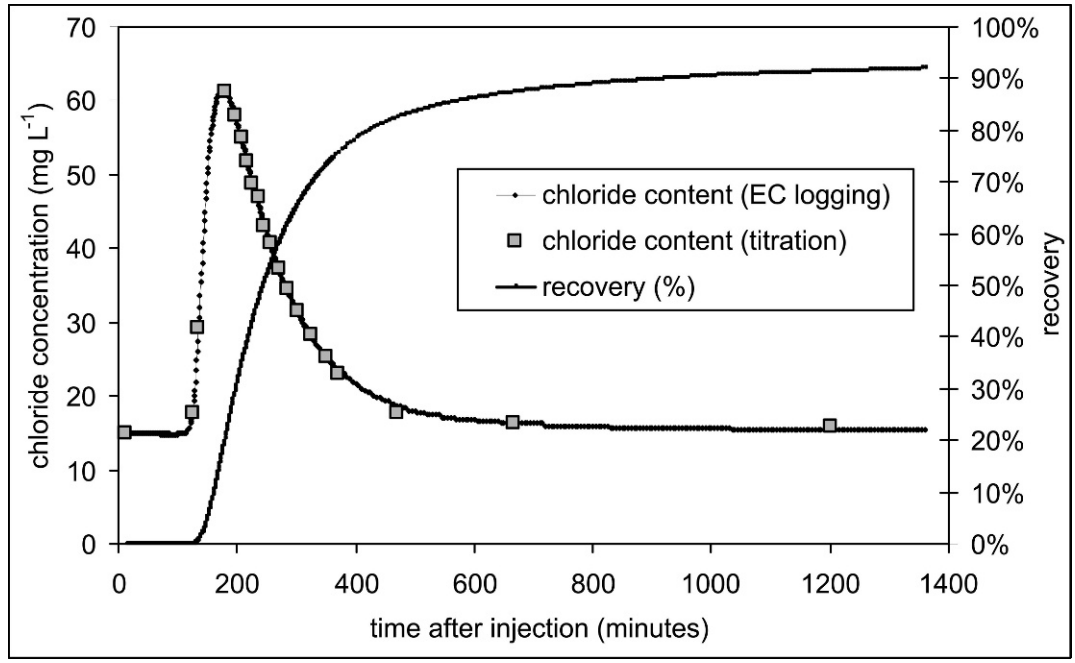

Figure 3. Chloride concentration based on argentometric titration and conductivity logging.

centroid is quite sensitive to the concentrations in the tail extending to longer times. Käss (1998) found that where breakthrough curves had very long tails (slightly increased concentration for a long time after the maximum concentration), the mean transit time is unsuitable. In such a case, the peak time may lead to better volume estimation. This is important for breakthrough curves affected by molecular diffusion into immobile water (mainly long-lasting breakthrough curves, several months and more, e.g., Goldscheider et al., 2003). In such case, the mean transit time may be considerably increased by exchange with immobile water, and thus, overestimates the volume of mobile water in the conduit.

In case of common karst conduits, where the flow at the injection point (Q_1) is often considerably smaller relative to the sampling point (Q_2), the conduit volume V is $Q_1 \times t < V < Q_2 \times t$, where Q is the stream flow rate or discharge and t is the mean tracer transit time. This is applicable if bifurcation (diversion of part of water outside the conduit) can be excluded based on nearly complete tracer recovery. If all adjoining conduits are similar to the conduit into which the tracer was introduced, the volume of whole connecting conduit system will be approximately equal to $Q_2 \times t$. On the contrary, if conduit flow is close to Q_1 for most of the underground path and only close to sampling point the conduit joins a stream with much higher discharge (Q_2), then the volume of conduit will be approximately equal to $Q_1 \times t$.

In case considerable diversion occurs (recovery far below 100%, no loss of tracer by other processes), the conduit volume V between injection and sampling point is $Q_1 \times t \times R < V$ where R is the ratio of tracer recovered at the sampling divided by tracer injected point. Diverging conduits are not counted into this volume.

In case that Q_1, Q_2, or both change over time, the discharge needs to be integrated over time to obtain conduit volume (Atkinson et al., 1973).

Conclusions

The isolated phreatic loop in a natural cave was used to test the reliability of tracer tests to estimate conduit volumes. The volume of a phreatic tube was measured by filling the drained phreatic loop by known discharge over known time period. Comparison of volume calculated from breakthrough curve data with the measured volume of karst conduit showed that volumes are best estimated using the mean transit time from a tracer test. In this case, the tracer test evaluation yielded conduit volumes very similar to the directly measured volume. This demonstrates that volume estimation by tracer tests may be quite precise for simple conduit geometries. On the other hand, using the first arrival or peak time in volume calculation will lead to a considerable underestimation of conduit volume compared to actuality and should be avoided except where breakthrough curves have extremely long tails.

Acknowledgements

Research was supported by institutional project No. MSM0021620855. Many thanks to Ondrej Jäger for help in the field and G.S. Springer, M. S. Field, A.L. Mayo, and a reviewer for very valuable suggestions for improving the manuscript.

REFERENCES

Atkinson, T.C., Smith, D.I., Lavis, J.J., and Whitaker, R.J., 1973, Experiments in tracing underground waters in limestones: Journal of Hydrology, v. 19, p. 323–349.

Atkinson, T.C., 1977, Diffuse flow and conduit flow in limestone terrain in the Mendip Hills, Somerset (Great Britain): Journal of Hydrology, v. 35, p. 93–110.

Birk, S., Liedl, R., and Sauter, M., 2004, Identification of localized recharge and conduit flow by combined analysis of hydraulic and physio-chemical spring responses (Urenbrunnen, SW Germany): Journal of Hydrology, v. 286, p. 179–193.

Bruthans, J., and Zeman, O., 2003, Factors controlling exokarst morphology and sediment transport through caves: Comparison of carbonate and salt karst: Acta Carsologica, v. 32, no. 1, p. 83–99.

Field, M.S., 2002, The QTRACER2 Program for Tracer Breakthrough Curve Analysis for Tracer Tests in Karstic Aquifers and Other Hydrologic Systems, Washington, D.C., U.S. Environmental Protection Agency, EPA/600/R-02/001, http://cfpub.epa.gov/ncea/cfm/recordisplay.cfm?deid=54930.

Field, M.S., and Nash, S.G., 1997, Risk assessment methodology for karst aquifers, (1) estimating karst conduit-flow parameters: Environmental Monitoring Assessment, v. 47, p. 1–21.

Ford, D.C., and Ewers, R.O., 1978, The development of limestone cave systems in the dimensions of length and depth: Canadian Journal of Earth Sciences, v. 15, p. 1783–1798.

Goldscheider, N., Hötzl, H., Käss, W., and Ufrecht, W., 2003, Combined tracer tests in the karst aquifer of the artesian mineral springs of Stuttgart, Germany: Environmental Geology, v. 43, p. 922–929.

Goldscheider, N., Meiman, J., Pronk, M., and Smart, C., 2008, Tracer tests in karst hydrogeology and speleology: International Journal of Speleology, v. 37, no. 1, p. 27–40.

Käss, W., 1998, Tracing Technique in Geohydrology, Rotterdam, Balkema, 581 p.

Smart, C.C., 1988, Quantitative tracing of the Maligne karst system, Alberta, Canada: Journal of Hydrology, v. 98, p. 185–204.

Thrailkill, J., Sullivan, S.B., and Gouzie, D.R., 1991, Flow parameters in a shallow conduit-flow carbonate aquifer, Inner Bluegrass Karst Region, Kentucky, USA: Journal of Hydrology, v. 129, p. 87–108.

L. Espinasa, S. Furst, T. Allen, and M.E. Slay – A new genus of the subfamily Cubacubaninae (Insecta: Zygentoma: Nicoletiidae) from caves in south-central and southwestern USA. *Journal of Cave and Karst Studies,* v. 72, no. 3, p. 161–168. DOI: 10.4311/jcks2009lsc0097

A NEW GENUS OF THE SUBFAMILY CUBACUBANINAE (INSECTA: ZYGENTOMA: NICOLETIIDAE) FROM CAVES IN SOUTH-CENTRAL AND SOUTHWESTERN USA

Luis Espinasa[1], Stephen Furst[1], Thomas Allen[2], and Michael E. Slay[3]

Abstract: The genus *Speleonycta* is erected, and *S. ozarkensis*, n. sp., is described and separated from other species of the subfamily Cubacubaninae. The type species was collected from several caves in the Ozark Plateau, while two more species, collected from a cave in Arizona and from a cave in California, remain under study. Morphology and preliminary analyses using histone DNA indicate that the new genus may be related to *Texoreddellia*, another nicoletiid from caves of Texas and northern Mexico.

Introduction

The subfamily Cubacubaninae in the hexapod family Nicoletiidae of silverfish is among the most important and common representatives of cave-adapted fauna in the Neotropics (Espinasa and Giribet, 2009), but they have a limited presence in caves of northern latitudes. Texas, where a species complex of at least six species in the genus *Texoreddellia* has been described (Espinasa and Giribet, 2009), appeared to be the northern limit of their distribution.

Nicoletiid specimens have been collected from several Ozark caves in Arkansas and Oklahoma. These collections are part of a larger and ongoing effort by The Nature Conservancy to conduct a comprehensive cave-fauna inventory, particularly in the caves of the southern Ozarks. These specimens represent a new genus of Nicoletiidae related to *Texoreddellia*. Despite being collected so sporadically, members of the new genus may actually have a wide distribution throughout the caves of the southwestern United States.

Materials and Methods

Dissections of holotypes were made with the aid of a stereo microscope and mounted as fixed preparations with Hoyer's solution. The remaining samples were left in a vial with ethanol. Illustrations were made with the aid of a camera lucida attached to a microscope. Specimens will be deposited in a collection at the American Museum of Natural History in New York.

Genomic DNA samples were extracted using Qiagen's DNEasy Tissue Kit by digesting a leg in lysis buffer from the paratype collected from Uno Cave, and from *Texoreddellia texensis* (Ulrich, 1902), *T. coahuilensis* Espinasa and Giribet, 2009, *T. aquilonalis* Espinasa and Giribet, 2009, and a specimen of the *T. texensis* species complex. Amplification and sequencing of the histone fragment was done as in Espinasa and Giribet (2009) following standard protocols and primers used in the past for nicoletiids. Chromatograms obtained from the automated sequencer were read and contigs made using the sequence editing software Sequencher 3.0. External primers were excluded from the analyses. Sequences were aligned with ClustalW2, and phylogram trees were obtained using PAUP 4.0 for neighbor-joining and parsimony-bootstrap method using heuristic search with 1,000 replicates.

Results and Discussion

Molecular data were obtained for one terminal from the specimen of Uno Cave (Table 1). The histone fragment was 328 bp long (primers excluded). Alignment with other species of the Cubacubaninae with ClustalW2 was trivial, as no gaps were needed. Both neighbor-joining and parsimony-bootstrap 50%-majority-rule consensus trees (Fig. 1A, B) showed the new species within a monophyletic group (90% bootstrap) with *Texoreddellia*. As such, the new species is granted exclusion from other genera of the Cubacubaninae. Nonetheless, the new species cannot be included within the *Texoreddellia* genus as it lacks the scales diagnostic of genus *Texoreddellia*. Furthermore, its sequence differs considerably (average of 52 bp; 15.8%) from the other species of *Texoredellia*, which is equivalent to the differences found among other genera of the Cubacubaninae, such as between *Squamigera*, *Prosthecina*, and *Anelpistina* (Fig. 1A). The specimens also have a unique appearance of the genital area not found in any other described species of the Cubacubaninae. Therefore, a new genus is proposed.

Speleonycta New Genus

Espinasa, Furst, Allen, and Slay

Diagnosis: A member of the subfamily Cubacubaninae without scales. Urosternum VIII of male flat posteriorly, without emarginations or projections in between the stylets of this segment. Paramera with a distal semi-eversible

[1] School of Science, Marist College, 3399 North Road, Poughkeepsie, NY 12601, luis.espinasa@marist.edu
[2] Academy of Natural Sciences, Philadelphia, PA
[3] Arkansas Field Office, The Nature Conservancy, 601 North University Avenue, Little Rock, AR 72705

Table 1. Nucleotide sequences of the histone from an individual from Uno Cave, Benton County, Arkansas, and four species of *Texoreddellia*. Asterisks reflect base position where all species shared the same nucleotide.

Species	DNA Sequence	Base Pairs
T. aquilonalis	TAGGAAGTCCACAGGAGGCAAGGCTCCTCGTAAACAGCTGGCAACGAAGGCAGCTCGCAA	60
T. texensis	TAGGAAGTCCACAGGAGGGAAAGCTCCTCGTAAACAGCTGGCAACGAAGGCAGCTCGCAA	60
T. coahulensis	TAGGAAGTCCACAGGAGGGAAAGCTCCTCGTAAACAGCTGGCAACGAAGGCAGCTCGCAA	60
Texoreddellia.sp.	-AGGAAGTCCACAGGAGGAAAAGCTCCTCGTAAACAGCTGGCAACGAAGGCAGCTCGCAA	59
S. ozarkensis	AAGAAAATCAACCGGAGGAAAAGCTCCGCGGAAGCAGTTGGCAACAAAGGCTGCTCGAAA	60
	** ** ** ** ***** ** ***** ** ** *** ******* ***** ***** **	
T. aquilonalis	GAGCGCCCCTGCCACTGGAGGAGTCAAAAAGCCACATCGCTACAGGCCAGGGACTGTAGC	120
T. texensis	GAGCGCCCCTGCCACTGGAGGAGTCAAAAAGCCACATCGCTACAGGCCAGGGACCGTAGC	120
T. coahulensis	GAGCGCCCCTGCCACTGGAGGAGTCAAAAAGCCACATCGCTACAGGCCAGGRACCGTAGC	120
Texoreddellia.sp.	GAGCGCCCCTGCCACTGGAGGAGTCAAAAAGCCACATCGCTACAGGCCTGGGACCGTAGC	119
S. ozarkensis	GAGCGCTCCCGCCACTGGAGGAGTCAAGAAACCCCATCGCTACAGGCCTGGAACCGTAGC	120
	****** ** ***************** ** ** ************** ** ** *****	
T. aquilonalis	TCTGAGGGAAATCAGGAGATACCAAAAGAGCACCGAGCTCCTCATTAGGAAGCTGCCCTT	180
T. texensis	TCTGAGGGAAATCAGGAGATACCAAAAGAGCACCGAACTCCTCATTAGGAAGCTGCCCTT	180
T. coahulensis	TCTTAGGGAAATCAGGAGATACCAAAAGAGCACCGAGCTCCTCATTAGGAAGCTGCCCTT	180
Texoreddellia.sp.	TCTGAGGGAAATCAGGAGATACCAAAAGAGCACCGAACTCCTCATTAGGAAGCTGCCCTT	179
S. ozarkensis	TCTGAGAGAGATCAGGAGATACCAGAAGAGCACGGAGCTTCTCATAAGGAAACTTCCCTT	180
	*** ** ** ************** ******** ** ** ***** ***** ** *****	
T. aquilonalis	CCAGCGGCTTGTCCGGGAAATAGCCCAGGATTTCAAAACTGATCTTCGGTTCCAGAGCTC	240
T. texensis	CCAGCGGCTTGTCCGGGAAATAGCCCAGGATTTCAAAACTGATCTTCGGTTCCAGAGCTC	240
T. coahulensis	CCAGAGGCTTGTCCGGGAAATCGCACAGGATTTCAAAACTGATCTGCGGTTCCAGAGCTC	240
Texoreddellia.sp.	CCAGCGGCTTGTCCGGGAAATAGCACAGGATTTCAAAACTGATCTTCGGTTCCAGAGCTC	239
S. ozarkensis	CCAGCGGCTGGTTAGGGAGATTGCTCAGGATTTCAAAACTGACCTTCGCTTCCAGAGCTC	240
	**** **** ** **** ** ** ****************** ** ** **********	
T. aquilonalis	TGCCGTCATGGCATTGCAGGAAGCTAGTGAGGCTTACTTGGTGGGGCTATTTGAGGACAC	300
T. texensis	TGCCGTCATGACATTGCAGGAAGCTAGTGAGGCTTACTTGGTGGGGCTATTTGAGGACAC	300
T. coahulensis	TGCCGTCATGGCATTGCAGGAAGCTAGTGARGCYTACTTRGTGGGGCTATTTGAGGACAC	300
Texoreddellia.sp.	TGCCGTCATGGCATTGCAGGAAGCTAGTGAGGCTTACTTGGTGGGGCTATTTGAGGACAC	299
S. ozarkensis	TGCAGTAATGGCTCTCCAAGAGGCWAGCGAGGCRTACTTGGTAGGCCTTTTTGAGGATAC	300
	*** ** *** * * ** ** ** ** ** ** ** ***** ** ** ** ******** **	
T. aquilonalis	CAACCTGTGCGCCATCCACGCCAAGCGA	328
T. texensis	CAACCTG----------	307
T. coahulensis	TAACCTGTGCGCCATCCATGCYAAGCGA	328
Texoreddellia.sp.	TAACCTGTGCGCCATCCATGCCAAGCGA	327
S. ozarkensis	CAACCTGTGTGCAATTCAYGCCAAACGA	328
	******	

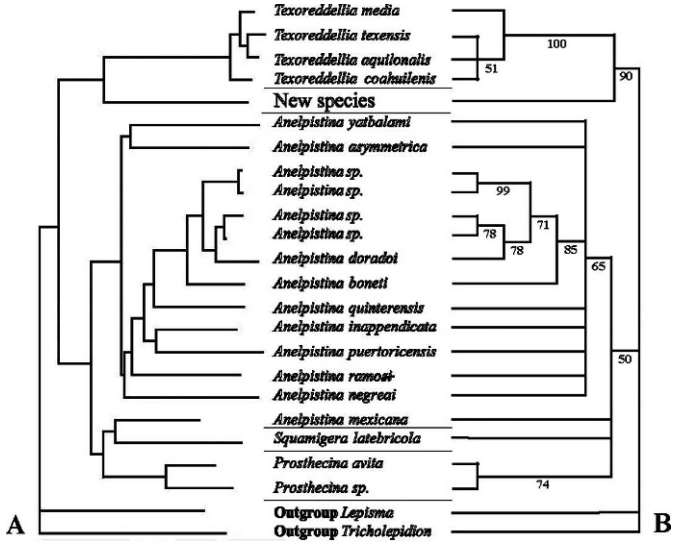

Figure 1. Distance and parsimony phylogram trees from histone-sequence data produced very similar topologies in which the new species is within a monophyletic group with *Texoreddellia* at the exclusion from other genera of the Cubacubaninae. A. Neighbor-joining; notice that the new species differs from the other species of *Texorredellia* by a distance equivalent to the differences found between the other genera *Squamigera*, *Prostecina*, and *Anelpistina*. B. Parsimony bootstrap 50%-majority-rule consensus trees.

vesicle and very long and specialized chaetae, their length being half or more the width of the paramera.

Description: Pedicellus of adult male with unicellular glands and with a blade-like spine not too scleritized. Mouthparts not specialized. Mandible strongly sclerotized apically with usual teeth. Galea apically with sensory pegs. Lacinia heavily sclerotized distally. First process of lacinia pectinate. Labium without prominent lateral lobes.

Tarsi with four articles. Praetarsi with three simple claws. Median claw glabrous, slender, and smaller than lateral claws. Urosterna II-VII subdivided into two coxites and one sternite. Urosterna VIII and IX of male entire. Median portion of sternites with 1 + 1 sublateral macrochaetae at hind borders, as well as 1 + 1 macrochoetae near suture at about middle of segment. Coxites on segments II–IX with stylets. Eversible vesicles on segments II-VI, pseudovesicles on VII. Urosterna III and IV of adult males apparently without modifications. Urosternum VIII of male straight posteriorly, without emarginations or projections in between the stylets of this segment. Tergum X with several subequal macrochaetae on posterior angles.

Point of insertion of paramera apparently not too deep. Paramera with a distal semi-eversible vesicle, somewhat similar to *Texoreddellia* (Wygodzinsky, 1973). Specialized chaetae very long, their length being half or more the width of the paramera. Stylets IX apparently without spines in males as seen in some species of *Prosthecina* or in *Anelpistina mexicana*, although some of the dorso-ventral macrochaetae may be scleritized. Opening of penis longitudinal. Cercus of male with sensory pegs. Appendix dorsalis without sensory pegs. Female with a subgenital plate.

Type species: *Speleonycta ozarkensis*, n. sp.

Etymology: From speliaon = Greek for cave and nycta = Greek for night. It references in Greek mythology the occupation of caves by Nyx, the primordial goddess of night.

Remarks: *Speleonycta* belongs to the Cubacubaninae (Mendes, 1988), characterized by subdivided abdominal sterna II-VII and fused coxites of abdominal segments VIII and IX. *Speleonycta* is distinguished from all other genera of this subfamily by the very long and specialized chaetae on the paramera. The type species of the new genus shares some characteristics with *Texoreddellia*, such as the paramera with semi-eversible vesicles, urosternum VIII of male straight posteriorly without emarginations or projections in between the stylets of this segment, and a blade-like spine in the pedicellus. None of these characteristics are present in any other of the genera of Cubacubaninae.

The new genus can easily be distinguished from *Texoreddellia* and *Squamigera* (Espinasa, 1999) by the absence of scales; from *Allonicoletia* (Mendes, 1992) by the presence of stylets on urosternite II; from *Prosthecina* (Silvestri, 1933) by the absence of conspicuous lateral lobes bearing numerous glandular pores in the submentum; from *Anelpistina* Silvestri, 1905 (= *Cubacubana* Wygodzinsky and Hollinger, 1977; syn. = *Neonicoletia* Paclt, 1979) as defined by Espinasa et al. (2007), by its urostenum VIII without emarginations or projections in between the stylets of this segment and its distinctive paramera.

Distribution: Specimens of this genus have been collected from Ozark caves in Arkansas and Oklahoma, and also from Arkenstone Cave, in Arizona, and Clough Cave, in California. The Arizona and California specimens are undescribed species currently under study. Specimens from both localities are clearly within the new genus, despite being geographically distant. Members of the new genus may actually have a wide distribution throughout the caves of the southern United States, despite being collected so sporadically.

Speleonycta ozarkensis Espinasa, Furst, Allen, and Slay

New Species (Figs. 2A–G, 3A–F, 4A–G)

Material: Holotype Oklahoma; Cherokee County, Single Barrel Cave (♂, body ~11 mm, tarsus 3rd leg 1.35 mm, 7/28/05, G. O. Graening and M. E. Slay col.). Paratypes: Arkansas; Benton County: Bear Hollow Cave (♀, 9 mm, no third leg, 12/7/00, M. E. Slay and G. O. Graening col.), and Uno Cave (♂, body 11mm, tarsus third leg 1.35 mm, 12/2/05, R. Rylee col.). Oklahoma; Delaware County: Black Hollow Cave (♀, body 12 mm, tarsus 3rd leg 1.5 mm, 7/29/05, G. O. Graening and M. E. Slay col.). All

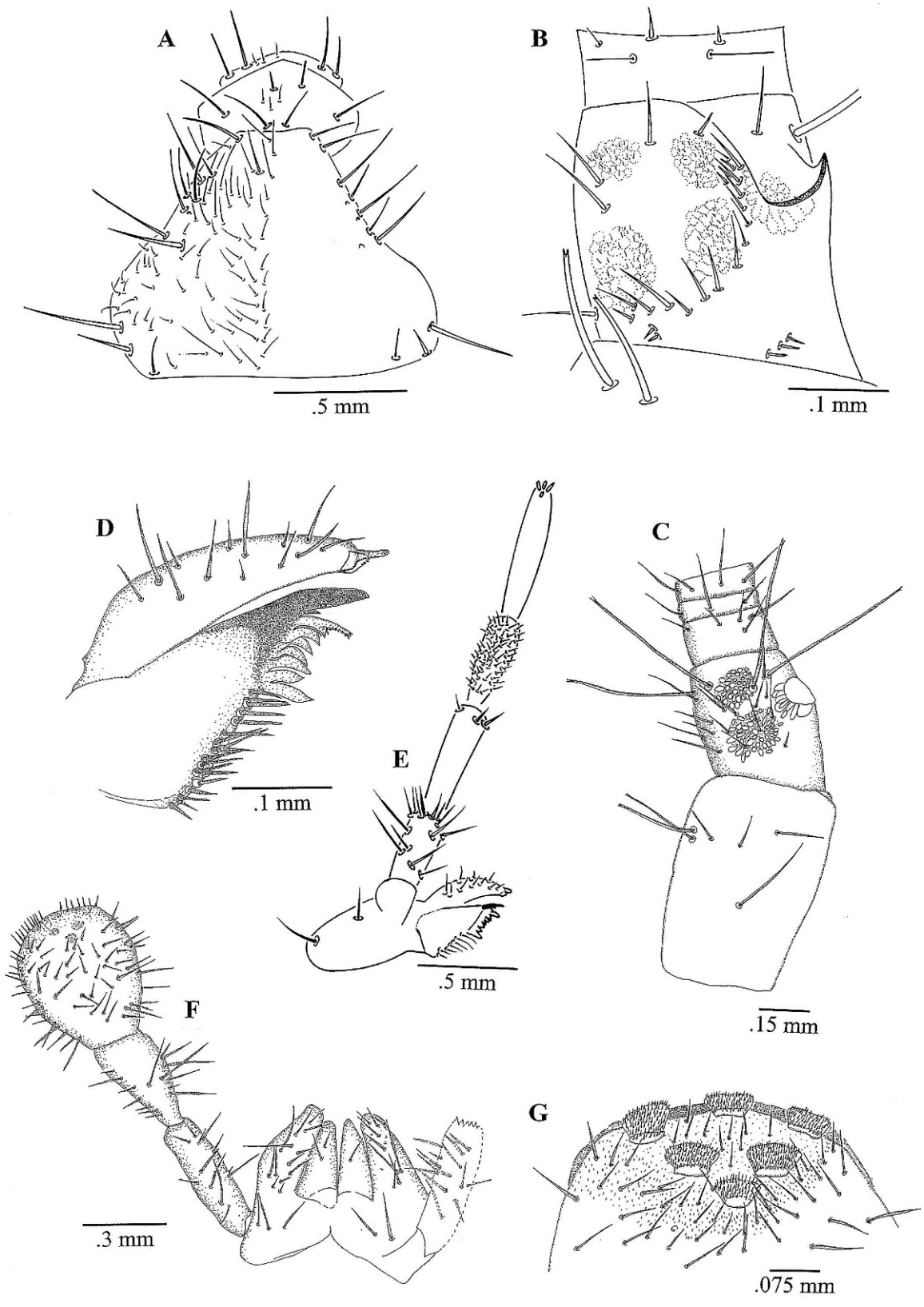

Figure 2. ***Speleonycta ozarkensis*** **n. sp., male. Microchaetae partially shown. A, head. B, pedicellus. C, base of antennae. D, galea and lacinia. E, maxilla. F, labium. G, apex of labial palp.**

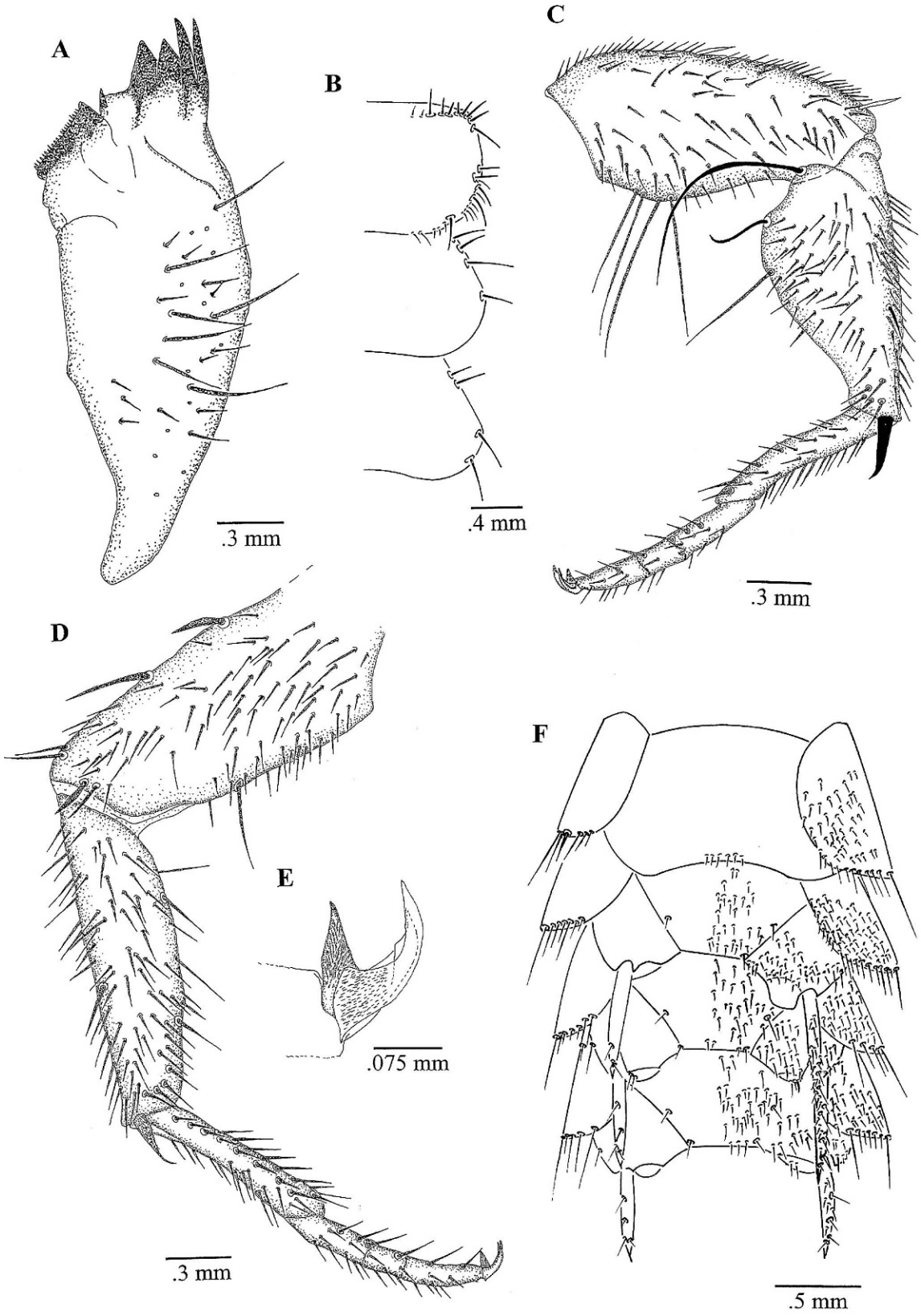

Figure 3. ***Speleonycta ozarkensis*** **n. sp., male. Microchaetae partially shown. A, mandible. B, thoracic nota. C, second leg. D, third leg. E, claws and endopodium. F, urosterna I–IV.**

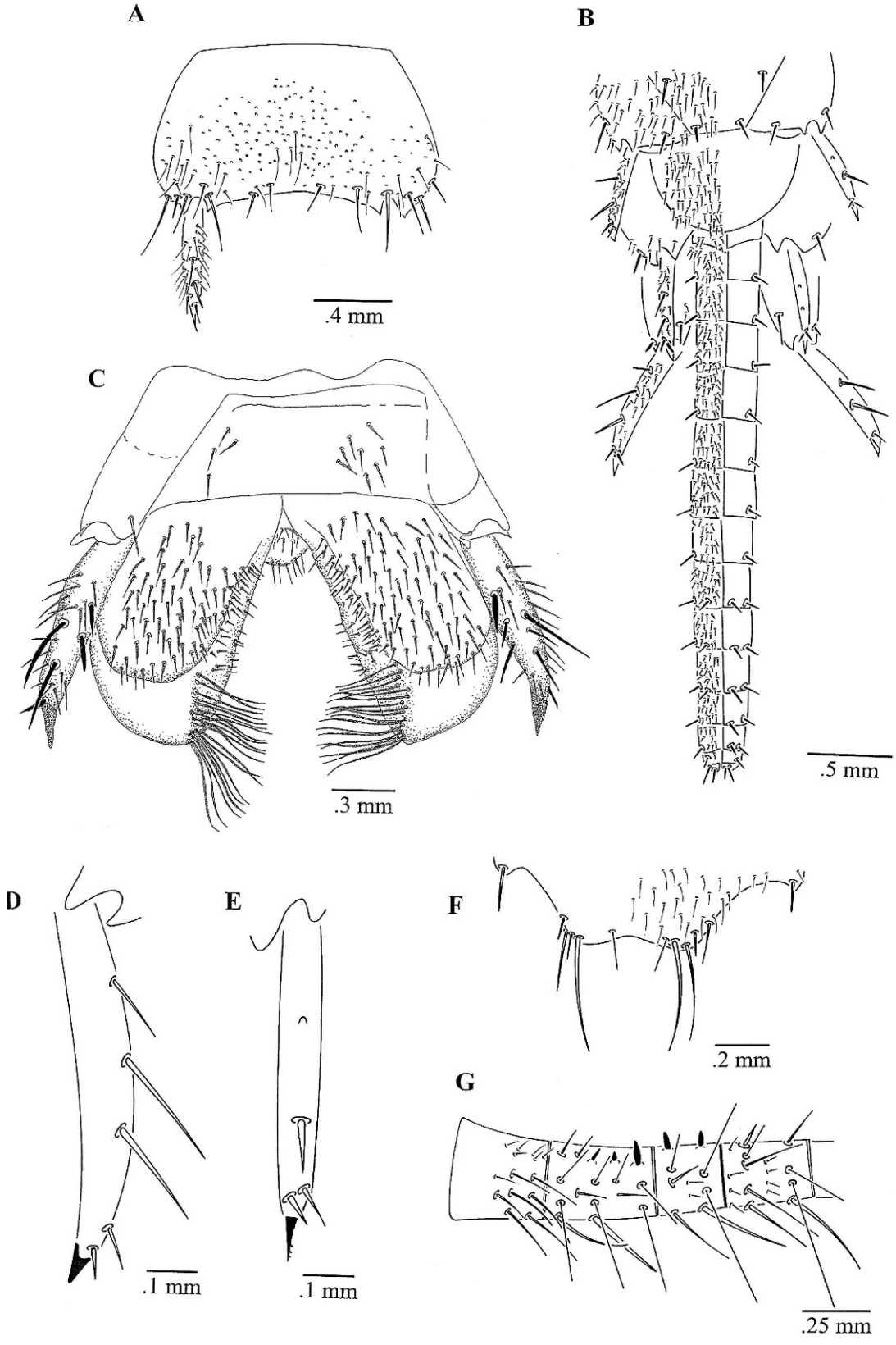

Figure 4. ***Speleonycta ozarkensis*** **n. sp., A, C–G, male. B, female. Microchaetae partially shown. A, urotergum VIII. B, ovipositor. C, genital area. D, stylets IX. E, stylets VIII. F, uroterguite X. G, cercus.**

caves, despite multiple collecting trips, have yielded only a single individual.

Description: Maximum body length of samples 12 mm. Antennae and caudal appendages broken in all specimens; their maximum conserved length was 1 mm and 0.5 mm, respectively. General color light yellow to white.

Head with macrochaetae and microchaetae as shown in Figure 2A, with about eight macrochaetae on border of insertion of antennae. Pedicellus of male shorter than first article and with clusters of unicellular glands. Four ventral clusters are bordered with a not very conspicuous row of microchaetae forming a *U*, and on outer border, a blade-like spine not very sclerotized and with more unicellular glands at its base (Fig. 2B, C). Basal articles of antennae of female simple.

Mouthpart appendages short, especially when compared with other cave nicoletiid species. Maxilla as shown in Figures 2D and 2E. Last article 1.5 times longer than penultimate. Apex of galea with two conules, one longer than wide and the other wider than long (Fig. 2D). Two teeth on lacinia. Labial palp as in Figures 2F and 2G, apical article distinctly longer than wide and longer than the next to last article. Penultimate article with a not very distinct bulge containing two macrochaetae. Labium and first article of the labial palp with macrochaetae. Mandible chaetotaxy as in Figure 3A, with many macrochaetae. Pro-, meso-, and metanota with several macrochaetae on postero-lateral margins, apart from several setae of varied sizes (Fig. 3B). Legs of medium size, hind tibia approximately 3.5 times longer than wide and slightly shorter than tarsus (Fig. 3D). On male holotype, tibia of second leg very stout (2 times longer than wide) with a large bulge with 3 distinctly long, sclerotized, and curved macrochaetae (Fig. 3C). Female legs simple. Claws short and with a hairy appearance (Fig. 3E) similar to other *Anelpistina* (Espinasa et al., 2007).

Abdominal sterna as in Figure 3F. Urosternum III and IV without modifications. Posterior margin of urosternum VIII of male straight, without emarginations or projections in between the stylets of this segment (Fig. 4A). Urosternum IX of male as in Figure 4C. Point of insertion of paramera in urosternum IX slightly below level of base of the stylets of this segment (Fig. 4C). Base of internal faces of coxal processes with one slightly sclerotized macrochaeta (Fig. 4C). Penis and paramera as in Figure 4C. Paramera very stout, with a distal semi-eversible vesicle, somewhat similar to *Texoreddellia* (Wygodzinsky, 1973), and with long specialized macrochaetae. Paramera attain apex of stylets IX.

Stylets IX stout and without small teeth on robust terminal spine. Stylets IX larger than others, without sensory cones, but dorso-ventrally with sclerotized macrochaetae (Fig. 4C). Ventrally with about three macrochaetae and an extra subapical pair (Fig. 4D). Other stylets have a terminal spine with small teeth and with about two macrochaetae and an extra subapical pair (Fig. 4E). Urotergite X protruding, shallowly emarginate in both sexes, posterior angles with several macrochaetae and a few relatively strong setae (Fig. 4F). Length of inner macrochaetae slightly longer than the distance between them.

Cercus of adult male straight, with several subequal annuli slightly longer than wide. Sensory pegs on second and third articles. Some pegs slightly bigger than others (Fig. 4G). Appendix dorsalis without sensory pegs. Female cercus and appendix dorsalis simple.

Subgenital plate of female rounded (Fig. 4B) to subparabolic. Ovipositor in largest adult female (12 mm) surpasses apex of stylets IX by 2 times the length of stylets (Fig. 4B). Gonapophyses with 15 or 16 annuli.

Postembryonic development: Both males were of same length (~11 mm) and had similar development in pedicellus and genital area. The male from Uno Cave had neither second legs nor cerci, so it is unknown if the three distinct macrochaetae are present in the legs or the pegs on the cerci. In both females (12 mm and 9 mm), ovipositor surpassing apex of stylets IX by 2 times the length of stylets.

Etymology: *ozarkensis*; Derived from the word Ozarks, the region where the species was discovered.

Remarks and distribution: Other nicoletiid specimens have been collected from Newton County (Tweet's Cave 10/21/01 and Wolf Creek Cave 11/11/00) in Arkansas and Delaware County (McGee's Cave 8/31/01) in Oklahoma, but were not available for examination. It is likely they belong to the same species. If so, the seven caves with the new species span about 100 miles from the Ozark Plateau. It is likely that the species is endemic to the cave systems of this karstic area. Despite multiple collecting trips, all caves have yielded only a single individual. Specimens of the different caves are at different stages of their postembryonic development, as well as being either male or female. The scarcity of specimens per population makes it difficult to determine how much of the variability is due to variation among populations, rather than to species differences.

Until recent studies, multiple cave populations of *Texoreddellia* spanning over 200 miles of Texan karst were assumed to be all included within a single species. It was not until molecular data were available that it was established they are in reality a complex of at least six closely related species (Espinasa and Giribet, 2009). DNA sequences in the new genus are available for only a single individual of a single locality. Until more specimens can be collected or more molecular data obtained, the possibility that this species is actually a complex of closely related species remains open.

Acknowledgments

We thank Nina Parker, chair of the Biology Department, Shenandoah University, for supporting the sequencing and the School of Science of Marist College for supporting the field expenses of one of us (SF) and the

publication of the manuscript. We thank Steve Hensley and Richard Stark (Oklahoma United States Fish and Wildlife Service), Bill Puckett (Poteau Public School District), Rhea Rylee (Arkansas United States Forest Service), The Nature Conservancy (Oklahoma Field Office, Arkansas Field Office), and several private landowners for facilitating and allowing access to these sites and others to look for additional specimens. Additional funding was provided by United States Fish and Wildlife Service (Oklahoma and Arkansas), United Stated Forest Service (Arkansas), Arkansas Game and Fish Commission, and The Nature Conservancy.

References

Espinasa, L., 1999, A new genus of the subfamily Cubacubaninae (Insecta: Zygentoma: Nicoletiidae) from a Mexican cave: Proceedings of the Biological Society of Washington, v. 112, no. 1, p. 52–58.

Espinasa, L., Flick, C., and Giribet, G., 2007, Phylogeny of the American silverfish Cubacubaninae (Hexapoda : Zygentoma : Nicoletiidae): a combined approach using morphology and five molecular loci: Cladistics, v. 23, no. 1, p. 22–40.

Espinasa, L., and Giribet, G., 2009, Living in the dark — species delimitation based on combined molecular and morphological evidence in the nicoletiid genus *Texoreddellia* Wygodzinsky, 1973 (Hexapoda: Zygentoma: Nicoletiidae) in Texas and Mexico, *in* Cokendolpher, J.C., and Reddell, J.R., eds., Studies on the Cave and Engogean Fauna of North America, Part V, Austin, Texas Memorial Museum Speleological Monographs 7, p. 87–100.

Mendes, L.F., 1988, Sur deux nouvelles Nicoletiidae (Zygentoma) cavernicoles de Grèce et de Turquie et remarques sur la systématique de la famille: Revue Suisse de Zoologie, v. 95, no. 3, p. 751–772.

Mendes, L.F., 1992, Novos dados sobre os tisanuros (Microcoryphia e Zygentoma) da América do Norte: Garcia de Orta Serie de Zoología, v. 16, no. 1–2, p. 171–193.

Paclt, J., 1979, Neue Beiträge zur Kenntnis der Apterygoten-Sammlung des Zoologischen Instituts und Zoologischen Museums der Universität Hamburg. VI. Weitere Doppel- und Bortenschwänze (Diplura: Campodeidea: Thysanura: Lepismatidae und Nicoletiidae): Entomologische Mitteilungen aus dem zoologischen Museum Hamburg, v. 6, no. 105, p. 221–228.

Silvestri, F., 1905, Materiali per lo studio dei Tisanuri. VI. Tre nuove specie di *Nicoletia* appartenenti ad un nuovo sottogenere: Redia (Firenze), v. 2, p. 111–120.

Silvestri, F., 1933, Nuovo contributo alla conoscenza dei Tisanuri del Messico: Bolletino del Laboratorio di Zoología general e agraria di Portici, v. 27, p. 127–144.

Ulrich, C.J., 1902, A contribution to the subterranean fauna of Texas: Transactions of the American Microscopical Society, v. 23, p. 83–101.

Wygodzinsky, P., 1973, Description of a new genus of cave Thysanuran from Texas (Nicoletiidae, Thysanura, Insecta): American Museum Novitates, no. 2518, p. 1–8.

Wygodzinsky, P., and Hollinger, A.M., 1977, A study of Nicoletiidae from Cuba (Thysanura), *in* Orghidan, T., Núñez Jiménez, A., Decou, V., Negrea, Şt., and Viña Bayés, N., eds., Résultats des Expéditions Biospéleologiques Cubano-Roumaines à Cuba, volume 2, Bucharest, Editura Academiei Republii Socialiste România, p. 317–324.

J. Lario and V. Soler – Microclimate monitoring of Pozalagua Cave (Vizcaya, Spain): application to management and protection of show caves. *Journal of Cave and Karst Studies,* v. 72, no. 3, p. 169–180. DOI: 10.4311/jcks2009lsc0093

MICROCLIMATE MONITORING OF POZALAGUA CAVE (VIZCAYA, SPAIN): APPLICATION TO MANAGEMENT AND PROTECTION OF SHOW CAVES

JAVIER LARIO[1] AND VINCENTE SOLER[2]

Abstract: This paper reports the results of a continuous monitoring program carried out in Pozalagua show cave (Vizcaya, Spain) between April 2001 and June 2004. The study focused on understanding the variations in the microclimatic parameters inside the cave to assess the effect of visitors and to design a visitor regime to minimize impact and optimize its carrying capacity. The main parameters susceptible to variations due to a massive influx of visitors are the internal temperature of the cave and the concentration of CO_2 in the cave air. Proposed management measures focus on reducing the human-induced variations of both parameters.

INTRODUCTION

Most show caves require physical modifications to allow visitor access. These modifications change the ventilation regimen, relative humidity, air temperature, and CO_2 in the cave environment (Hoyos et al., 1998; Pulido-Bosch et al., 1997; Fernández-Cortés et al., 2006a; Russel and MacLean, 2008). For example, increased condensation from respiration has been shown to cause a decline in air quality leading to degradation of speleothems (Pulido-Bosch et al., 1997; Sarbu and Lascu, 1997; Baker and Genty, 1998; Sanchez-Moral et al., 1999; Fernández-Cortés et al., 2006a, 2006b; Russell and MacLean, 2008). As has been pointed out by Russel and MacLean (2008), the effect of increased CO_2 exhaled by cave visitors is another parameter that has a major impact on show caves (Huppert et al., 1993; Gillieson, 1996; de Freitas, 1998; de Freitas and Banbury, 1999), since levels of CO_2 above 2400 ppm can potentially increase the deterioration of speleothems, and levels above 5000 ppm can be dangerous to humans (Kermode, 1979).

This paper presents the results of a continuous monitoring program carried out in Cueva de Pozalagua show cave between April 2001 and June 2004. The study focused on understanding the variations of the microclimatic parameters inside the cave to evaluate the effect of visitors, and on developing an optimum visitor regime to minimize the effect of those visitors on the cave by optimizing its carrying capacity. Previous results recorded for one year (2001–2002) were presented in Lario et al. (2005).

Any tourist area must consider the carrying capacity of the overall resource as essential to management of the environment (Cigna, 1993; Huppert at al., 1993; Hoyos et al.,1998; Mangin et al., 1999; Calaforra et al., 2003; Fernández-Cortés et al., 2006b), but some authors have also pointed out the difficulties of quantifying the carrying capacity, given the large number of variables involved and the subjectivity of some of these (Middaugh, 1977; Hammitt and Cole, 1987; Hoyos et al., 1998). In evaluating this capacity, the challenge lies in quantifying the acceptable limit for changes in a parameter in the karstic environment. The carrying capacity can be defined as the maximum number of visitors per unit of time that will maintain a critical factor or parameter within defined, natural limits. The parameter most susceptible to change will be the critical factor in calculating visitor capacity (Cigna, 1993; Hoyos et al., 1998).

Ideally, this type of study should begin with the installation of instrumentation to perform background monitoring of the cave prior to any alteration in the natural conditions and before any tourist activity. Almost one year of microenvironmental recording without human disturbance would be required (Sanchez-Moral et al., 1999; Michie, 2005). In this case, the study was initiated after some years of tourist activity and after some human modifications to the cave's natural environment, including the opening of the current entrance using explosives and the closing of two natural entrances to control access to the cave. It is, therefore, very difficult to establish the natural conditions of the cave prior to human visits. Consequently, in this study we use a relative background, which means the least-modified microclimate conditions due to tourism activity. This study only focuses on cave management as it is related to the effect of visitors on the cave's microclimate. Any other impact related to tourist activity in the cave has not been considered.

LOCATION AND GEOLOGICAL SETTING

Cueva de Pozalagua is located in the western part of the province of Biscay, northern Spain (Fig. 1) and is geologically located on the southern flank of the Carranza anticline, which is mainly made up of Urgonian limestone

[1] Facultad de Ciencias, Universidad Nacional de Educación a Distancia – UNED, Senda del Rey, 9, 28040 Madrid, Spain, javier.lario@ccia.uned.es
[2] Instituto de Productos Naturales y Agrobiología, CSIC. Avda.Astrofísico Fco. Sánchez, La Laguna, 38206 Tenerife, Spain

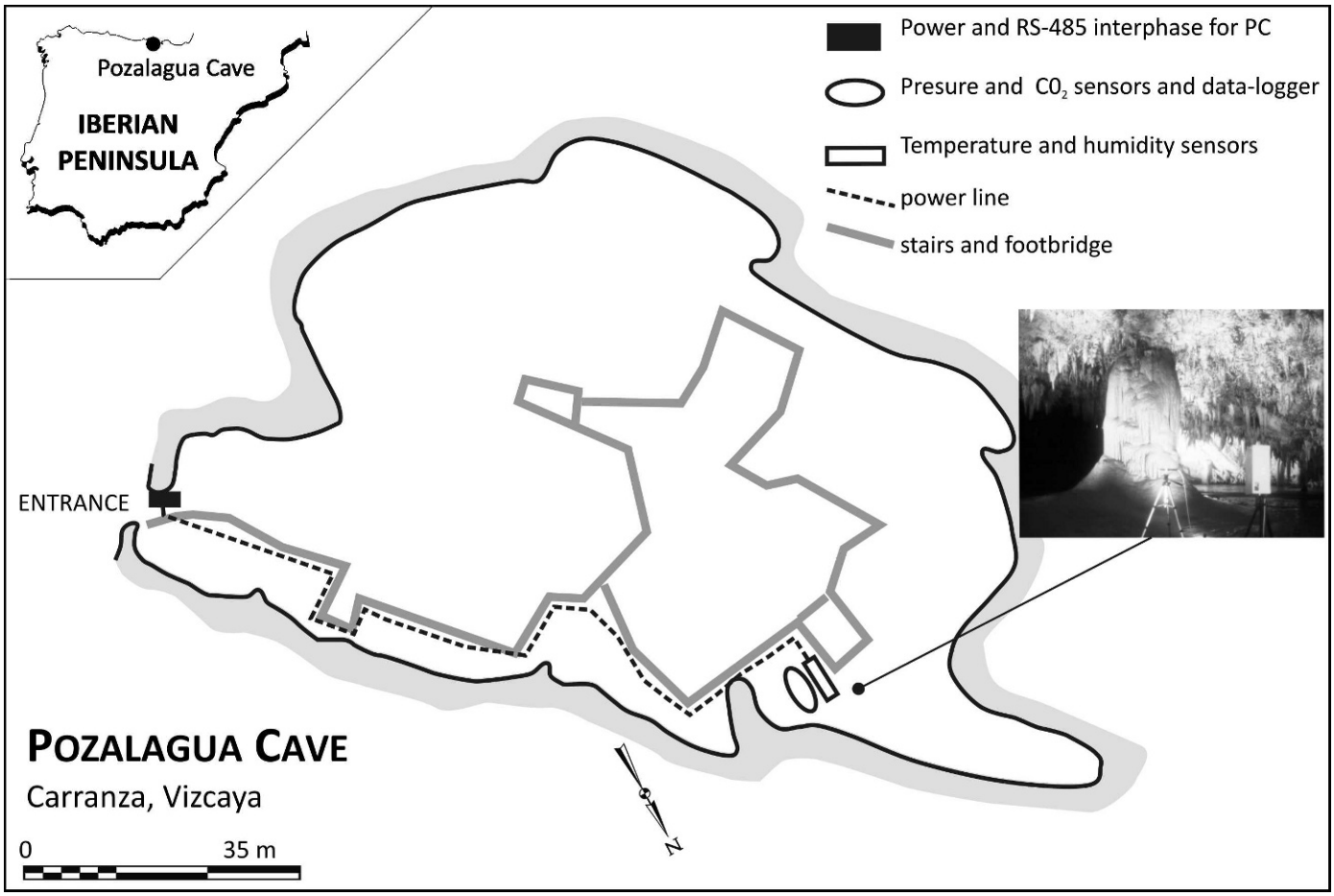

Figure 1. Location and plan map of Cueva de Pozalagua.

(IGME, 1978). The cave is part of a larger karstic system with an area of 15 km^2 (Ugarte, 1989).

The limestones that make up the Carranza karstic system have different compositions and textures, corresponding to a large extent to reef and para-reef limestones of the Urgonian facies (Jurassic-Cretaceous transition). These appear in great banks of massive or diffuse stratification, with approximately 1-m-thick individual white and black limestone layers, accompanied by breccias. In the fracture zones are irregular strips of calcification and dolomitization generated by the circulation of hydrothermal fluids. The limestone dips gently (15° to 20°) towards the southeast, and the dip is above 30° in some places in the fault zones. In the case of Pozalagua, the cave developed at the limestone and the dolomite contact generated by a fault striking N145°E where hydrothermal fluids have circulated.

Cueva de Pozalagua consists of a main chamber 125 m in length, 70 m in width, and 12 m of height (Fig. 1). The cave, due to the profusion of several phases of speleothems and the collapse of blocks, displays two levels with a difference of 4 to 5 m between them. At the present time, the entrance has a metal door and metal stairs descending 3 m. The public route through the cave is covered with a metal grid and a footbridge to the sides. Illumination is varied, with a system of cool-lights and warm-lights. The most attractive feature of the cavity is the large amount of eccentric stalactites (also called helictites).

METHODS: MONITORING THE MICROENVIRONMENTAL PARAMETERS

Research was carried out by a consulting company in collaboration with the Carranza council. It is based on an 8-channel, 16-bit data acquisition system (DAS), with storage capacity for 32,000 measurements. The system was equipped with a battery to sustain its operation for short periods of time (6 to 7 days) in case of power outages. In addition, a visual alarm system was set up to facilitate detection by workers in the cave of a possible failure in the DAS.

A set of sensors and signal-conditioning units was used:

- Air temperature sensor (T) with a Pt100, measurement range between 0–50 °C with a resolution of 0.01 °C.
- CO_2 sensor based on non-dispersive spectrometry with infrared radiation, double beam, 1 ppm resolution and 0–7000 ppm measurement range.

- Capacitive-type relative-humidity sensors with a 0–100% measurement range and a resolution of 0.1%.
- Atmospheric-pressure sensor with a silicon-diaphragm detector temperature balanced, barometric range and 0.1 hPa (0.1 mbar) resolution.
- The ^{222}Rn concentration was measured by means of a Pylon AB5 scintillometer with a continuous passive radon detector (CPRD). This equipment was calibrated periodically with a ^{222}Rn calibration standard cell model Pylon 3150 and RNC standard radioactive sources of known activity concentration (Chau et al., 2005). An automatic recording system was programmed to store records every hour.

The system was completed by a stabilized power supply, located at the entrance of the cave, with regulated outputs of +24V, +12V, and −12V and load tension of the back-up battery. This power source included surge protectors in case of spikes produced in the power line by atmospheric storms.

Sensors and DSA were situated in the Versalles Chamber, where the largest number of helicites and other spelothems are located and where visitors stop for periods of 10 to 15 minutes. Data points were recorded every 10 minutes.

Transmission of data to the cave entrance was by means of a low-voltage line and an RS485 interface. An RS485/RS232 converter was used to communicate from a personal computer to the DAS. In this way, all routine operations of unloading data, verification of the sensors, and starting the equipment were controlled from outside the cave. The locations of the different elements of the measurement system are detailed in Figure 1.

Microenvironmental Parameters Record and Results

Microenvironmental parameters were measured inside the cave from April 1, 2001, to June 30, 2004, with an interval of either 10 or 20 minutes; the recording interval was changed during the different seasons to reflect different tour frequencies. Because of failures in the electric system or sensors, some gaps in the record were supplied by means of measurements taken with portable instruments. We used the weather dataset provided by the Basque Meteorology Service (station G065 Cerroja-Karrantza, Bizkaia) located at an altitude of 677 m for the climatic parameters outside the cave.

Management of the Cave

There was no limit to the number of visitors inside the cave during the entire recording period. When possible, each group did not exceed 30 people, although this number increased greatly during holiday periods and on bank holidays. The visiting hours are 11 a.m. to 5 p.m. during winter and 10 a.m. to 7 p.m. during summer. On Mondays, the cave is closed to the public, except during holiday periods or on bank holidays.

Each group of visitors spends between 40 and 50 minutes inside the cave. There is a break of about 10 minutes between groups, but not if it is a busy day. The door is opened only for the entrance and exit of visitors and remains closed during the visit. Lights are always on during open hours.

The number of visitors during the recorded period was 151,315, with a peak of 1,389 visitors on one day and an average of 170 visitors per day. The daily number of visitors was recorded by the cave guides at our request. The results obtained on the variations in the microenvironmental parameters of the cave during the period studied, together with the outside climatic parameters, are shown in Figure 2.

Relative Humidity of the Air

The relative humidity in the cave is always over 97%, very close to saturation. This is characteristic of an underground environment and common inside caves. In this case, the saturated state is favored by the fact that thermal oscillations inside the cave are very small. In addition, there is water present in the cave. Because of the little variation, the data are not displayed in any of the figures.

Atmospheric Pressure

Atmospheric pressure inside the cave is very close to that outside. The average pressure inside the cave is 979 hPa, with a maximum of 998 hPa and a minimum of 949 hPa. During the recorded period there were stable periods during summer and the beginning of winter and variable periods at the end of winter and during spring, as well as at the beginning of autumn.

Air Cave and Outdoor Temperature

Mean air cave temperature (internal temperature, T_{int}) during the studied period was 12.96 °C but increased since the beginning of the study, most likely due to the massive numbers of visitors entering the cave. As Figure 2 shows, the underground temperature is influenced by the outdoor cycle, but with a time lag due to the low thermal conductivity of the rock. Inside the cave, there are two well-differentiated periods: six months of thermal rise (from May to October) and six months of thermal fall (from November to April). The minimum temperature recorded was 12.78 °C, and the maximum was 13.39 °C, which coincided with a very large number of visitors during October 2002. Therefore, the annual temperature inside the cave fluctuates about 0.5 to 0.6 °C, including the effect of visitors. It is difficult to calculate the effect of visitors in detail, because there is no record of temperatures before the cave was opened to tourism, but, even so, we selected a period with the maximum temperature inside the cave (October-November), and using temperatures taken during

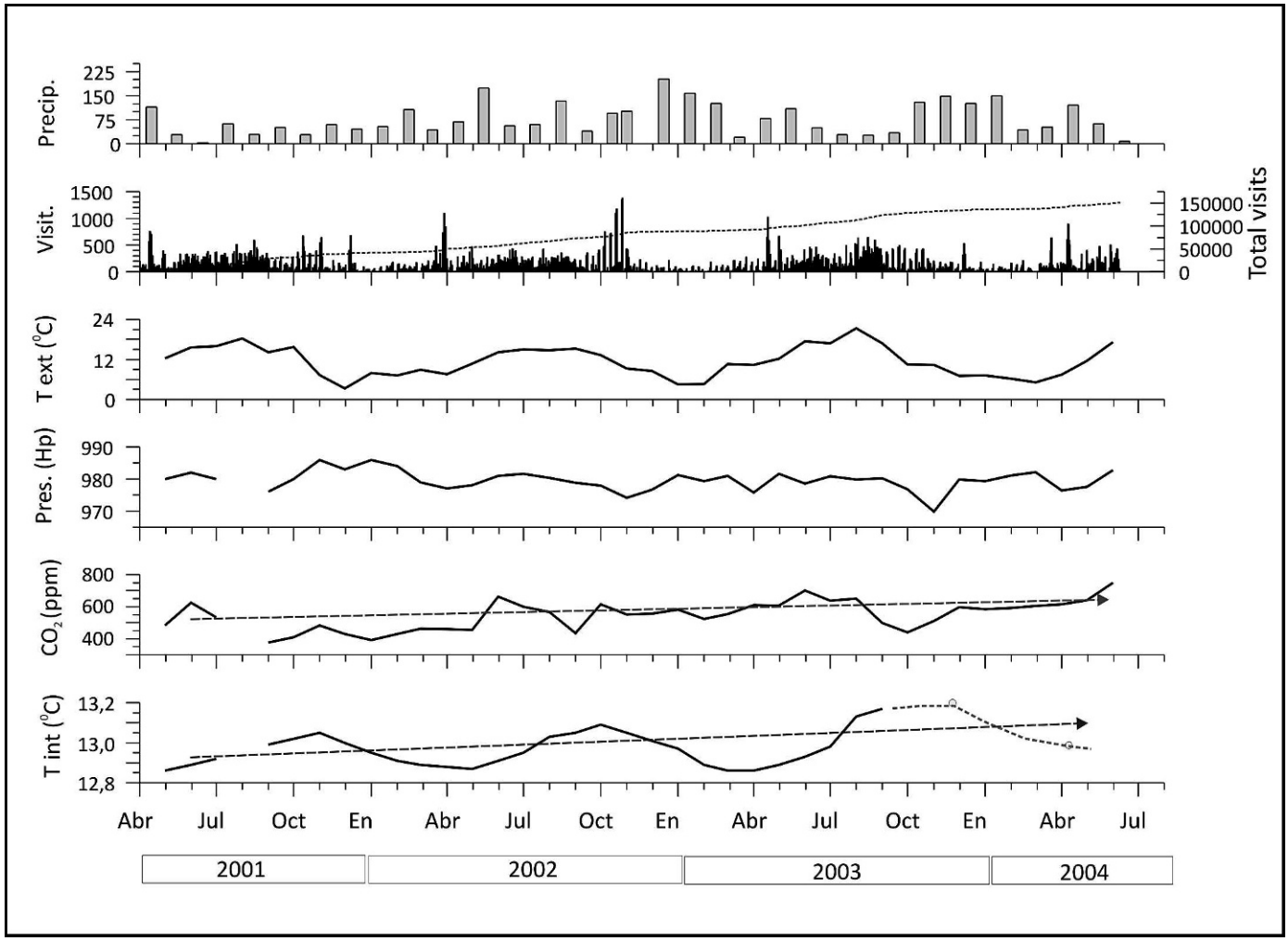

Figure 2. Microclimatic data from 2001 to 2004 (monthly averages except visitor numbers).

the night and during periods without visitors, we estimate that the annual temperature range, without the effect of visitors (relative background), would be 0.25 to 0.30 °C. By means of the same procedure, we calculated that maximum temperature inside the cave without the cumulative influence of visitors would be less than 13.05 °C. That value is surpassed on multiple occasions due to the influx of visitors.

Also, the occurrence of high numbers of visitors during the Easter holidays, just when the cave should reach its natural minimum temperature, provokes a break in the natural trend. A similar effect can be shown during the maximum annual temperature period, in October-November, again coinciding with an increase of visitors on bank holidays.

Using linear regression during a complete annual recording period (April 2001 to April 2002), we estimate that the mean temperature of the cave increases by 0.04 °C/yr, which was confirmed by the data of the following years. This phenomenon will be detrimental to the cave and should be taken into account in its management.

The mean outdoor temperature (external temperature, T_{ext}) was 11.44 °C, with a minimum of −6.3 °C and a maximum of 37.1 °C during the recording period. The mean is lower than the mean cave temperature mainly because T_{int} is not the natural one but is modified by visitors.

CHANGES IN T_{int}

In order to evaluate the effect of visitors on the daily record of microenvironmental parameters, a period with both low (nil) and high (>250 visitors/day) numbers of visitors was chosen. Figure 3 shows the period June 3–8, 2001. Variation in T_{ext} is low because there is a stable situation, with a maximum during midday and a minimum late at night.

During visit days there is an overall rise in T_{int}, which also reflects each group of visitors entering the cave. The maximum increase recorded is 0.21 °C on June 3, which amounts to 84% of the natural annual variation (0.25 °C). Recovery to the temperature previous to visits took about 12 h 15 min, similar to that of June 5 (12 h 45 min). These

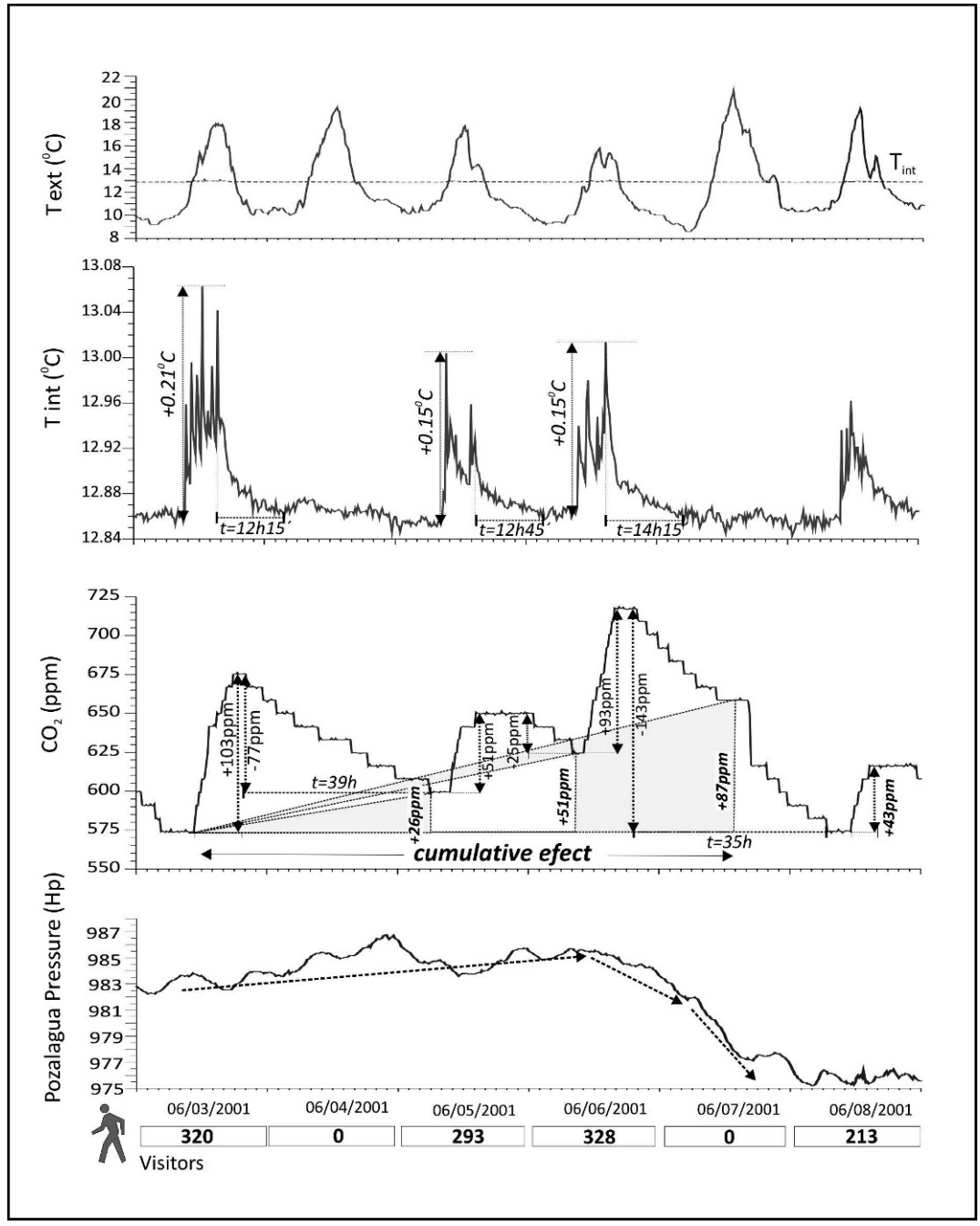

Figure 3. Evolution of main microclimate parameters during heavy use of the cave (June 2001).

values are considered the typical T_{int} recovery time after a visit day during most of the year. The next day (June 6) the recovery time was slightly longer (14 h 15 min), showing a possible cumulative effect of days with large numbers of visitors.

CO_2

The mean annual concentration of CO_2 recorded inside the cave was 570 ppm, with a minimum of 325 ppm and a maximum of 1060 ppm, corresponding to a massive influx of visitors. The presence of only thin soil cover above the cave is likely to be the cause of these low values, as the soil is largely responsible for the total dissolved CO_2 in the vadose zone (Baldini et al., 2006). The evolution of CO_2 over a year-long period shows that the cave is the upper part of a deep karstic system. Periods with higher natural concentration of CO_2 are related to a rise in T_{ext}, and occur once it is above T_{int} and remains there. Using the same methodology as for T_{int}, it is possible to estimate that the maximum value in semi-natural conditions (relative back-

ground) would be lower than 600 ppm, giving an annual natural variation of 300 ppm.

CHANGES IN CO_2

During massive influxes of visitors (holiday periods and bank holidays), a significant increase in CO_2 levels, with slow recovery to previous levels, is produced (Fig. 2). We used the period between June 3 and 8, 2001, to evaluate CO_2 levels during periods with no visitors and days with large number of visitors (Fig. 3). Visits by 290 to 300 people per day provoked an increase of 50 to 100 ppm of CO_2 in the cave environment. Recovery to previous levels before the entry of visitors was not completed during the daily cycle, but continued during the next day because there were no visitors on June 4, for a total recovery of 75% in 39 h. On June 5 the recovery ceased because there were almost 300 visitors. Finally, during a day without any visits (June 7), total recovery of previous CO_2 levels was reached after 35 h.

Drops in CO_2 concentration are also related to atmospheric pressure variations. During June 6 and 7 there was an abrupt fall in external atmospheric pressure that favored cave ventilation. This probably accounts for the quick and full recovery after the visitors of June 6. During stable weather, the CO_2 concentration does not recover fully between visitor days, as on June 3 and 4.

THE EFFECT OF BUSY PERIODS ON MICROENVIRONMENTAL PARAMETERS: EASTER HOLIDAYS 2002

To check the effect of busy holiday periods on the microenvironmental parameters inside the cave, the 2002 Easter holiday was studied in detail (Fig. 4). Between March 28 and April 1, 2002, there were 3574 visitors, with a maximum of 1100 visitors on Good Friday. The increase in T_{int} during the maximum influxes of visitors (always over 600 visitors/day) ranges from 0.16 to 0.23 °C (65% to 92% of the natural annual variation). These largest daily T_{int} increases also provoke an increase in the recovery time from approximately 12 h seen in Figure 3. So, during the four days of heavy visits, there was an accumulated T_{int} increase after each day of 0.05 to 0.07°C (20 to 28% of annual range), and it took 72 h during days with few or no visits for the temperature to fully recover. This cumulative warming effect could also be partly related to the increase in T_{ext}, because the cave door was open during the entrance and exit of visitors. From March 28 to March 31 there was an increase in minimum T_{ext} of 6 °C. Nevertheless, the effect is offset by the natural cooling trend in the cave during this season, and also because of the T_{ext} fall of 8 °C during the following two days. Busy days will cause greater warming inside the cave if there is also a warming trend outside the cave.

These changes can also be observed in the CO_2 record. The direct daily increase varies between 185 and 280 ppm. The rest period of 16 h between the closing of the cave and the next day's opening is not enough for recovery to the levels prior to the visits. Actually, much more time is needed (nearly 35 h; see Fig. 2). Because there is not enough time to recover original CO_2 levels between visits, the total CO_2 cumulative effect is nearly 400 ppm, more than doubling the values registered previous to the large numbers of visitors at Easter.

This example confirms that the cave atmosphere needs a much longer time to return to previous CO_2 values after heavy use than is needed for temperature recovery. The total time with high visitor influence is the same (ca. 95 h) for both, but overall about 118 h is necessary to recover the original CO_2 levels, while only 72 h are needed to return to the original T_{int} values. It should also be considered that this happened during a favourable situation in which the average T_{ext} was lower than T_{int}, and also that there was a drop in atmospheric pressure. Under different circumstances the recovery time would probably be longer.

Another impressive data set can be seen in Figure 5, which shows the period for August 2003. During this time, there were 11,981 visitors to the cave. Using the same methodology and focusing only on the cumulative increase in minimum daily T_{int} during the whole month that represents nearly 75% of the annual range (Figure 2), there is an increased step in the T_{int} record, which never reached the original level during the study period.

^{222}RN

The level of ^{222} Rn was measured from October 19, 2002, to January 16, 2004. Mean annual concentration of ^{222}Rn recorded inside the cave was 838 Bq m^{-3}, with a minimum of 228 Bq m^{-3} and a maximum of 1568 Bq m^{-3}. Radon levels in karstic systems depend on a complex interrelation of different factors, both external and internal (Kies et al., 1997): outside-inside temperature differences, wind velocity, atmospheric pressure variations, humidity, karstic geomorphology and porosity, and radium content in the sediments and rocks. Since ^{222}Rn is not related to human presence, it could be used as an independent indicator of cave ventilation. Low values show ventilation of the cave, while high values show a decrease in air flow inside the cave. The ^{222}Rn concentration should show a good correlation with evolution of natural CO_2 values. Negative or inverse correlation is an indicator of CO_2 increase due to human activity.

DISCUSSION

Cave microclimate is controlled by external and internal factors. The alteration of cave microenvironmental conditions causes a break in the natural dynamic equilibrium of the cave system. In order to reduce visitor impact, cave managers need to understand the factors that contribute to the cave microclimate to define and maintain an appropriate range of environmental conditions for each particular cave system (Gillieson, 1996; de Freitas, 1998;

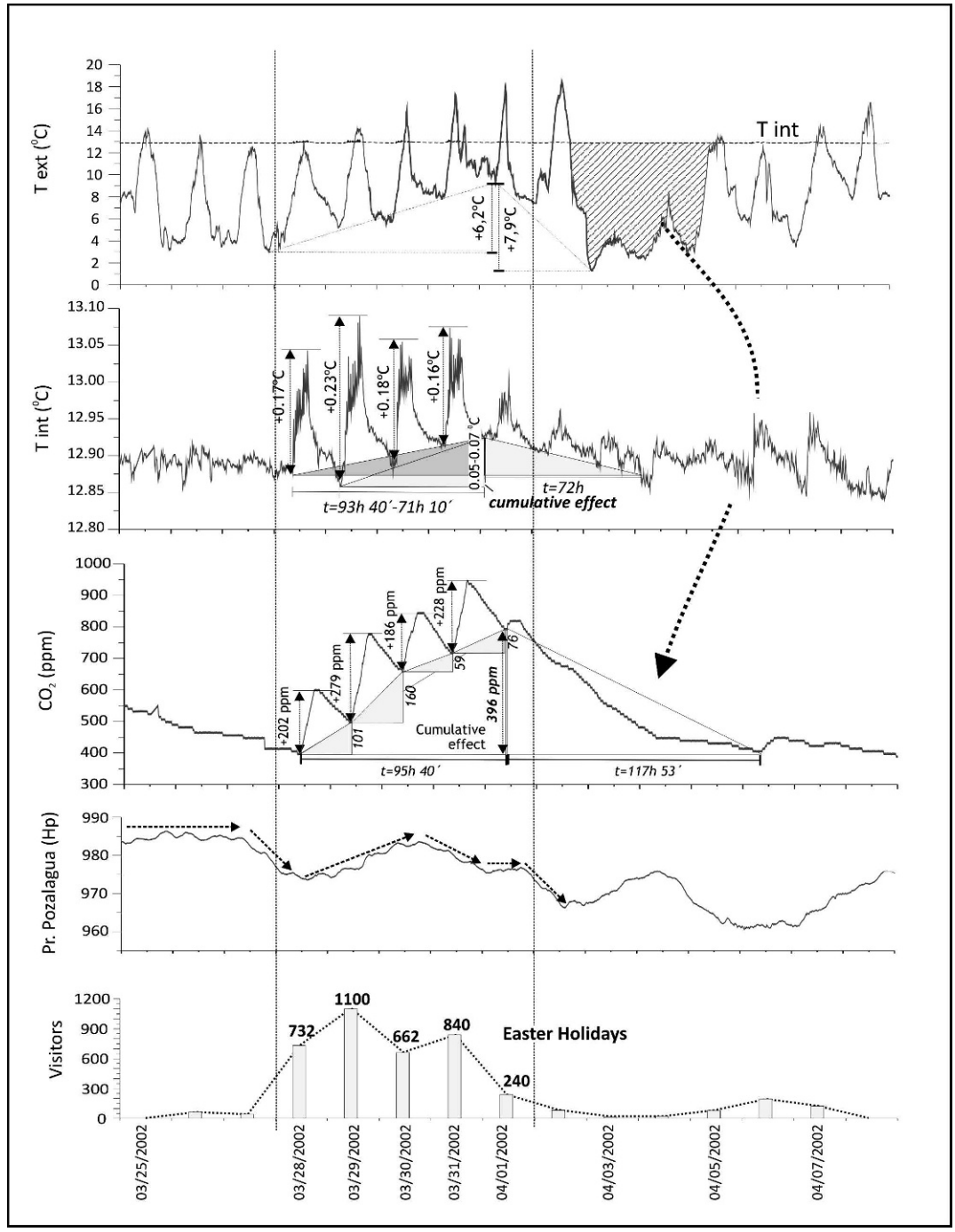

Figure 4. Evolution of main microclimate parameters during heavy use of the cave (Easter holidays 2002).

Fernández-Cortés et al., 2006b; Russel and MacLean, 2008).

Helicites growing in the cave, its greatest tourist attraction, are directly related to the occurrence of various factors (Lario et al, 2005): low water-infiltration velocities, hydrochemistry of the infiltration waters (affected by the lithology around the cave), and the physical-chemical equilibrium between the cave atmosphere and the infiltration water. This last point is the one factor affected by cave visitors causing changes to temperature, water vapor, and CO_2 concentrations. All these variations affect the physical-chemical equilibrium, and are also very important for colonization by microbial communities and for corrosion of the speleothems and host rock.

From the analysis of data obtained during the study, it is possible to conclude that Cueva de Pozalagua has a low natural temperature range (0.25 °C) compared to other shallow caves close by, such as Altamira Cave (1.6 °C,

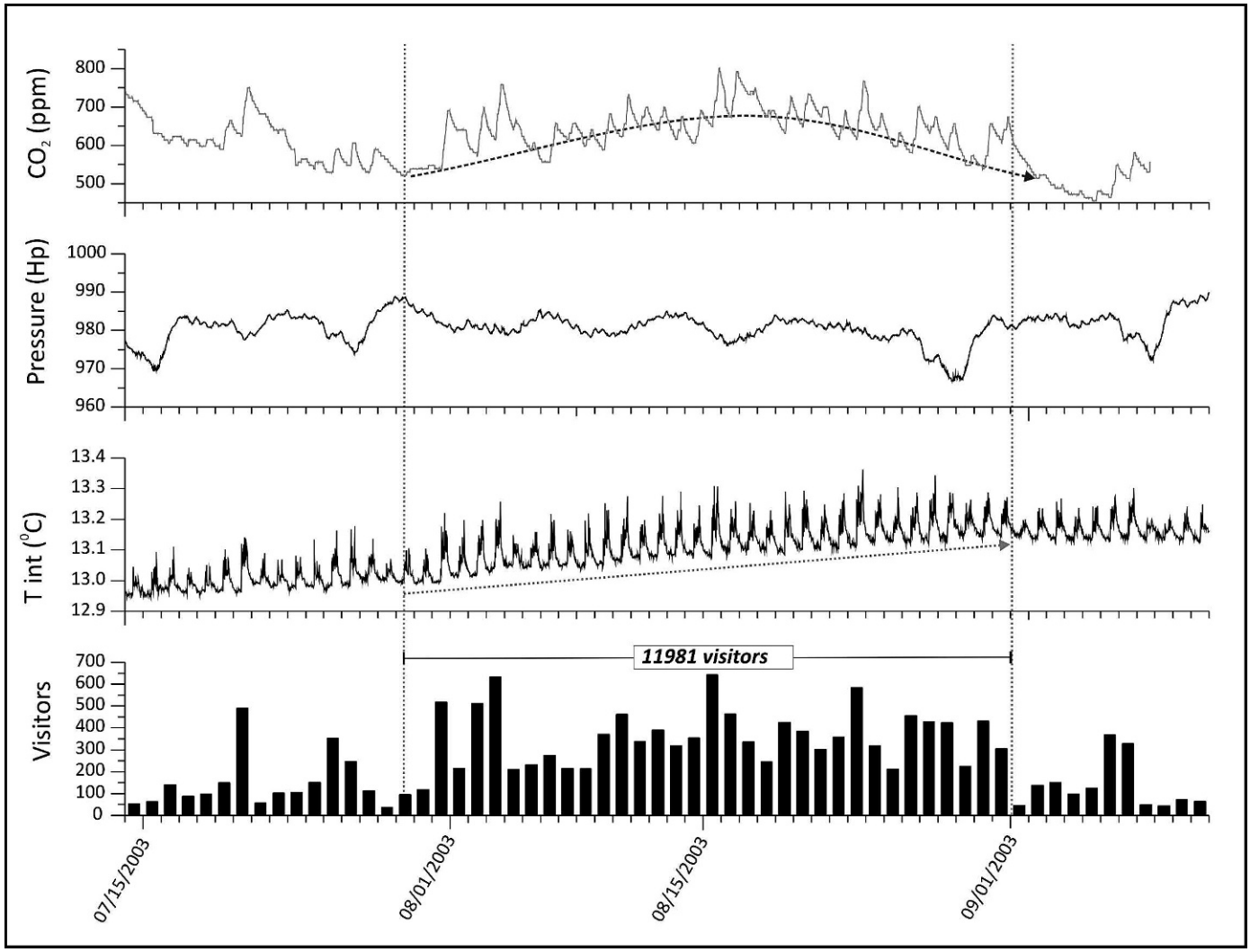

Figure 5. Evolution of main microclimate parameters during heavy use of the cave (August 2003).

Sanchez-Moral et al., 1999). Also, the average annual natural concentration of CO_2 is moderate to low (448 ppm), with an annual variation range of 300 ppm. Recovery from a day of visits requires a long time (12 h for T_{int} values and 35 h for CO_2). These characteristics show a high degree of isolation of the cave relative to changes in external climatic conditions. In these conditions, any change inside the cave will remain and accumulate over time, modifying the fragile physical-chemical equilibrium of the system. This is confirmed by the warming trend of the cave observed during this study. Due to this special characteristic of the cave, proposals for modifying the visitor regime should focus on avoiding disrupting the equilibrium of the system. Obviously, for complete success, the best case scenario is the absence of any human influence. In order to minimize the effect of visits, it is useful to calculate the visitor carrying capacity of the cave to establish the number of visitors per day that does not irreparably deteriorate the cave.

T_{int} AS A LIMITATION FACTOR

Figure 6a shows a direct relation between daily visits and net increase in T_{int} calculated during periods without cumulative effect. There is dispersion in data when there are few visitors, but there is a good correlation when the number of visitors is over 100. The dispersion of data on the days with few visits is most likely related to varying stopping times in the Versalles Chamber, while during busy days, the stopping time in the Versalles Chamber is more controlled and is the same during all visits. Therefore the correlation line obtained is useful to predict the increase in T_{int} after a day of 100 to 700 visitors.

Maximum T_{int} recorded in the cave without the cumulative effect of visits was lower than 13.05 °C. Hence the proposed visiting regime needs to be adjusted in order not to surpass this T_{int} and, consequently, to maintain the natural annual range. As was recorded, this T_{int} was frequently surpassed, and on more occasions during October-November. From the average monthly T_{int}

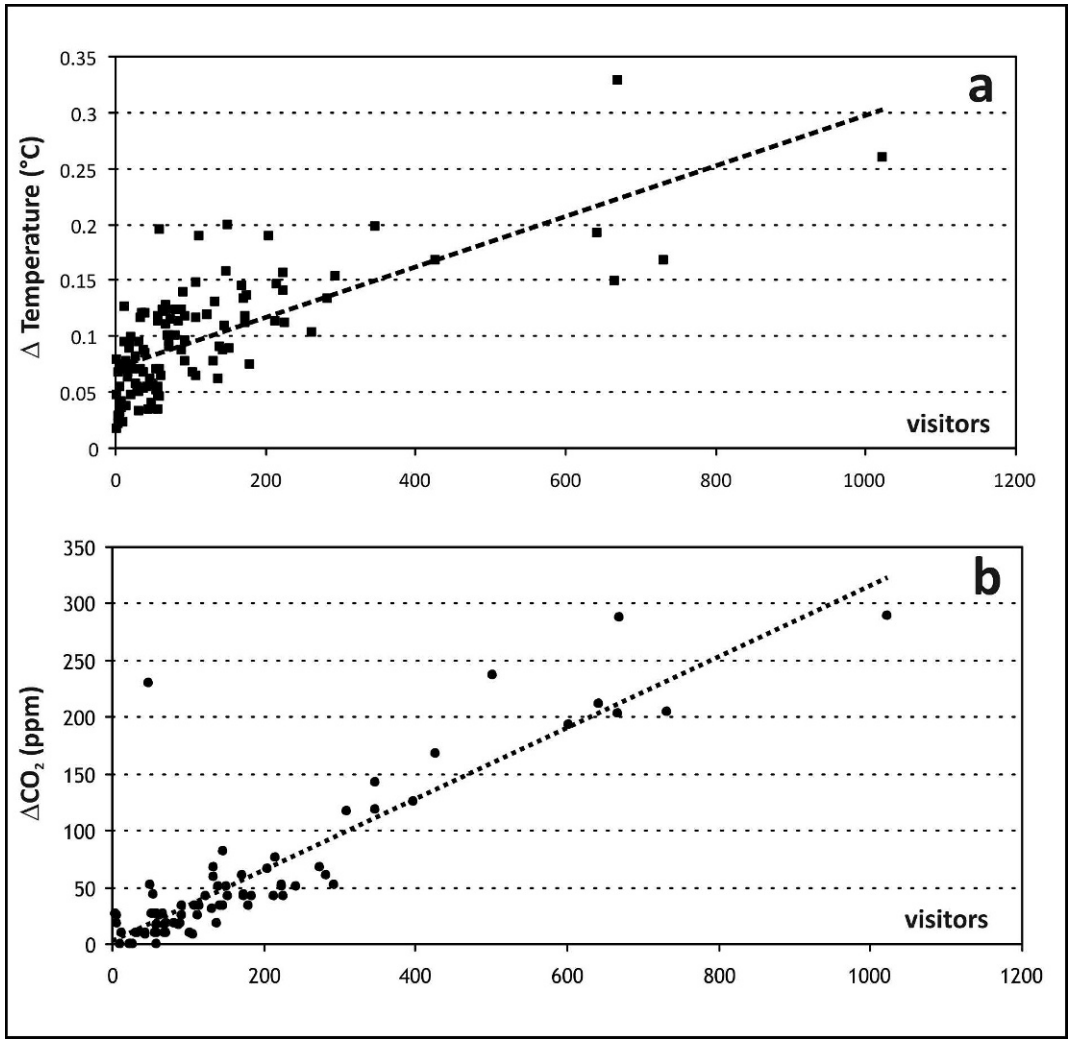

Figure 6. Relation between daily visits and net increase in T_{int} (a) and CO_2concentration (b) calculated during periods without cumulative effect.

recorded, the limitation criterion is to not exceed the maximum estimated natural T_{int}. For example, in June, with an average T_{int} of 12.89 °C, the maximum number of visitors allowed per day is estimated at 275. These visitors provoke an increase in T_{int} of 0.16 °C, which is the maximum allowable in order to not surpass the maximum T_{int} under natural conditions. Using these criteria, it was possible to assess the recommended numbers of visitors per day during each month (Table 1).

CO_2 as a Limitation Factor

The maximum value of CO_2 concentration inside the cave during undisturbed periods would be under 600 ppm and the limiting criteria should not surpass these concentration levels. Figure 6b shows a direct relation between daily visits and net increase in CO_2 concentration calculated during periods without cumulative effect. In this case, the correlation is clearer than in the case of T_{int}, and the correlation line allows calculation of the CO_2 concentration increase that would be produced by 100 to 1000 visitors. The proposed number of visitors per day for each month is presented in Table 2.

Combination of Both Factors: T_{int} and CO_2

Table 3 was calculated combining both factors and using the most restrictive of each. The table shows the recommended maximum number of visitors per day during each month to avoid surpassing the natural capacity of the cave to return to a stable situation. Because we observed the cumulative effect of massive visits during the three years of study and we know the first period (2001–2002), we used the numbers calculated for this period because they were obtained during the stage in which the cave was less affected by visits. It must also be taken into consideration that all the microenvironmental parameters obtained were affected by the visitors themselves and that the truly undisturbed original conditions of the cave are unknown. Also, during the recording period, some building

Table 1. Recommended maximum number of visitors/day each month using cave indoor temperature as a limiting factor.

Month-Year	Average T_{int} (°C)	Recommended maximum increase in T_{int} (°C)[a]	Maximum number of visitors/day[b]
05-2001	12.86	0.19	362
06-2001	12.89	0.16	282
07-2001	12.92	0.13	214
08-2001	…	…	…
09-2001	12.99	0.06	24
10-2001	13.02	0.03	0
11-2001	13.05	0.00	0
12-2001	13.00	0.05	7
01-2002	12.95	0.10	131
02-2002	12.91	0.14	224
03-2002	12.89	0.16	271
04-2002	12.88	0.17	305
05-2002	12.87	0.18	330
06-2002	12.91	0.14	230

[a] 13.05°C–average
[b] (a−0.0492/0.004)

Table 2. Recommended maximum number of visitors/day each month using cave CO_2 as a limiting factor.

Month-Year	Average CO_2 (ppm)	Recommended maximum increase in CO_2 (ppm)[a]	Maximum number of visitors/day[b]
05-2001	484	116	311
06-2001	626	0	0
07-2001	533	67	176
08-2001	…	…	…
09-2001	376	224	614
10-2001	409	191	522
11-2001	482	118	318
12-2001	429	171	467
01-2002	391	209	573
02-2002	430	170	464
03-2002	463	137	370
04-2002	460	140	380
05-2002	425	175	477
06-2002	563	37	90

[a] 600 ppm-average
[b] (a−4.7289/0.3567)

and conditioning work was carried out in the cave and the environment (changes to the lighting system, building an interpretation center at the entrance of the cave, stabilization of the nearby quarry) without notifying the research team, so the influence of these on the microenvironmental record is not evaluated in this paper.

CONCLUSIONS: CARRYING CAPACITY AND PROPOSAL FOR MODIFICATION OF VISITOR REGIME

As previously explained, carrying capacity can be defined as the maximum number of visitors per unit of time while maintaining the critical factor or parameter within its natural fluctuation limits. Thus, the parameter most susceptible to change will be considered the critical factor for calculating visitor capacity (Cigna, 1993; Hoyos et al., 1998; Calaforra et al., 2003).

In our case, not only the number of visitors per day and distribution per month calculated using the limiting factors (T_{int} and CO_2) is proposed, but also some changes in the visitor schedule would help to optimize visiting conditions, and therefore, increase the carrying capacity of the cave. These proposals are focused on reducing the increase in CO_2 and T_{int} values generated by visitors, and also on reducing the cumulative effect of these visits and the cave recovery time.

Table 3. Recommended maximum number of visitors/day each month.

Month	Critical Factor T_{int} Maximum number of visitors/day	Critical Factor CO_2 Maximum number of visitors/day	Combination of both critical factors Maximum number of visitors/day
January	131	573	131
February	224	464	224
March	271	370	271
April	305	380	305
May	330	477	330
June	230	90	90
July	214	176	176
August	No Data	No Data	…
September	24	614	24
October	0	522	0
November	0	318	0
December	7	467	7

Table 4. Proposed visitors regime (carrying capacity).

Month	Maximum number of visitors/day
January	125
February	225
March	275
April	300
May	330
June	90
July	175
August	50
September	50
October	0
November	0
December	50

After adjusting values of Table 3, the recommendations for modifying visit management are:

- Reduce the visit time inside the cave to a maximum of 30 minutes with a minimum waiting time between visits of 30 minutes. Due to the dimensions of cave passages and corridors, the ideal group of visitors should not exceed 25 to 30 people per visit.
- Close the cave weekly. Every week the cave requires almost one day without visits. Closing of the cave one day per week during normal weeks, and two days after periods with large numbers of visitors, should be rigorously observed.
- Control of the proposed maximum number of visitors per day during each month (Table 4). Closing the cave after the summer (October-November) or, if this is not possible, opening only during weekends and not exceeding 100 visitors per day.
- Shut down the lighting system between groups of visitors. Change the lighting system from ''all-on'' to a ''partial'' lighting system controlled by the cave guides.

Since, as we have explained, the original undisturbed microenvironmental levels of the cave have not been recorded, the carrying capacity should be interpreted as a changing parameter that needs to be adjusted depending on the response of the cave to the visit regime proposed. Once the measures proposed take effect and the current cumulative effect decreases, a further record of the evolution of the microenvironmental parameters would permit adjustment of the visitor regime and optimization to minimize the effect of visitors on the cave.

Aknowledgements

Thanks to the Carranza Council and the guides of the cave. This is a contribution to IGCP Project 513, Global Study of Karst Aquifers and Water Resources.

References

Baker, A., and Genty, A., 1998, Environmental pressures on conserving cave speleothems: effects of changing surface land use and increased cave tourism: Journal of Environmental Management, v. 53, p. 165–175.

Baldini, J.U.L., Baldini, L.M., McDermott, F., and Clipson, N., 2006, Carbon dioxide sources, sinks, and spatial variability in shallow temperate zone caves: Evidence from Ballynamintra Cave, Ireland: Journal of Cave and Karst Studies, v. 68, no. 1, p. 4–11.

Calaforra, J.M., Fernandez-Cortés, A., Sanchez-Martos, F., Gisbert, J., and Pulido-Bosch, A., 2003, Environmental control for determining human impact and permanent visitor capacity in a potential show cave before tourist use: Environmental Conservation, v. 30, no. 2, p. 160–167.

Chau, N.D., Chruściel, E., and Prokólski, L., 2005, Factors controlling measurements of radon mass exhalation rate: Journal of Environmental Radioactivity, v. 82, p. 363–369.

Cigna, A., 1993, Environmental management of tourist caves: the examples of Grotta di Castellana and Grotta Grande del Vento, Italy: Environmental Geology, v. 21, p. 173–180.

de Freitas, C.R., 1998, Cave monitoring and management: The Glowworm Cave, New Zealand, *in* Cave and Karst Management in Australasia XII. Proceedings of the Twelfth Australasian Conference on Cave and Karst Management, Waitomo, Carlton South, Victoria, Australasian Cave and Karst Management Association, p. 55–66.

de Freitas, C.R., and Banbury, K., 1999, Build up and diffusion of carbon dioxide in cave air in relation to visitor numbers at the Glowworm Cave, New Zealand, *in* Cave Management in Australasia XIII. Proceedings of the Thirteenth Australasian Conference on Cave and Karst Management, Mount Gambier, South Australia, Carlton South, Victoria, Australasian Cave and Karst Management Association, p. 84–89.

Fernández-Cortés, A., Calaforra, J.M., Jiménez-Espinosa, R., and Sánchez-Martos, F., 2006a, Geostatistical spatiotemporal analysis of air temperature as an aid to delineating thermal stability zones in a potential show cave: Implications for environmental management: Journal of Environmental Management, v. 81, p. 371–383.

Fernández-Cortés, A., Calaforra, J.M., and Sánchez-Martos, F., 2006b, Spatiotemporal analysis of air conditions as a tool for the environmental management of a show cave (Cueva del Agua, Spain): Atmospheric Environment, v. 40, p. 7378–7394.

Gillieson, D., 1996, Caves: Processes, Development, Management, Oxford, Blackwell, 324 p.

Hammitt, W., and Cole, D., 1987, Wildland Recreation: Ecology and Management, New York, John Wiley & Sons, 341 p.

Hoyos, M., Soler, V., Cañaveras, J.C., Sánchez-Moral, S., and Sanz-Rubio, E., 1998, Microclimatic characterization of a karstic cave: human impact on microenvironmental parameters of a prehistoric rock art cave (Candamo Cave, northern Spain): Environmental Geology, v. 33, p. 231–242.

Huppert, G., Burri, E., Forti, P., and Cigna, A., 1993, Effects of tourist development on caves and karst, *in* Williams, P.W., ed., Karst Terrains: Environmental Changes and Human Impact, Cremlingen-Destedt, Germany, Catena (supplement 25), p. 251–268.

IGME, 1978, Mapa Geológico de España, escala 1:50.000, Hoja 60, Valmaseda.

Kermode, L.O., 1979, Cave corrosion by tourists, *in* Cave Management in Australia 3: Proceedings of the 3rd Australian Conference on Cave Tourism and Management, Mt. Gambier, South Australia, Carlton South, Victoria, Australasian Cave and Karst Management Association, p. 97–104.

Kies, A., Massen, F., and Feider, M., 1997, Measuring radon in underground locations, *in* Virk, H.S., ed., Rare Gas Geochemistry, Amritsar, Punjab, Guru Nanak Dev University, p. 1–8.

Lario, J., Sánchez-Moral, S., Soler, V., Cañaveras, J.C., and Cuezva, S., 2005, Caracterización microambiental de la Cueva de Pozalagua (Vizcaya): aplicación a la gestión y protección de cavidades turísticas: Estudios Geológicos, v. 61, p. 41–59.

Mangin, A., Bourges, F., and D'Hulst, D., 1999, La conservation des grottes ornées: un problème de stabilité d'un système naturel (l'exemple de la grotte préhistorique de Gargas, Pyrénées francaises): Comptes rendús de l'Académie des Sciences de Paris, Sciences de la Terre et des Planètes, v. 328, p. 295–301.

Michie, N.A., 2005, On the placing of objects in caves, *in* Cave management in Australasia 15: Proceedings of the 15th Australasian Conference on Cave and Karst Management, Chillagoe Caves and Undara Lave Tubes, North Queensland, Carlton South, Victoria, Australasian Cave and Karst Management Association, p. 51–52.

Middaugh, G., 1977, Practical experiences with carrying capacity, *in* Aley, T., and Rhodes, D., eds., National Cave Management Symposium Proceedings, Mountain View, Arkansas, October 26–29, 1976: 1976, Albuquerque, Speleobooks, p. 6–8.

Pulido-Bosch, A., Martín-Rosales, W., López-Chicano, M., Rodríguez-Navarro, C.M., and Vallejos, A., 1997, Human impact in a tourist karstic cave (Aracena, Spain): Environmental Geology, v. 31, no. 3–4, p. 142–149.

Russel, M.J., and MacLean, V.L., 2008, Management issues in a Tasmanian tourist cave: Potential microclimatic impacts of cave modifications: Journal of Environmental Management, v. 87, p. 474–483.

Sanchez-Moral, S., Soler, V., Cañaveras, J.C., Sanz, E., Van Grieken, R., and Gysells, K., 1999, Inorganic deterioration affecting Altamira Cave: quantitative approach to wall-corrosion (solutional etching) processes induced by visitors: Science of the Total Environment, v. 243, p. 67–84.

Sarbu, S.M., and Lascu, C., 1997, Condensation corrosion in Movile Cave, Romania: Journal of Cave and Karst Studies, v. 59, no. 3, p. 99–102.

Ugarte Elorza, F.M., 1989, Geomorfología de las unidades kársticas situadas en los montes vascos, *in* Durán, J.J., and Lopez-Martinez, J., eds., El Karst en España, Sociedad Española Geomorfología (Monorafía 4), p. 121–130.

GUIDE TO AUTHORS

The *Journal of Cave and Karst Studies* is a multidisciplinary journal devoted to cave and karst research. The *Journal* is seeking original, unpublished manuscripts concerning the scientific study of caves or other karst features. Authors do not need to be members of the National Speleological Society, but preference is given to manuscripts of importance to North American speleology.

LANGUAGES: The *Journal of Cave and Karst Studies* uses American-style English as its standard language and spelling style, with the exception of allowing a second abstract in another language when room allows. In the case of proper names, the *Journal* tries to accommodate other spellings and punctuation styles. In cases where the Editor-in-Chief finds it appropriate to use non-English words outside of proper names (generally where no equivalent English word exists), the *Journal* italicizes them. However, the common abbreviations i.e., e.g., et al., and etc. should appear in roman text. Authors are encouraged to write for our combined professional and amateur readerships.

CONTENT: Each paper will contain a title with the authors' names and addresses, an abstract, and the text of the paper, including a summary or conclusions section. Acknowledgments and references follow the text.

ABSTRACTS: An abstract stating the essential points and results must accompany all articles. An abstract is a summary, not a promise of what topics are covered in the paper.

STYLE: The *Journal* consults The Chicago Manual of Style on most general style issues.

REFERENCES: In the text, references to previously published work should be followed by the relevant author's name and date (and page number, when appropriate) in parentheses. All cited references are alphabetical at the end of the manuscript with senior author's last name first, followed by date of publication, title, publisher, volume, and page numbers. Geological Society of America format should be used (see http://www.geosociety.org/pubs/geoguid5.htm). Please do not abbreviate periodical titles. Web references are acceptable when deemed appropriate. The references should follow the style of: Author (or publisher), year, Webpage title: Publisher (if a specific author is available), full URL (e.g., http://www.usgs.gov/citguide.html) and date when the web site was accessed in brackets; for example [accessed July 16, 2002]. If there are specific authors given, use their name and list the responsible organization as publisher. Because of the ephemeral nature of websites, please provide the specific date. Citations within the text should read: (Author, Year).

SUBMISSION: Effective July 2007, all manuscripts are to be submitted via AllenTrack, a web-based system for online submission. The web address is http://jcks.allentrack2.net. Instructions are provided at that address. At your first visit, you will be prompted to establish a login and password, after which you will enter information about your manuscript (e.g., authors and addresses, manuscript title, abstract, etc.). You will then enter your manuscript, tables, and figure files separately or all together as part of the manuscript. Manuscript files can be uploaded as DOC, WPD, RTF, TXT, or LaTeX. A DOC template with additional manuscript specifications may be downloaded. (Note: LaTeX files should not use any unusual style files; a LaTeX template and BiBTeX file for the *Journal* may be downloaded or obtained from the Editor-in-Chief.) Table files can be uploaded as DOC, WPD, RTF, TXT, or LaTeX files, and figure files can be uploaded as TIFF, EPS, AI, or CDR files. Alternatively, authors may submit manuscripts as PDF or HTML files, but if the manuscript is accepted for publication, the manuscript will need to be submitted as one of the accepted file types listed above. Manuscripts must be typed, double spaced, and single-sided. Manuscripts should be no longer than 6,000 words plus tables and figures, but exceptions are permitted on a case-by-case basis. Authors of accepted papers exceeding this limit may have to pay a current page charge for the extra pages unless decided otherwise by the Editor-in-Chief. Extensive supporting data will be placed on the *Journal*'s website with a paper copy placed in the NSS archives and library. The data that are used within a paper must be made available. Authors may be required to provide supporting data in a fundamental format, such as ASCII for text data or comma-delimited ASCII for tabular data.

DISCUSSIONS: Critical discussions of papers previously published in the *Journal* are welcome. Authors will be given an opportunity to reply. Discussions and replies must be limited to a maximum of 1000 words and discussions will be subject to review before publication. Discussions must be within 6 months after the original article appears.

MEASUREMENTS: All measurements will be in Systeme Internationale (metric) except when quoting historical references. Other units will be allowed where necessary if placed in parentheses and following the SI units.

FIGURES: Figures and lettering must be neat and legible. Figure captions should be on a separate sheet of paper and not within the figure. Figures should be numbered in sequence and referred to in the text by inserting (Fig. x). Most figures will be reduced, hence the lettering should be large. Photographs must be sharp and high contrast. Color will generally only be printed at author's expense.

TABLES: See http://www.caves.org/pub/journal/PDF/Tables.pdf to get guidelines for table layout.

COPYRIGHT AND AUTHOR'S RESPONSIBILITIES: It is the author's responsibility to clear any copyright or acknowledgement matters concerning text, tables, or figures used. Authors should also ensure adequate attention to sensitive or legal issues such as land owner and land manager concerns or policies.

PROCESS: All submitted manuscripts are sent out to at least two experts in the field. Reviewed manuscripts are then returned to the author for consideration of the referees' remarks and revision, where appropriate. Revised manuscripts are returned to the appropriate Associate Editor who then recommends acceptance or rejection. The Editor-in-Chief makes final decisions regarding publication. Upon acceptance, the senior author will be sent one set of PDF proofs for review. Examine the current issue for more information about the format used.

ELECTRONIC FILES: The *Journal* is printed at high resolution. Illustrations must be a minimum of 300 dpi for acceptance.

Journal of Cave and Karst Studies

Volume 72 Number 3 December 2010

Grant Funding Available. The National Speleological Foundation offers modest grants for cave- and karst-related research. Information at www.speleofoundation.org